3D FEM & Multibody System Coupling of Railroad Dynamics with

Vibration of Surrounding Building Structure

by

Sarvesh Masurekar
B.S (University of Mumbai) 2015

Thesis submitted in partial fulfillment of the requirements
for the degree of Master's of Science in
Mechanical Engineering
in the Graduate College of the
University of Illinois at Chicago, 2018

Chicago, Illinois

Defense Committee:
Dr.Craig Foster, Chair and Advisor
Dr.Michael Scott , Department of Mechanical and Industrial Engineering
Dr.Didem Ozevin, Department of Civil and Materials Engineering

To my family and friends

who constantly supported me

throughout this journey

ACKNOWLEDGEMENTS

Firstly, I must express my very profound gratitude to my parents for providing me with immense support and continuous encouragement throughout my years of study and through the process of researching. This accomplishment would not have been possible without them.

I would specially like to thank my advisor, Dr. Craig Foster from the CME department who has always guided me in the right direction by sharing his expertise throughout this research. It has helped me generate great interest in the field of Finite element analysis under his mentorship. I would also like to thank Dr.Michael Scott and Dr. Didem Ozevin for their presence on my thesis committee.

I would like to thank my lab mate, Ahmed El-Ghandour for helping me learn ANSYS APDL and MATLAB to apply in this project and helping me understand finite element concepts clearly. Finally, I would like to thank my friends who have always been a constant support.

TABLE OF CONTENTS

LIST OF TABLES

LIST OF FIGURES

FIGURE   **PAGE**

LIST OF FIGURES(CONTINUED)

LIST OF ABBREVIATIONS

FE   Finite Element

MBS   Multibody Systems

FFR   Floating frame of reference

ANCF   Absolute Nodal Coordinate Formulation

SAMS   Simulation of Articulated Mechanical Systems (multibody software)

MAPDL   Mechanical ANSYS Design Parametric Language

<u>SUMMARY</u>

Rail transportation of both passengers and goods plays a vital and evolving role in US society and worldwide. Particularly with the introduction of higher-speed rail in the US, new problems need to be addressed efficiently and economically. One such issue is the effect of vibrations from rail traffic on nearby buildings. In extreme cases, vibrations may lead structural fatigue, but occupant comfort is generally the controlling issue.

Computer analysis techniques have been shown to be an effective tool for examining a variety of problems. In this work, we perform a coupled finite element and multibody analysis of vibration in buildings due to a passing train. The model of the track, substructure, and building is constructed in commercial finite element software, and modal analysis is performed to identify the important vibration characteristics. This information is imported into the multibody analysis software, which performs a dynamic analysis of wheel-interaction in the time domain. We then reconstruct the full displacement and accelerations from the modal displacement to evaluate the vibration magnitudes of the building.

<u>KEYWORDS</u>: FINITE ELEMENT ANALYSIS, MODAL ANALYSIS, MULTIBODY DYNAMICS, NODAL ELIMINATION, FLOATING FRAME OF REFERENCE.

INTRODUCTION

In the field of railway engineering, there is a rising interest in ground borne vibrations due to railway tracks and control methods which can be resorted to minimize it by means of various modifications in the track structure. This thesis is focused upon quantifying the vibrations that are produced due to passing trains on an adjacent building structure by using computational techniques.

1.1 Vibrations in building:

Vibrations are generated through the interaction of a passing train with the rail track and are transmitted to the ground and thereby to the structures in the vicinity. Ground vibrations induced by railway can cause discomfort on local building occupants near rail lines. The problems and its solutions are still not fully understood even though the current field of research is constantly progressing. Factors such as wheel and rail roughness, propagation of waves through soil, soil damping, vehicle speed and dynamic properties of a train greatly affect the amplitude and frequency of vibrations that are experienced.

Along with the occupant discomfort, one more concern is the structural damage in buildings due to fatigue which can result in catastrophic failure if exposed to prolonged vibrations. While in most buildings occupant comfort controls, in some structures this may be a concern.This complex problem can be broken down into 3 steps:

1. Vehicle- rail dynamic interaction, which is the main source of vibration.
2. Transmission of vibrations from the rail-track through the soil to the walls of the building.
3. Energy propagation from the foundation into the building.

With the advent of advanced technology, research pertaining to this topic is advancing given a more concerned approach towards the safety and comfort of people, and economy of design.

1.2 <u>Rail track and substructure</u>

The railway industry has been continuously developing new technology coming out with solutions to specific requirements. The traditional railway model is a system with rails, rail pads and sleepers laid on a track substructure consisting of top layer of ballast, intermediate layer of subballast and bottom layer of subgrade. The primary function of track substructure is to pass on the applied loads from the moving train to the subgrade safely as well as control water drainage. The dynamic load is transmitted by the train onto the rail track and is transmitted to the sleepers through the fasteners and rail pads. In order to reduce the stress in the substructure, this load should be spread out to a large area. The wheel – rail contact force which is due to the moving weight of the train is transmitted from a smaller area of a few cm^2 through rails, fasteners and sleepers to a larger area of square meters in the subgrade.

Rails are normally made of steel and are welded or bolted together. The cross ties or sleepers with the help of fasteners keep the rail in place. They are typically made of wood, though concrete ties are used in some newer applications. Their job is to receive the load from the rail above and distribute it to the ballast. The sleepers also grip the entire superstructure to the ballast.

Ballast is a material made up of crushed hard stones and rocks which are coarse-sized and non-cohesive grains of relatively uniform gradation laid on top of the track subgrade. It supports

the rail and sleepers as discussed in AREMA (31).The track structure consisting of rails and sleepers is supported by this ballast layer against lateral, longitudinal and vertical forces from the train.

To keep the track accurately aligned and in level, the sleepers are fastened to the rails and embedded in the ballast. The rail fasteners are an integral part of the track structure since they help in keeping the connection between the rail and sleepers intact and act as spring-dampers to help absorb vibrations generated by the motion of the train.

The ballast layer has many important roles to perform:

1. Providing proper resistance to absorb shock from dynamic loading,
2. Minimizing movement of the sleeper by resisting the longitudinal, transverse and vertical forces from the train.
3. Distribution of the load coming from the sleepers to avoid permanent settlement of the track and to protect the subgrade from high stresses.
4. Assisting fluid drainage.

The subballast forms a permeable zone between the ballast and subgrade, preventing migration of fine particles from the subgrade to the ballast .It also reduce stresses in the subgrade.

Subgrade is the third layer below ballast and subballast which provides a stable foundation. The subgrade does undergo some strain due to constantly applied stress. The main function of the subgrade is to support the track structure with minimum deflections. To lower the deflection, the subgrade needs to be stiffer. This can be ensured by using techniques like compaction, in situ densification and by providing a good drainage system.

1.3 <u>Computational modeling of rail problems</u>

Due to increasing computational power, techniques have been developed to reduce the expenses that come along with experimentation, various computer models have been suggested in this field of rail research.

1.3.1 <u>Rail-Wheel contact theory</u>

Many rolling contact theories have been put forward to calculate the tangential contact forces which are expressed as a function of the relative velocity between wheel and the rail and stiffness co-efficients given in Kalker's table[2]. These theories concluded that calculating the contact forces at the wheel-rail contact area is very important to study the dynamic performance of vehicle track system.

Moncef Toumi et al. (1) developed a three-dimensional finite element model to study the frictional rail-wheel rolling contact with increased spin effect in elasticity with three different analyses: explicit dynamic, implicit quasi-static and implicit moderate energy dissipation analysis. The theory proposed in this paper affirms that shear stresses that are generated in the contact area between wheel and the rail subjected to high pressure are one of the most important factors leading to its damage. Therefore to determine the dynamic performance of vehicle track system, calculating the contact forces acting over this contact patch is a very important step.

Xin Zhao (2) et al in their research emphasized on how vehicle dynamics, rolling contact fatigue, wear and plastic deformation are affected by the rolling contact of the wheel. Here, analytical and computer-based numerical approaches were highlighted since there were no experimental techniques to determine contact stress under dynamic conditions. The wheel-rail

contact is traditionally divided into normal and tangential parts for study. The normal problem is associated with the contact patch and the pressure distribution under certain elastic conditions while the tangential problem deals with the friction, where the major focus is to determine surface shear stress, also known as tangential traction. The micro-slip, the relative velocity between the rail and the wheel surface was also examined. They focused more on the tangential problem and modeled the problem with 3D transient finite elements with a fine mesh at the patch to establish a contact solution, which was verified with Hertzian contact theory. Hertz theory is an analytical model to calculate normal forces in a contact in a simplified way.

Modeling of wheel wear helps in understanding how a wheel design behaves and enables modification to minimize the wear rate, which indirectly decreases the vehicle rail contact forces. A real-time analysis is possible when the finite element model is coupled with multibody dynamics software to calculate the vehicle motion. The solutions obtained by these models have to employ some simplifications such as neglecting surface roughness, which may lead to inaccurate analysis of wear on the rail profile. To overcome this, Rovira et al.(3) used a combination of rolling contact algorithm on FASTSIM and experimental methods to solve the contact problem by measurement of ultrasonic reflection. Here, wear is calculated by an energy dissipation approach named T-gamma.

1.3.2 <u>Vibration propagation through soil</u>

An extensive number of mechanisms are associated with the transmission process of vibrations through the soil, hence it is quite difficult to predict railway induced ground vibrations. For over two decades, there have been a many studies to model the propagation of vibrations induced by passing railways in the surrounding buildings. These models have been developed to determine the transmission of vibration from the time-dependent force applied to the track. The

vibration was subsequently quantified by studying the modal response of the track, ballast and the sub-structure in time domain.

In his research, Hunt (4) presented a methodology where the numerical model was simplified to an infinitely long track with an isotropic infinite half-space and the building structure was considered to be lumped mass attached to a spring. He suggested that this simplifies the process to calculate vibration spectra in the building present in the proximity of the rail.

Gutowski and Dym (5) highlighted three origins of intricacies that have to be faced while predicting the vibration propagation through the soil:

1. The complexity in understanding soil behavior.

2. Trouble in defining accurate soil properties.

3. Difficulty in accurately modeling the vibration source.

In his research, Galvin Dominguez et al.(6) carried out numerical simulations using finite element method where two dimensional models were used to examine the impact of various soil parameters and also the design of the building. He also explained that the study of wave propagation through the ground is material dependent. He has described distribution of pressure waves (P-waves), which displace particles parallel to the direction wave propagation giving rise to compressions and rarefactions, and shear waves (S-waves), where the particles are moving perpendicular to the wave propagation giving rise to crests and troughs. Certain empirical models concluded that softer materials such as clay are correlated with high vibrations.

To determine resonant frequencies in the ground in an elastic model, the three determining factors are Poisson's ratio, Elastic modulus, density and geometry of the soil layers. The knowledge of resonant frequencies of both soil and building would be beneficial to avoid the high vibration levels.

In order to bypass extreme computational resources, Georges Kouroussis (7) took to a decoupled approach which considered developing a coupled lumped mass model of the soil using only finite element modeling and then studying the vehicle –track dynamics separately. This model interprets the effects of seismic wave amplification by initially performing modal analyses of the building and the vehicle. It helps in studying the structural response of a building located nearby in case the source frequencies, which can be problematic if close to natural frequency of the building.

In his theory, Krylov (8) stated that mechanical properties of the track and parameters of soil and train which include nonlinearity in static contact of track-soil combination are the contributing factors when it comes to studying the ground-borne vibrations due to moving train. Also the distance between adjacent sleepers, train speed and the distance between wheel axle and carriage influence the rail induced vibrations. Verbraken (9) employed a finite element model to determine vibrational velocities in the building.

1.4 <u>Wave barriers to reduce vibration</u>

In order to counter the influence of vibrations on structural damage in building and comfort of people inside, an assessment of the effect of vibration is necessary. A parametric study of wave barriers to reduce train induced vibration was carried out by Yeong-Bin Yang and Hsiao-Hui Hung (10). In this study, the effectiveness of three different wave barriers, the elastic foundation, infilled trench, and open trench, is examined by different finite element schemes. It adopted a mathematical model having a two-dimensional geometry containing railway cross-section, the wave barrier and the substructure and the dynamic load of the train simulated as harmonic load in a vertical direction. This study concluded that all three wave barriers have the potential to isolate

vibrations that occur due to high frequency. L.Andersen et al. (11), in their study, proved how open trenches are useful in reducing vertical ground vibrations.

M.Sanayei et al. (12) proposed a wave propagation mathematical model which predicted velocity ratios, velocities and impedances analytically. The analytical predictions were validated with experimentally measured floor vibrations and they turned out to be similar. This result implied that the upper floor vibrations can be relieved by increasing the thickness of a lower level floor in the building, which is called the blocking floor. The measured feedback of the scaled building using different thickness slabs at the first floor and the predicted response were analyzed, and it was concluded that blocking floor has the capacity to mitigate structural vibration transmitted to the floors above it.

1.5 Coupling MBS and FEM

Multibody system dynamics is an approach that has been growing widely in the field of railway engineering. Complex problems having interconnected rigid and flexible systems are modeled using algebraic and differential equations. The multibody systems that consists of these rigid and deformable are interconnected by joints are explained in detail in Shabana et al. (15). This approach is extensively used in examining the interaction between rail and the wheels to extract and calculate an important set of information in the domain of railroad dynamics. The rail deformations and the contact forces between the rail and the wheel are investigated using multibody dynamics code.

Ebrahimi (13) discussed the multibody dynamics for problems involving unilateral contact between constrained and non-constrained planar deformable bodies giving rise to kinematic relationships controling the behavior of contact considering effect of deformations.

In his study of unsupported sleepers in the rail track system, Recuero et al. (16) used a non-linear MBS approach to understand the effect of sleeper loss of support on the system. The creepages which depend on the deformation of the rail were analysed here along with the system frequencies. Kumaran et. al(14) explained different methods to study the rail-wheel interaction dynamics. Shabana et.al (15) and Recuero et. al (16) modeled the rail-wheel contact for a moving train using Multibody system dynamics. A new multibody system method was developed by Rosario Chamorro et.al (17) to model flexibility of the rail which was based on floating frame of reference formulation. This formulation was incorporated with MBS code to simulate the motion of railroad vehicles. It used shape functions which are defined in the trajectory frame of reference to determine the deformations. To study the rail-wheel interactions, coupling of finite element method and multibody analysis has become a very useful approach. Tanabe et. al (18) studied the rail wheel interaction dynamics on a high speed train using a coupled finite element and multibody model. By using finite element method, Galvin et al. (19) studied the rail-wheel interaction in trains which travel with high speeds. Liang et al. (20) used MBS approach to model the lateral impact on trains running on ballasted track. El-Ghandour et al.(21) investigated the train substructure interaction under dynamic loading by using a coupled technique between finite element method and multibody dynamics. The floating frame of reference technique was used in this research to study the effect of the substructure on rail-wheel interaction. Also a bridge approach problem was investigated for problems due to the stiffness variation of the track from softer substructure to stiffer foundation on the bridge.

In this thesis, we used a coupled approach between finite element method and multibody dynamics to model the rail and the substructure below it that can inspect the wheel-rail interaction and determine the contact forces which give rise to the substructure deformations. We created a

finite element model of the track system which included the geometry as well as the material properties of the rail, sleepers, fasteners, track substructure and a concrete framed building nearby. The model was built in commercially available FE ANSYS software using Mechanical ANSYS Parametric Design Language (MAPDL). Modal mass and stiffness data is then extracted after performing modal decomposition on the model and this is then imported into a multibody software SAMS. The multibody system code is used to simulate the moving train over the rail structure and study the contact forces that are generated due to this interaction using a contact algorithm. The floating frame of reference technique was used to formulate the forces in the simulation driven by multibody code. The FFR technique formulated by Shabana et al.(15) analyses the dynamics of a multibody system which undergoes small strains and large relative rotations. Here, in this research the techniques adopted by El-Ghandour et al.(21) were used but they were further extended to calculate the nodal displacements and nodal accelerations from the corresponding modal values. Later, the strains and stresses were also determined in the substructure.

The order of the chapters and a brief description of the content present in it is as follows: Chapter 2 discusses the creation of finite element model of the rail, substructure and the building in Mechanical ANSYS APDL. Chapter 3 outlines the modal analysis performed on the model to extract modal information. Chapter 4 discusses the multibody dynamic analysis and formulations used in this system. Chapter 5 explains how the results are reconstructed back into the finite element software after calculating it in MATLAB. Chapter 6 analyzes a numerical example and the results obtained for the analysis and finally Chapter 7 summarizes the thesis and suggests directions for future work in this research.

CHAPTER 2

<u>FINITE ELEMENT MODEL</u>

The finite element method is one of the most effective methods for solving the differential equations associated with many problems on complex geometries. It helps perform complex engineering analysis and provides a useful computational tool as it reduces the need to test multiple scenarios for experimenting on difficult prototypes in indefinite situations. The power of this tool can greatly reduce the cost of the project. The finite element method is capable of producing extremely accurate results to many engineering problems with complex geometries, material properties and boundary conditions.
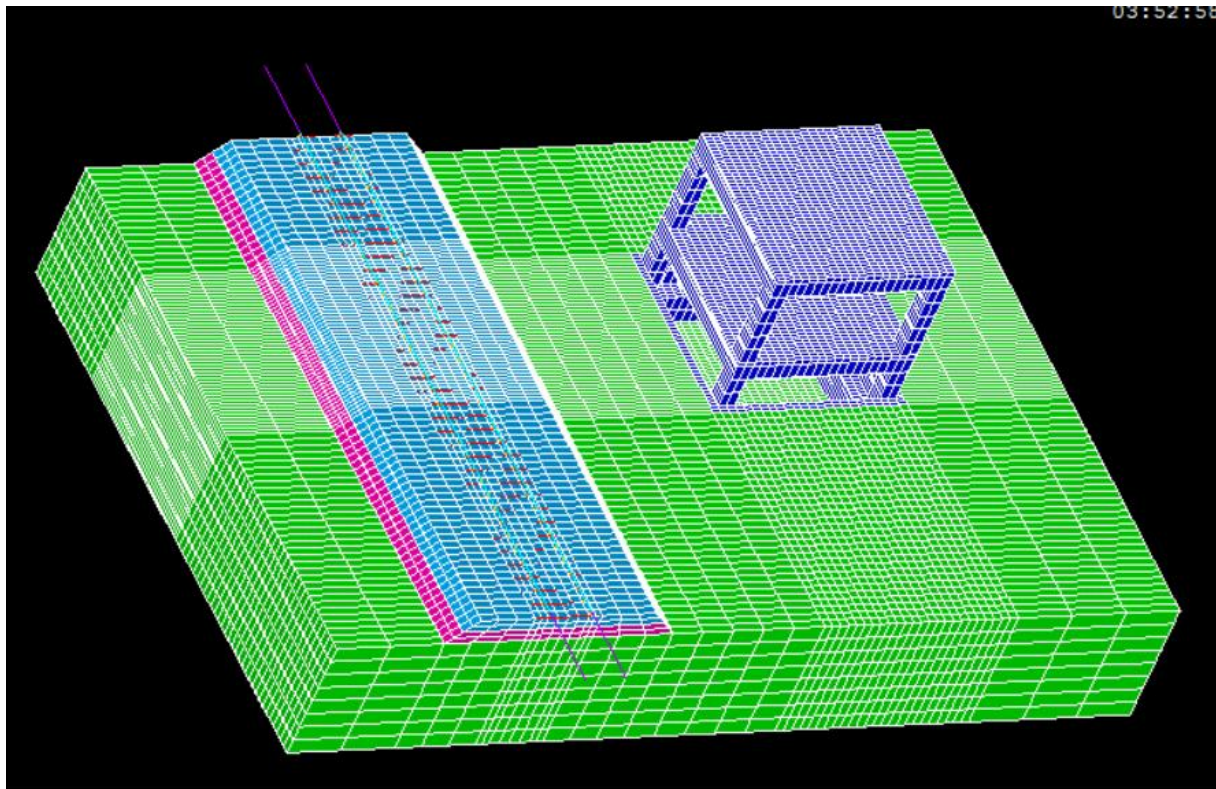
Figure 1: FE model of the entire rail system with an adjacent building structure

2.1 <u>GEOMETRICAL DIMENSIONS & MATERIAL PROPERTIES</u>

In this research, the three dimensional finite element model of the rail along with the adjacent building structure is being built in a commercial software package ANSYS M-APDL (Mechanical ANSYS Parametric Design Language). With this finite element software package, we build a 3D model of the rails, sleepers, fasteners that connect them together and the substructure beneath the rail assembly including the ballast, subballast and the subgrade .We also model a two story concrete building in the vicinity of the rail system.

The rails and the sleepers are modeled using three dimensional beam elements (BEAM 188). The three substructure layers of ballast, subballast, the subgrade and the concrete building are all modeled using 8-node hexahedral brick element (SOLID185). Spring-damper elements (COMBIN14) are used to model the fasteners and rail pads that connect the deformable rail with the sleepers and help ease off the deformation between rail and sleepers.

8-node brick elements tend to be stiff in bending and when using full integration schemes, the material behaves badly for higher Poisson's ratio or plastic behavior. However, employing selective reduced integration as b-bar methods reduce shear locking and volumetric locking. The 20 node brick elements are not so favorable for dynamic analysis. A general mass matrix is difficult to generate. So naturally, to reduce the computational time and avoid complications in the analysis since we have elastic material properties, we prefer to use 8 node brick elements with three translational degrees of freedom associated with each node.

The modal damping coefficient values used for this model was 3% as this roughly reflects the damping in the soil that dominates the geometry. It was concluded that keeping the modal damping coefficient to a minimum of 3% also gives better results and better cancels out wave reflection effects over a model where there is no modal damping.

The material properties and dimensions are described briefly in the table given below:

TABLE I: Finite element model dimensions and material properties

Description	Value	Unit
Length of the rigid rail	3	m
Length of the flexible rail	21.6	m
Gauge length	1.5113	m
Stiffness of the rail	210e9	N/m^2
Density of the rail	7700	kg/m^3
Poisson's ratio of the rail	0.3	
Cross-sectional area of the rail	64.5e-4	m^2
Second moment of inertia of the rail-Iyy	2010e-8	m^4
Second moment of inertia of the rail-Izz	326e-8	m^4
Timoshenko shear coefficient for the rail	0.34	
Length of a sleeper Length	2.5	m
Gap between sleepers	0.6	m
Stiffness of a sleepers	64e9	N/m^2
Density of a sleeper	2750	kg/m^3
Stiffness coefficient of a pad	26.5e7	N/m
Damping coefficient of a pad	4.6e4	N.s/m
Poisson's ratio of a sleeper	0.25	
Cross-sectional area of a sleeper	513.8e-4	m^2
Second moment of inertia of a sleeper	18907e-8	m^4
Timoshenko shear coefficient for a sleeper	0.83	
Stiffness of the ballast	260e6	N/m^2
Density of the ballast	1300	kg/m^3
Poisson's ratio of the ballast	0.3	
Stiffness of the subballast	200e6	N/m^2
Density of the subballast	1850	kg/m^3
Poisson's ratio of the subballast	0.35	
Stiffness of the subgrade	200e6	N/m^2
Density of the subgrade	1850	kg/m^3
Poisson's ratio of the subgrade	0.35	
Ballast depth	4.8	m
Subballast depth	0.5	m
Subgrade depth	0.5	m
Density of the concrete building	2500	kg/m^3
Poisson's ratio of the concrete building	0.25	
Stiffness of the concrete building	31e9	N/m^2
Height of the building	8.2	m
Width of the building	7.2	m
Perpendicular Distance between rail and building	9.15	m

2.2 **BOUNDARY CONDITIONS**

- As the sleepers, modeled using beam elements are connected to the solid brick elements, the torsional degrees of freedom associated with them are constrained.

- The beam elements have six degrees of freedom: 3 translational and 3 rotational while the 8-node brick elements have 3 translational degrees of freedom at each node. Therefore the rotational degrees of freedom of the nodes common to both of them are constrained to maintain connectivity and avoid floating-redundant degrees of freedom.
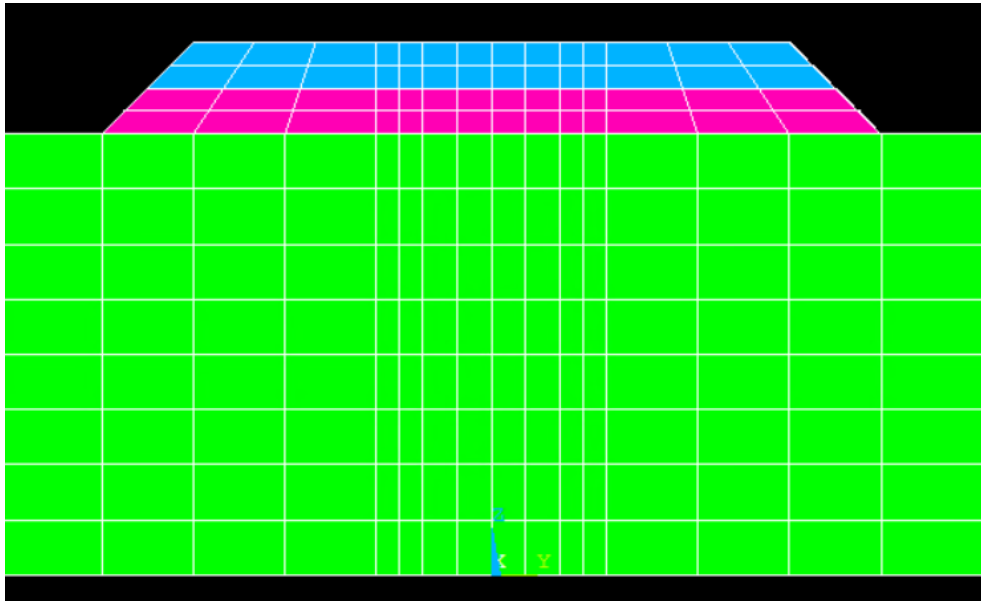
Figure 2: A front view of the FE mesh model for 3 different layers: ballast, subballast and the subgrade made up of solid brick elements.

- The rail track is divided into two sections: the rigid section and the deformable section.
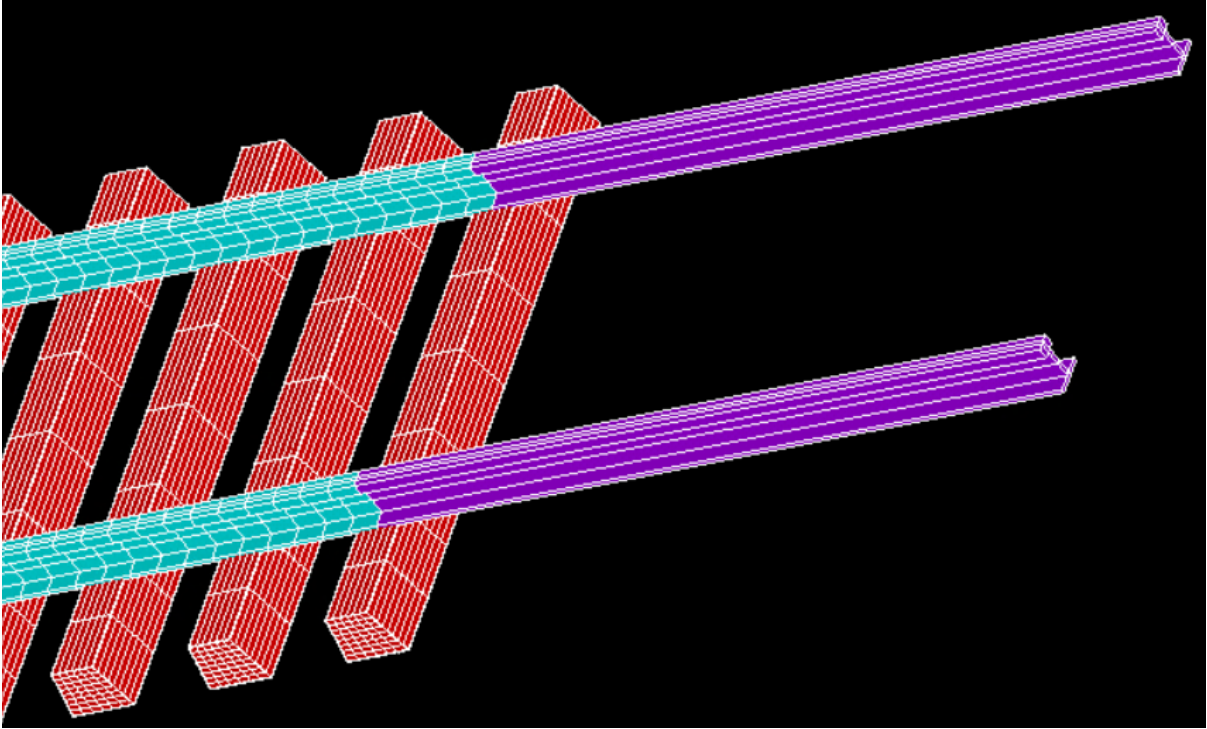
Figure 3:3D view of the FE model of the rail and sleepers showing transition from rigid to flexible.

- Though the Figure(3) may appear to show meshing on the flexible rail, they are modeled with beam elements as shown in Figure (4).
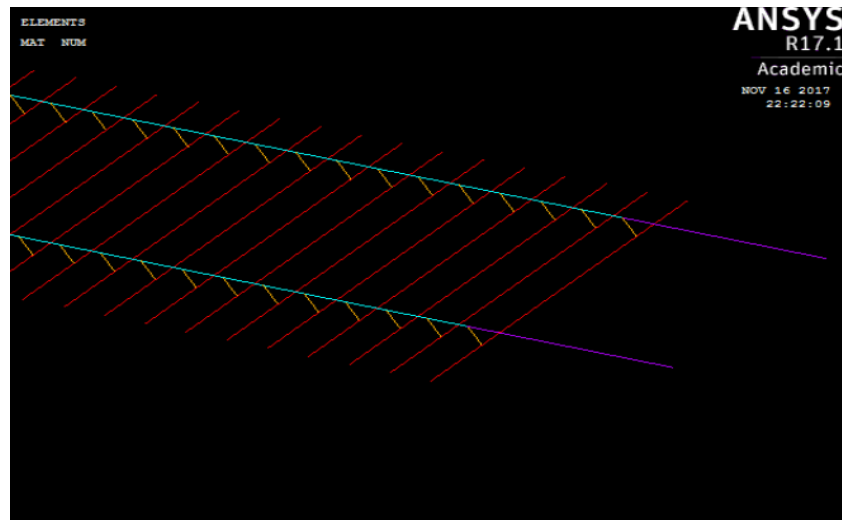
Figure 4:3D view of the beam elements used for rail, sleepers and damper springs.
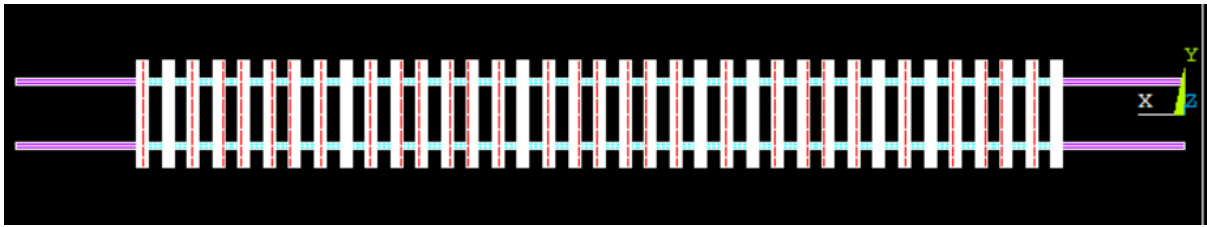
Figure 5:Top view of the FE model of the rail

- The rigid section is designed to form a track before and after the deformable part of the rail. It has all its degrees of freedom constrained. It is done to avoid the initial sudden impact of the wheelset which is dropped from a small distance initially and an unwanted sharp noise in the analysis at the beginning of the simulation.
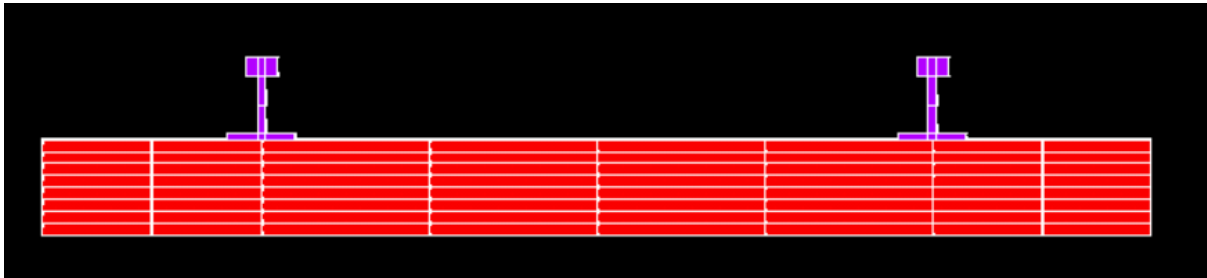
Figure 6: Front view of the FE model of the rail
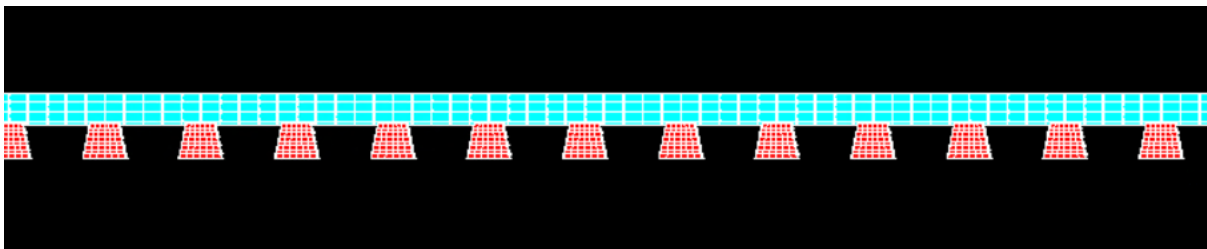
Figure 7: Side view of the FE model of the rail

- Building a section of rigid rail before and the after a flexible rail assures smooth transition and avoids very large rail deflections initially.

- The substructure is constrained on all sides in the longitudinal direction to avoid out of plane motion.

- The bottom side of the subgrade is fully fixed and constrained for all degrees of freedom to make sure it is consistent with the physical behavior of the soil and its attachment with the hard rock below it.

- The common nodes between the beam elements of the rail and the spring elements have their rotational degrees of freedom constrained for torsional movement since the vertical load of the train doesn't contribute much to the track's torsional rotation along the direction of motion of the railway.

- Also, the remaining two rotational degrees of freedoms for these common nodes are constrained to ensure smooth motion of the rail at these connection points. The fasteners largely constrain this movement.
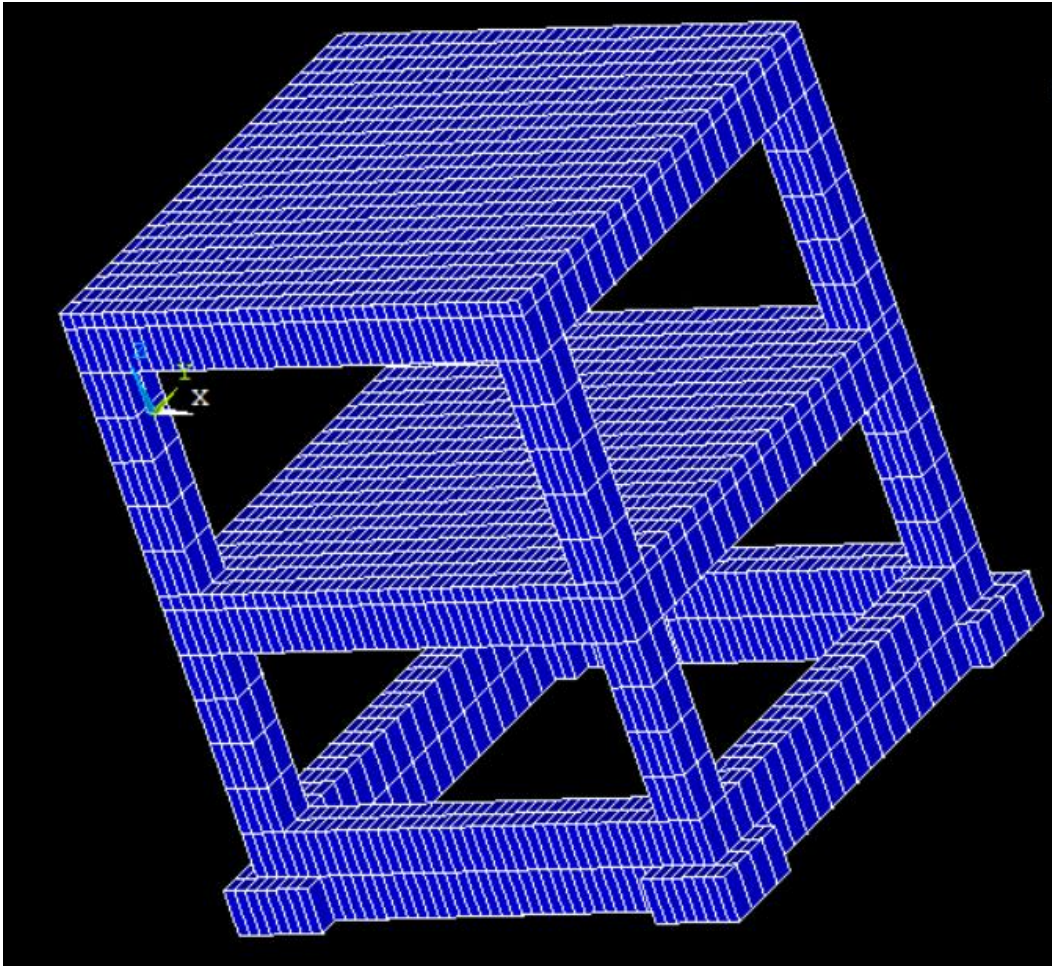
Figure 8:3-D FE model of the building structure

- A two story building structure of height 8.2 meters with 7.2 m x 7.2 m length and width is made of concrete. The FE model of this structure is built using 8 node brick elements with three translational degrees of freedom at each of its nodes.

- To ensure that the model is realistic; the span of beams, height of columns and dimensions of slabs constructed at each level meet the structural design norms of an actual building.
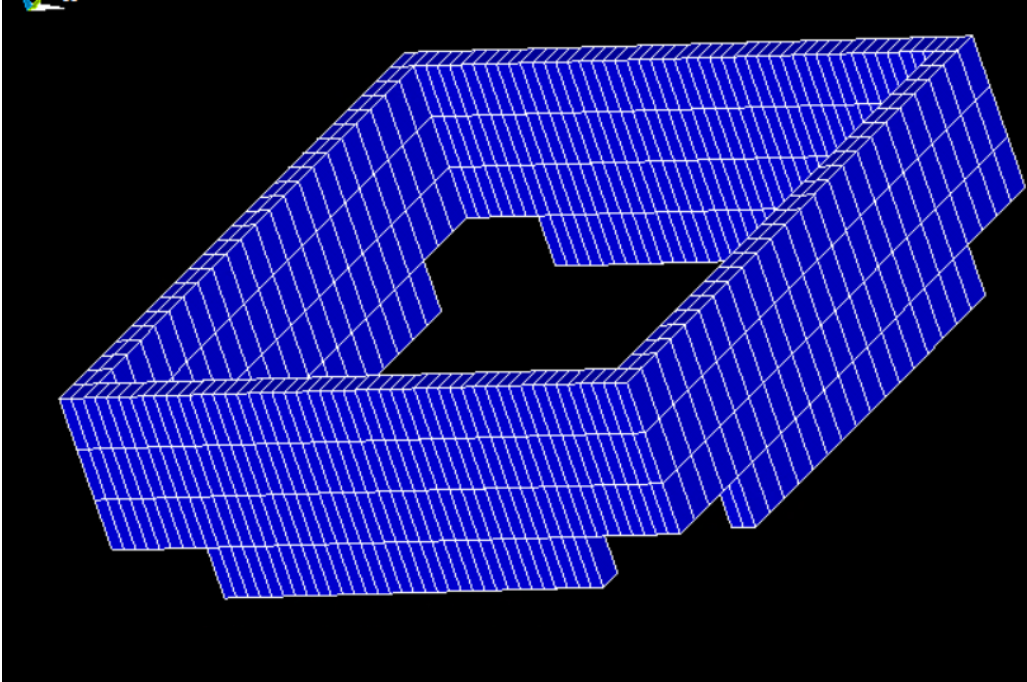
Figure 9:FE model of Foundation wall of the building made up of concrete
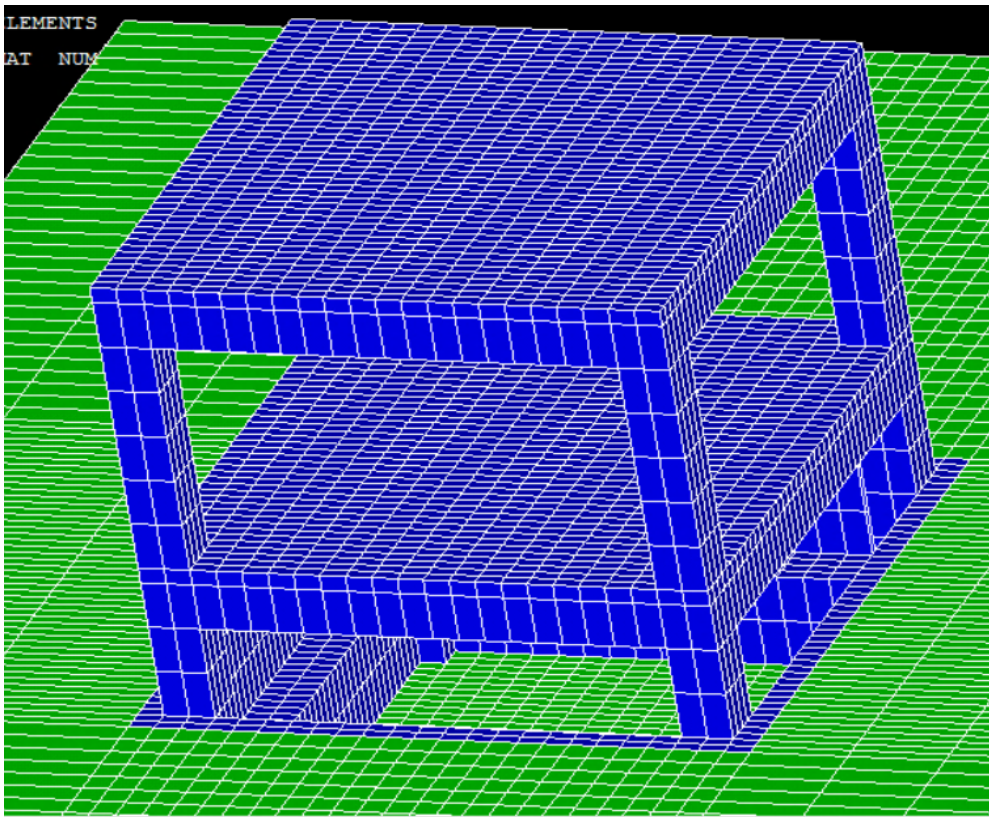
Figure 10:3-D FE model of the building structure with the foundation and subgrade surrounding it

- Also to ensure stability of the building, it has a foundation of 2.4 meters below the substructure level firmly standing on four 1.2 x 1.2 x 1.2 meter high flexible footings forming the base of this building.

- The foundation has concrete wall of 2.4 meters surrounding its basement level from all the four directions which helps to keep the soil in place around the building.

- Also, it is made sure that each co-incident node at the connection of two adjacent elements is merged to maintain connectivity and continuity.

CHAPTER 3

MODAL ANALYSIS

The modal superposition method is basically a technique for linear dynamic analysis that calculates and superimposes individual vibration mode shapes of a model to calculate the displacement in time history. Its main purpose is to reduce the computational cost of a simulation by finding shapes and frequencies at which the structure will naturally vibrate when there is a loading effect. By knowing the fundamental frequencies of a system after performing modal analysis, it gives an understanding of how to approach the designing phase of a system since exciting the geometry at its fundamental frequency can cause resonance which may lead to structural damage to the system.

The mode shapes indicate the configurations in which the body vibrates naturally. For rail vibrations in buildings, the principal interest is the lateral displacement pattern. Usually a small number of mode shapes of the lower order frequencies dominate the motion. Hence, it is possible to ignore many of the higher modes, which are generally less accurate in numerical models anyway. Selecting the important modes saves both memory and simulation time.

In our model of the three-dimensional railroad structure, we perform modal analysis to generate the mode shapes from the eigenvectors after calculating the eigenvalues, which represent the squares of the fundamental frequencies.
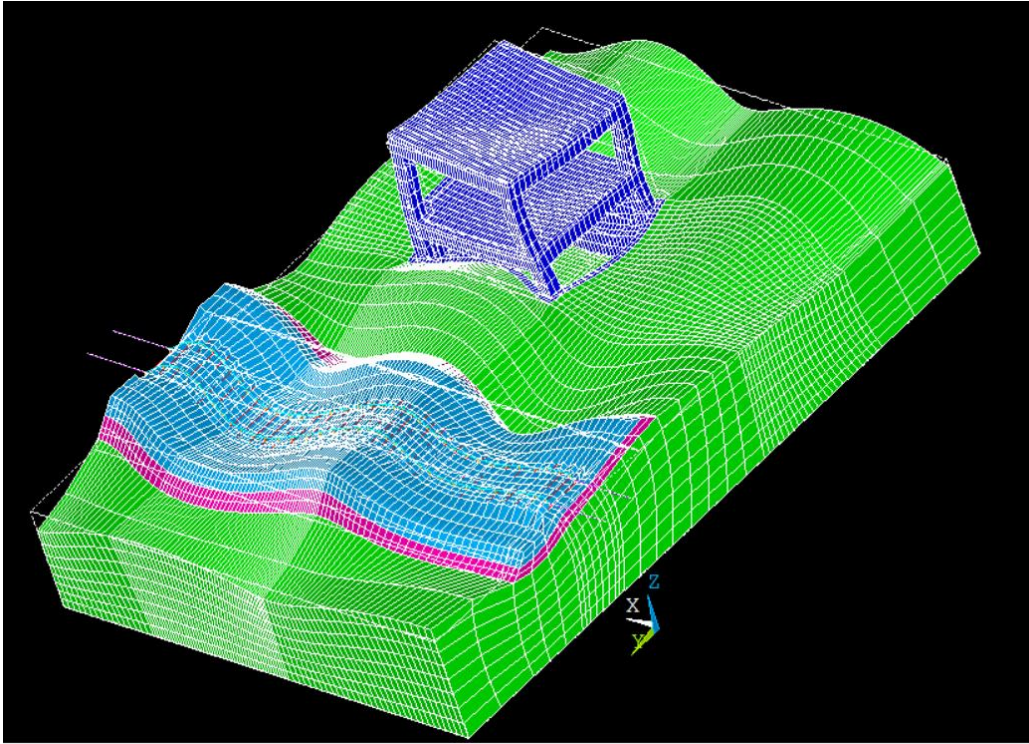
Figure 11:A deformed shape of a lower mode at frequency of 22 Hz
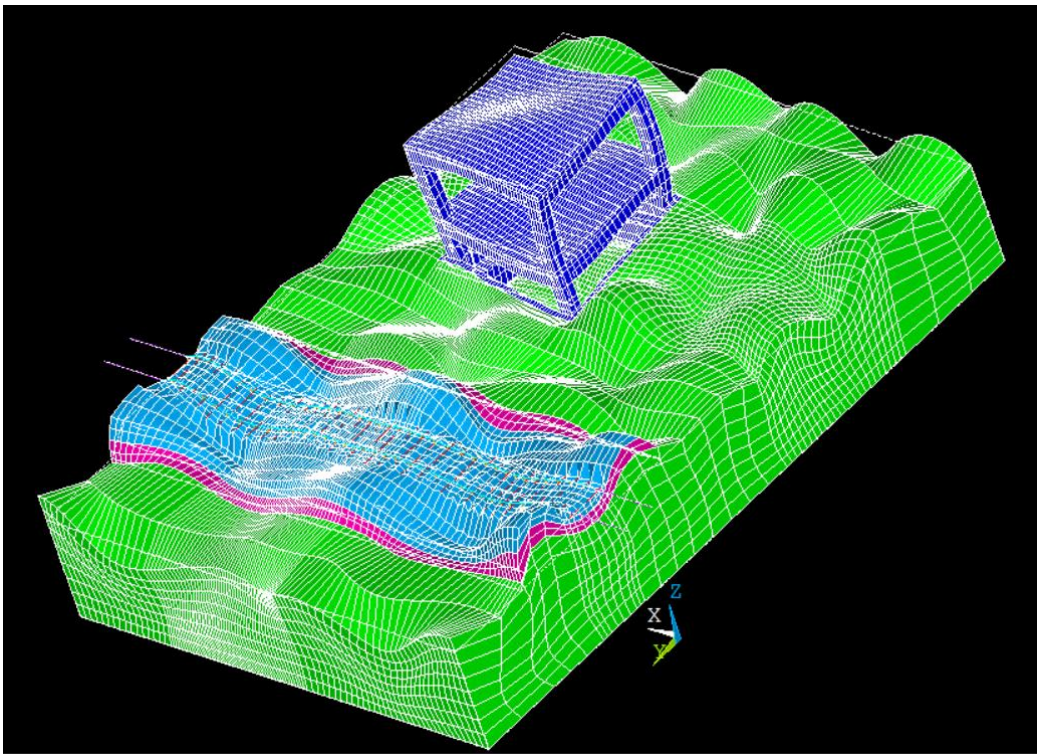
Figure 12:A deformed shape of a lower mode at frequency of 45 Hz

The modal mass matrix and the stiffness values are extracted when we run the modal analysis for the entire model. Before running the multibody dynamic analysis in the time domain, this information taken from the modal analysis is then used as input parameters. It is used to simulate the interaction between the rail and the wheel further.

Further investigating rail induced vibrations, research done by El Ghandour et.al (21) clearly shows that the number of mode shapes that needs to be extracted has to be comparatively large in order to derive accurate results. A large number of modes is necessary when there is a concentrated load and when this load is moving, the effect is compounded. El Ghandour et al.(21) demonstrated in their research that convergence in vertical displacement in the middle flexible section of the rail is achieved at approximately 300 modes and since the difference in the displacement at 300 and 350 modes was only 0.24%, we have extracted 300 modes for our problem. While extracting the modes, it ensured that all mode shapes covered deformation in all directions, as well as torsional motion was considered. The frequency range for the extracted modes in our example is between 9.56 Hz and 57.87 Hz.

Of all mode extraction methods that are normally used in modal analysis, here we have adopted Block Lanczos method in the finite element package since it is recommended to be used for solid elements since it is more computationally efficient. Block Lanczos method is powerful when it searches for Eigen-frequencies in a given part of eigenvalue spectrum. Also, the convergence rate of Eigen-frequencies is same while extracting lower end modes, mid-range modes and higher end modes.

3.1 <u>PreSAMS</u>

The modal analysis data extracted from finite element software ANSYS, which needs to be fed to the multibody dynamic code to perform the simulation in SAMS (Simulation of Articulated Mechanical System Software), has to be altered according to the input format that is accepted by it. This information is first read by the pre-processing code PreSAMS to feed the nodal mass into the multibody dynamics code as an input file. In the next step, the degrees of freedom that are associated directly with the rail geometry only are considered and rest of them are eliminated by a nodal elimination technique which is performed in script. The part of these matrices that form the modal mass of only the rail nodes are extracted separately and given as main input to the multibody dynamics code. The modal mass and stiffness is reformatted into a file in the input format required by SAMS.

CHAPTER 4

MULTIBODY DYNAMICS MODEL

Multibody dynamics is a method of numerical simulation that considers the interaction among connected rigid and flexible bodies. The study of multibody dynamics helps to build numerical models of the connections between the bodies using force elements such as spring dampers as well as kinematic constraints such as various types of joints depending on the constraints put in the degree of freedoms.

In our research, once the modal analysis is performed in the finite element software, the modal information including the mode shapes and natural frequencies are used as input to the multibody dynamics code. Then the dynamic analysis for the rail-wheel interaction in the time domain is run to find the wheelset displacement, wheel-rail contact forces and the modal displacements for the rail system. To determine the displacement of the bodies over the rail substructure in this research, we use the floating frame of reference technique. This technique was adopted by El-Ghandour et al.(21) and Recuero et al. as well in their research to examine the performance of rail and wheel interaction, though Recuero used a simplified spring-damper model for the substructure.

4.1 Floating frame of reference

The floating frame of reference (FFR) technique is a finite element formulation method that utilizes non-isoparametric elements to describe rigid body motion and small deformation of a system. It is important that the element shape functions used in floating frame of reference finite element formulation method express arbitrary rigid body translations and rotations in all directions.

This condition is favorably met by most of the non iso-parametric finite elements that employ infinitesimal rotations as nodal coordinates. As shown in Figure (14), Vlasenko and Kasper (22) explained how floating frame of reference is used to obtain the relative motion of the system of the elastic coordinates with respect to the reference coordinates. The floating frame of reference takes into account the flexibility of the bodies and associates it with the equations of motion.

Within FFR formulation, it is possible to reduce number of degrees of freedom in individual bodies using modal analysis. This approach effectively reduces the body to a set of desired mode shapes with many fewer degrees of freedom. The deformation of the flexible bodies in the multibody system can then be easily determined using this reduced model. This technique is suitable for small deformations as in case of deformation of the rail but its application to large relative rotations between separate bodies is permissible. In case of large deformations, FFR can result in large numerical error.In that case, a different approach called the Absolute Nodal Co-ordinate Formulation (ANCF) can be employed. With regards to the current problem of interest, the floating frame of reference formulation can be used since the deformations are small and hence we can get proper results. Hence, FFR is applied here in our system to model rail flexibility. This approach has been verified by Rathore (23) in his work. He also showed that for the determining the creepages, contact points and the normal forces that are applied, deformations of the rail can be taken into account in FFR.

The elements are considered as a part of the rigid and flexible body system. The motion of the component, for example the suspended wheelset, is described with respect to the absolute fixed frame of reference. Each of the rails is defined by two interconnected models, the geometric model and the finite element model. The surface of the rail, which must be modeled accurately to determine the contact of the wheel and the rail in the time domain is detailed by the geometric

model whereas the elastic properties in the materials used in the system are handled by the finite element model.
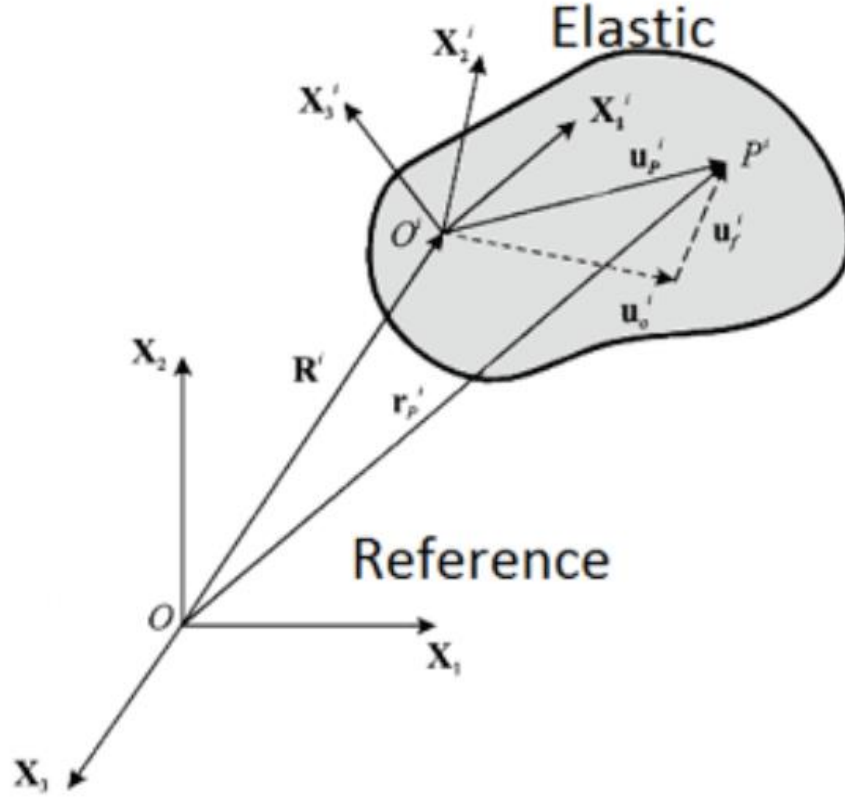
Figure 13:Representation of a deforming body in reference frame.

The point on the rail in the geometric model is defined by the equation:

$$r^r = R^i + A^r (\overline{R}^{ip} + A^{ip}\overline{\overline{u}}^{ip})$$

where r^r is defined by an arbitrary point on the surface of the rail. R^i describes the location of the coordinate system of the rail track with respect to the global coordinate system.

$\overline{R}^{ip}$ defines the position of the coordinate system of the rail profile with respect to the track's

coordinate system. A^{ip} defines the orientation of the rail profile coordinate system with respect to

the track's coordinate system. $\overline{\overline{u}}^{ip}$ is the position of the point on the rail surface in the frame of

reference of the rail. $\overline{\overline{u}}^{ip}$ is defined by a point traced on the profile curve swept along the rail space

curve to describe the contact surface. This equation used by Rathore et al.(23) to demonstrate

floating frame of reference was earlier derived by Shabana (24).
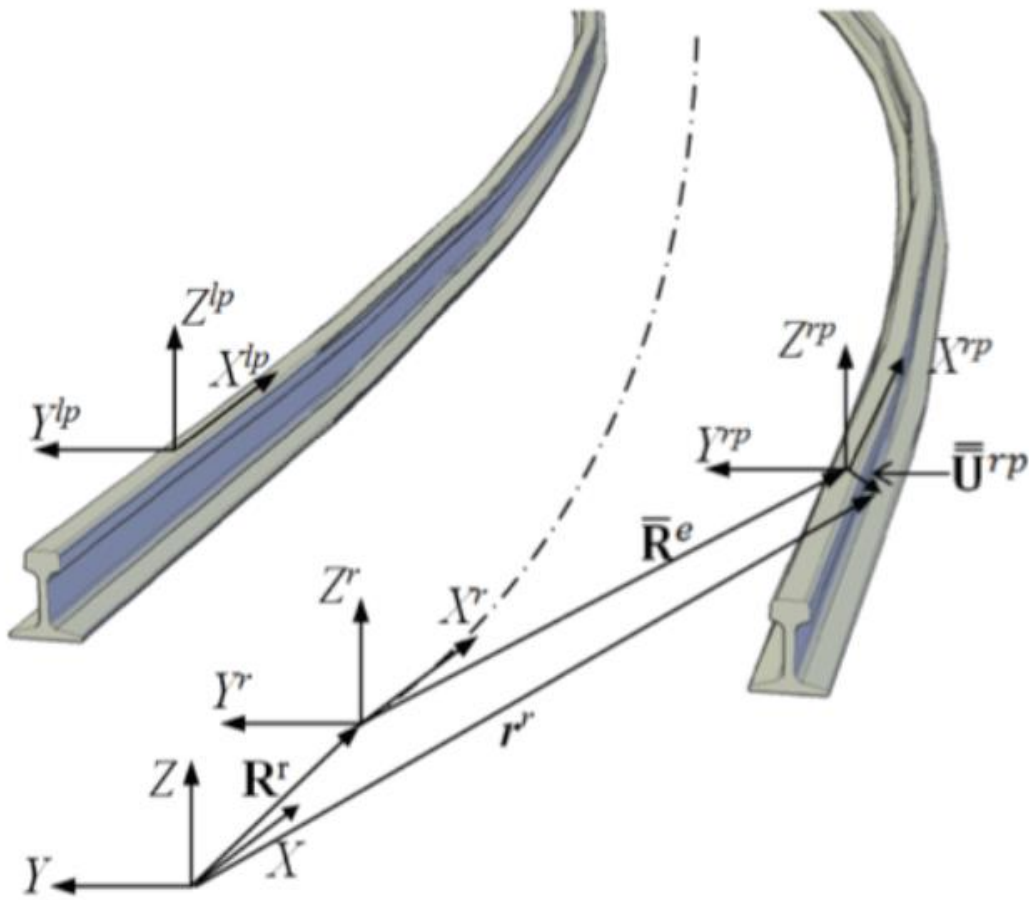
Figure 14:Floating frame of reference of the rail and track geometry

As described in Shabana (24), the rail space curve is defined by the modal positioning principle using Absolute Nodal Coordinate Formulation (ANCF) technique. The position of the point on the 3D beam element can be represented by the following equation:

$$\overline{R}^{ip}\left(x^i, y^i, z^i\right) = S(x^i, y^i, z^i)e^i(t)$$

where $\mathbf{S}$ is the shape function matrix for the ANCF 3D beam element given by Shabana (27) and e^i is vector comprising of nodal coordinates which are time dependent. The shape function represent position and the first order spatial derivatives of the rail space curve and the position. x^i, y^i and z^i are the local coordinates that are defined in the ANCF element coordinate system. In order to consider the deformation of the finite element model, e^i should be constantly updated with time. The ANCF element vector's nodal coordinates e^i, are updated from the finite element model using the floating frame reference formulation technique. It is not necessary that the nodes of the finite element model and nodes of the geometric model should coincide as shown in Figure (15).

A point of the FE model of the rail geometry can be represented with the following given equation described by Shabana (24):

$$r^{ij} = R^i + A^i \left(\overline{u}_o^{ij} + \overline{u}_f^{ij}\right) \quad , \qquad j = 1,2,3,4, \dots, n_e$$

where $\mathbf{R}^i$ is the reference point of the track's coordinate system. $\mathbf{A}^i$ represents the track's coordinate system's orientation with respect to the global coordinate system, and n_e represents the number of elements in the FE model of rail i. The position of the point in the reference and deformed configurations are defined by the vectors $\overline{u}_o^{ij}$ and $\overline{u}_f^{ij}$ respectively.

Here, $\overline{\boldsymbol{u}}_o^{ij}$ and $\overline{\boldsymbol{u}}_f^{ij}$ can further be defined by the following expressions:

$$\overline{\boldsymbol{u}}_o^{ij} = \boldsymbol{S}_b^{ij} \boldsymbol{B}_c^{ij} \boldsymbol{e}_{bo}^i \quad , \qquad \overline{\boldsymbol{u}}_f^{ij} = \boldsymbol{S}_b^{ij} \boldsymbol{B}_c^{ij} \boldsymbol{B}_r^i \boldsymbol{B}_m^i \boldsymbol{q}_f^i$$

where $\boldsymbol{S}_b^{ij}$ is the finite element shape function matrix of the element j , $\boldsymbol{B}_c^{ij}$ represents the Boolean element connectivity matrix , $\boldsymbol{B}_r^i$ is the reference condition matrix which defines element displacement field, $\boldsymbol{B}_m^i$ represents the modal matrix extracted from the finite element model which is described by the vibrational modes for the analysis, $\boldsymbol{e}_{bo}^i$ is the finite element coordinates vector in the undeformed configuration, $\boldsymbol{q}_f^i$ describes the elastic degrees of freedom in the equations of motion in the form of a modal displacement vector.
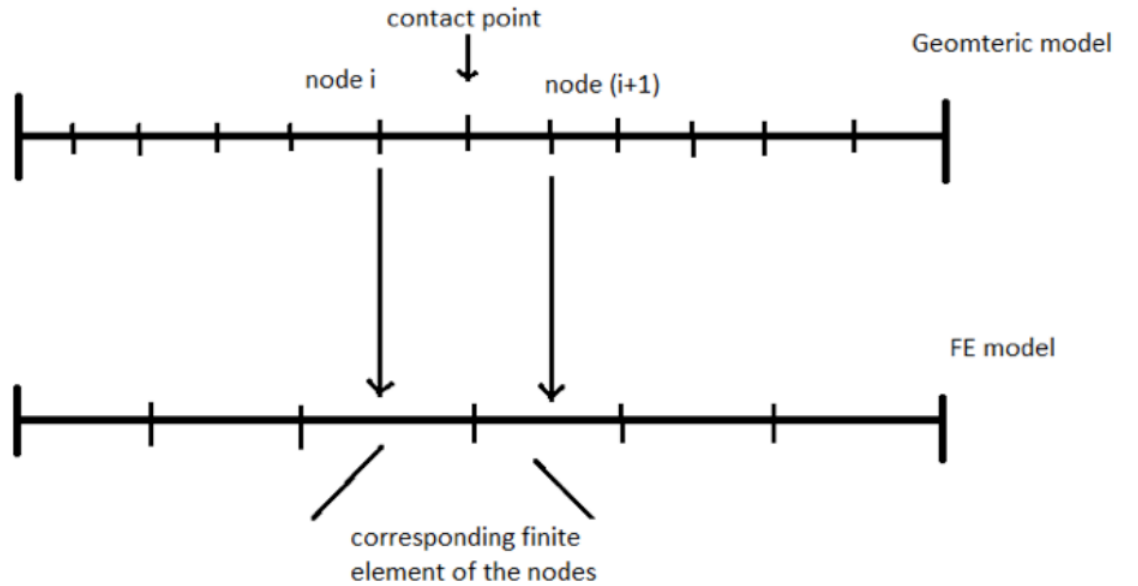
Figure 15:Floating frame of reference of the rail and track geometry

4.2 Contact formulation:

Many simplified techniques have been put forward in numerous research papers to evaluate the contact forces and trace the contact path between two interacting bodies. In their research, Meli and Pugi (25) approximated the contact position by using the linear superposition principle. They used the Elastic Contact Formulation for Algebraic Equations (ECFA) approach given by Shabana et al.(24) to determine the contact point location. This technique allows the wheel to have six degrees of freedom with respect to the rail since it does not treat the governing equations as constraints. Small penetrations and separation between the rail and the wheelset are allowed in this algorithm, which is not exact but can approximate the contact very well. The surface contact is defined in terms of two non-generalized coordinates which are also known as surface parameters. This method of using parameters to locate any point on a contact surface simplifies the problem. The following four equations given by Shabana (15) usually solved iteratively gives the contact point location for a wheel rail pair:

$$E(s) = [t_1^r.r^{wr} \quad t_2^r.r^{wr} \quad t_1^w.n^r \quad t_2^w.n^r]^{\text{T}} = 0$$

Here $E(s)$ represents the contact point location, t_i^j is the tangent vector of surface j with respect to surface parameter i, r^{wr} is the relative position of the contact point on the wheel with respect to the rail and n^r is the normal vector at the point of contact on the rail.

The solution for the equation should be tested for a contact or small separation. This is calculated by determining the value of δ from the equation $\delta = r^{wr}.n^r$, where a positive value indicates separation between the rail and wheel and a negative value means that there is penetration. If the value of δ is negative implying that there is contact between the rail and the wheel, then the normal force is calculated as per the formula $F^N = -K_H \delta^{3/2} - C \dot{\delta} |\delta|$,

where F^N is the normal force, K_H is the Hertzian constant, C is the damping constant and $\dot{\delta}$ is the time derivative of the penetration value. On the basis of Kalker's theory (26), Shabana et al.(15) formulated a procedure to compute dimensions of the Hertzian contact ellipse, tangential and spin creepages and thereby the tangential creep forces and creep spin moment. To take into consideration the rail deformation effect on the determination of the contact point, the element that's in contact has to be determined first and subsequently the rail geometry is updated by an iterative process which is further used in the calculation of the tangential and spin creepages at the corresponding Hertzian contact patch.

4.3 The nodal elimination technique used for coupling:
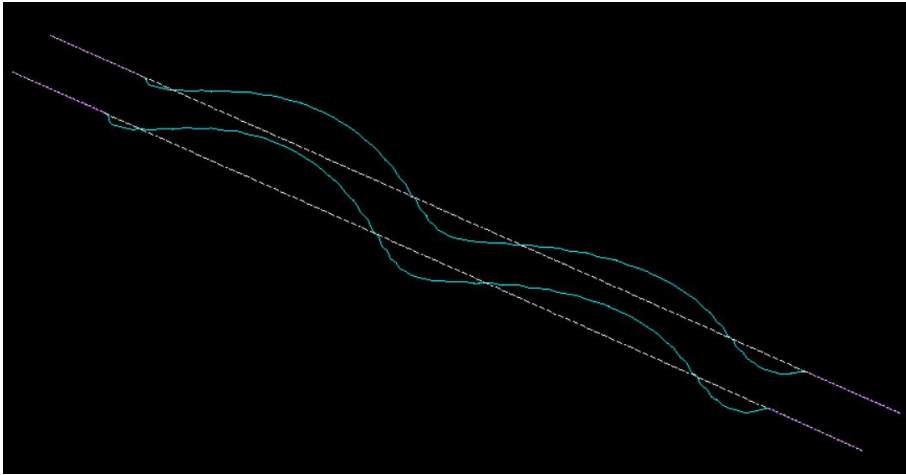
Figure 16:Mode shape of the rail only at a lower frequency of 15 Hz
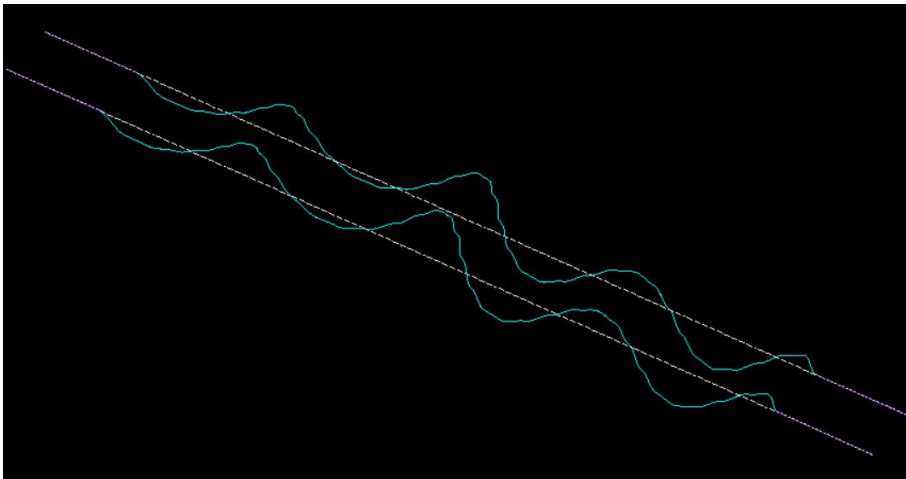
Figure 17:Mode shape of the rail only at a higher frequency of 52 Hz

In this research, after performing the modal analysis for the entire system, a nodal elimination technique was used to further improve the efficiency of the multibody simulation. The nodal elimination technique extracts only the modal information corresponding to the nodes of the

rail. This method helps in reducing the number of degrees of freedom of the model and thereby decrease the size of the matrices input into SAMS. Since only the rail nodes directly come in contact with the surface of the suspended wheelset, the other information is not needed. By using this nodal reduction technique, we can create more complex finite element model with more details and degrees of freedom. It should, of course be ensured that appropriate number of modes are extracted for the system to cover all kinds of expected displacement patterns in the body. In our model, since the load under study is both moving and highly concentrated, 300 mode shapes were extracted to consider for the above mentioned fact. Modal analysis and nodal elimination are very economical when it comes to the computation cost in the linear case.

After nodal elimination technique is performed to shrink the data for entire system down to only the rail nodes, it is used as an input to the software package SAMS to run the dynamic analysis between the articulated systems, which is explained further in the next section.

4.4 <u>Wheel rail interaction in SAMS:</u>

Nowadays, with easy access to fast and high capacity computational power, many analyses of mechanical systems that involve interacting rigid and flexible components rely on multibody dynamics for accurate solutions. A very standard application of a multibody system analysis is dynamics between rail and wheel contact, and SAMS has been developed to evaluate and study this interaction. The model suggested by Kumaran et al.(14) briefly explains how contact forces are generated on the rail due to the moving wheel considering the dynamics of the rail wheel interaction. The multibody code takes into account the time-dependent force conditions, which are applied in the time domain. SAMS calculates these wheel-rail contact forces as well as the modal displacements, velocities and accelerations. The details of the method by which the computation is carried out, is discussed in the following sections.

.   A PreSAMS file is used as an input to SAMS which is generated after performing the nodal elimination of the model. This PreSAMS file contains the data for mode shapes, natural frequencies, modal mass and stiffness of the model is used by SAMS to solve sets of differential and algebraic equations to evaluate the displacements, velocities and accelerations.

The multibody code uses the reduced modal data from PreSAMS and the mechanical properties of the wheelset such as its mass, moments of inertia, the stiffness and the damping coefficient to simulate the interaction.

TABLE II : Mechanical properties of the wheelset used in SAMS.

Description	Value	Unit
Mass	1568	kg
Ixx	656	$kg.m^2$
Iyy	168	$kg.m^2$
Izz	656	$kg.m^2$
$K_{l1}=k_{l2}$	13500	N/m
$K_{t1}=k_{t2}$	25000	N/m
$c_{l1}=c_{l2}$	1000	N.s/m
$c_{t1}=c_{t2}$	0	N.s/m

The analysis is made for an average speed of a train with the wheelset moving at 30 m/s, which is approximately equal to 67 miles per hour. The wheelset models have previously been developed in SAMS.SAMS has two sets of wheelsets developed already: the unsuspended wheelset and the suspended wheelset. The unsuspended wheelset is connected with the rail track geometrically while the suspended wheelset is independent of the finite element model of the rail.
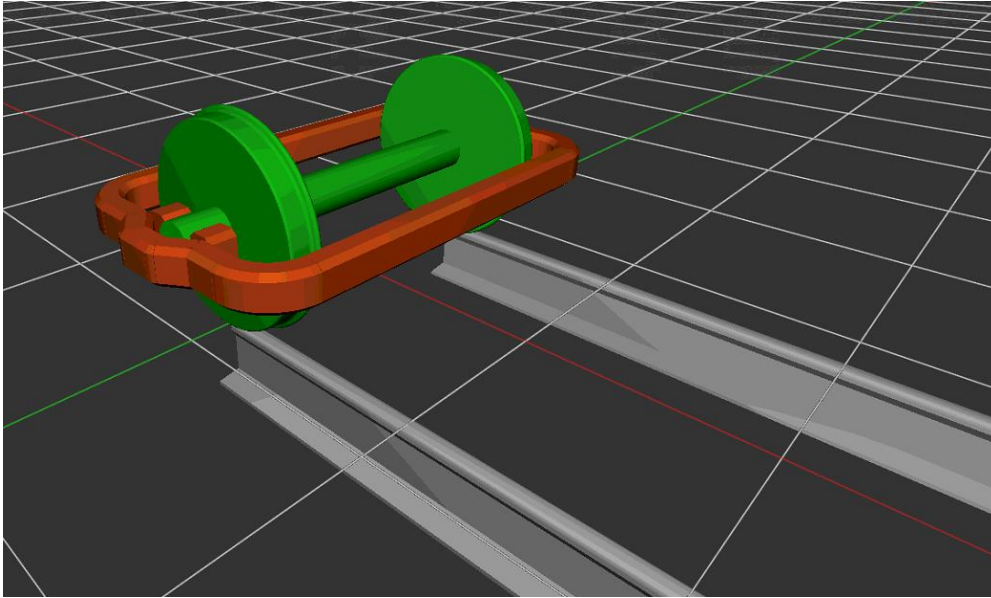
Figure 18:Suspended wheelset model used in SAMS

The suspended wheelset is used for this analysis as shown in the Figure (18). For this suspended wheelset analysis, a SamsdataT.dat file is used as an input, which was extracted from the PreSAMS file as the output. To create the coordinates of geometric nodes for the wheelset, the multibody code uses the coordinates of the nodes from the actual finite element model of the rail.

The stiffness and the mass matrix data of the sleepers, ballast, substructure and the building structure are linked to the nodes of the rails through the mode shapes and hence in the multibody analysis, but only the rail nodes are needed to study the dynamics of wheel-rail interaction.

4.5 <u>Multibody system code using SAMS (Simulation of articulated mechanical systems):</u>

The mathematical formulation derived by Shabana (15) that determines the relation between the modal forces and the nodal contact forces is solved by SAMS:

$$(\boldsymbol{Q}_e)_f = \Psi\,(i)^t \boldsymbol{f}$$

where $\boldsymbol{f}$ is the nodal force which is applied on the rail nodes, $\Psi\,(i)^t$ is the i ᵗʰ generalized eigenvector which is extracted from the finite element model, and $(\boldsymbol{Q}_e)_f$ is modal force which has to be calculated.

The nodal force applied on the nodes is represented as a vector form given below:

$$\boldsymbol{f} = \left\{ \begin{matrix} \boldsymbol{f}_r \\ \boldsymbol{f}_o \end{matrix} \right\}$$

where force on the nodes that are not on the rail and are not considered for the simulation and eliminated are represented as $\boldsymbol{f}_o$ and the force on the nodes that are a part of the rail and considered for the multibody analysis is represented by $\boldsymbol{f}_r$. Since in this scenario, the forces on the nodes that are not on the rail are zero, it is ignored and only $\boldsymbol{f}_r$ is used for further computation. Thus, the equation is simplified to:

$$(\boldsymbol{Q}_e)_f = \Psi_r\,(i)^t \boldsymbol{f}_r\,,$$

where $\Psi_r\,(i)$ is the eigenvector reduced down to only the rail nodes. After computing the modal forces, the next step is the calculation of the modal displacements, modal velocities and the modal accelerations by solving equations of motion, which are discussed next.

4.6 Equations of motion:

The augmented form of the multibody equations derived by Shabana et al.(15) are used in this research. Differential and non-linear algebraic constraint equations are simultaneously solved in this augmented method to find the solutions for the equations of motion. This augmented equation is given as:

$$\begin{bmatrix} m_{rr} & m_{rf} \\ m_{fr} & m_{ff} \end{bmatrix} \begin{bmatrix} \ddot{q}_r \\ \ddot{q}_f \end{bmatrix} = \begin{bmatrix} (Q_e)_r \\ (Q_e)_f \end{bmatrix} + \begin{bmatrix} (Q_v)_r \\ (Q_v)_f \end{bmatrix} - \begin{bmatrix} C_{q_r}^T \\ C_{q_f}^T \end{bmatrix} \lambda - \begin{bmatrix} 0 \\ K_{ff}q_f \end{bmatrix}$$

where m_{rr} is the inertia matrix for reference coordinates, m_{rf} and m_{fr} are the inertia matrices that dynamically couple elastic and reference coordinates, q_f is the elastic modal coordinates vector that represents track and substructure flexibility in the floating frame reference formulation while q_r is the rigid body coordinates vector. $(Q_e)_r$ and $(Q_e)_f$ are the generalized external forces vectors in the rigid and elastic coordinates respectively, $(Q_v)_r$ and $(Q_v)_f$ represent the quadratic velocity inertia forces vector in rigid and elastic coordinates respectively, C_{q_r} and C_{q_f} are the Jacobian matrices as a result of the constraints for the rigid and elastic coordinates respectively, K_{ff} is the stiffness matrix of the rail track and λ is the vector of Lagrange multipliers.

Lagrange multipliers and generalized accelerations are calculated by solving the equations of motion and then using the explicit Adams Bashforth predictor-corrector numerical integration technique as discussed by Shampine and Gordon(28), Independent velocities and the coordinates are determined. The dependent velocities and coordinates are thereafter calculated afterward for the subsequent time step of the equation, and this computation is continued until the final time step is reached. A sparse matrix solver is used in multibody system to solve for reference and elastic accelerations to improve simulation speeds.

CHAPTER 5

RECONSTRUCTION OF RESULTS

El-Ghandour et al (21) in their research created a practical model of the substructure but it focused more on the effect of interaction between rail and the wheel. The increase in level of contact force and the rate of increase in rail surface wear was analyzed but substructure behavior was never fully studied. Here, by reconstructing the nodal displacements from the modal data, we are studying the response of the entire substructure as well as the discomfort that is being caused to the occupants due to the impact of the pressure and longitudinal waves on the building. The parameter that we are focusing on is acceleration at various sections of the building structure such as the flexible footing and different levels of columns and slabs.

After running the multibody simulation in SAMS (Simulation of Articulated Mechanical System) for the moving suspended wheelset on the rail, the time dependent outputs obtained are modal displacements, modal velocities and modal accelerations. In this research, the parameters of interest are displacements and accelerations in particular, in the building. Since the mode shapes and natural frequencies are already extracted from the modal analysis performed earlier, this information along with the modal displacements and modal acceleration given by SAMS as output is sufficient to derive the nodal displacements along with nodal accelerations and reconstruct it over rest of the model including the ballast, subballast, subgrade and the building structure on which we are focusing.

The equation that helps us derive nodal displacements and nodal accelerations is derived by Shabana et al. and is given as:

$$\boldsymbol{U}_f = \Psi(i)^t \, \boldsymbol{q}_f$$

$$\ddot{\boldsymbol{U}}_f = \Psi(i)^t \ddot{\boldsymbol{q}}_f$$

where $\Psi(i)^t$ is the matrix for the 300 mode shapes of the whole structure that were extracted during modal analysis, $\boldsymbol{q}_f$ and $\ddot{\boldsymbol{q}}_f$ are the modal displacement and modal acceleration vectors obtained from the MBS code as output and $\boldsymbol{U}_f$ and $\ddot{\boldsymbol{U}}_f$ are the nodal displacement and nodal acceleration vectors of the whole structure.

The computation of these nodal displacements and acceleration from their respective modal parameters extracted from the multibody code is performed in MATLAB and then, using ANSYS APDL, it is reconstructed over each and every node of the model.

Once the displacements are calculated, the elastic stress and strain values can be determined. With the nodal velocities, damping stresses may also be calculated. While not the focus of this study, these quantities may be important for other studies.

CHAPTER 6

RESULTS

6.1 Numerical example

The numerical model used in this research is a three dimensional system of rail, sleepers, fasteners, ballast, sub-ballast and sub-structure. El-Ghandour et al. (21) used a similar model in their research. The schematic diagram below represents the levels of different layers of the substructure. In our model, the subgrade is extended to the area surrounding in nearby building.
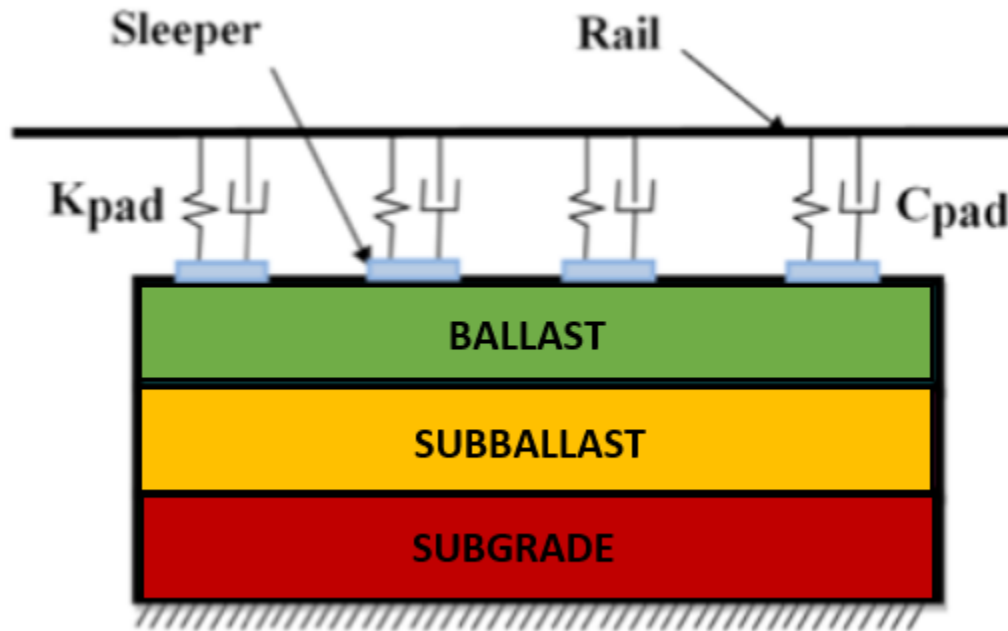
Figure 19:Schematic diagram of the finite element model representing the layers of the substructure. K_{pad} and C_{pad} are the stiffness and damping, respectively, taken from the fastener and pad assembly.

6.2 Contact forces
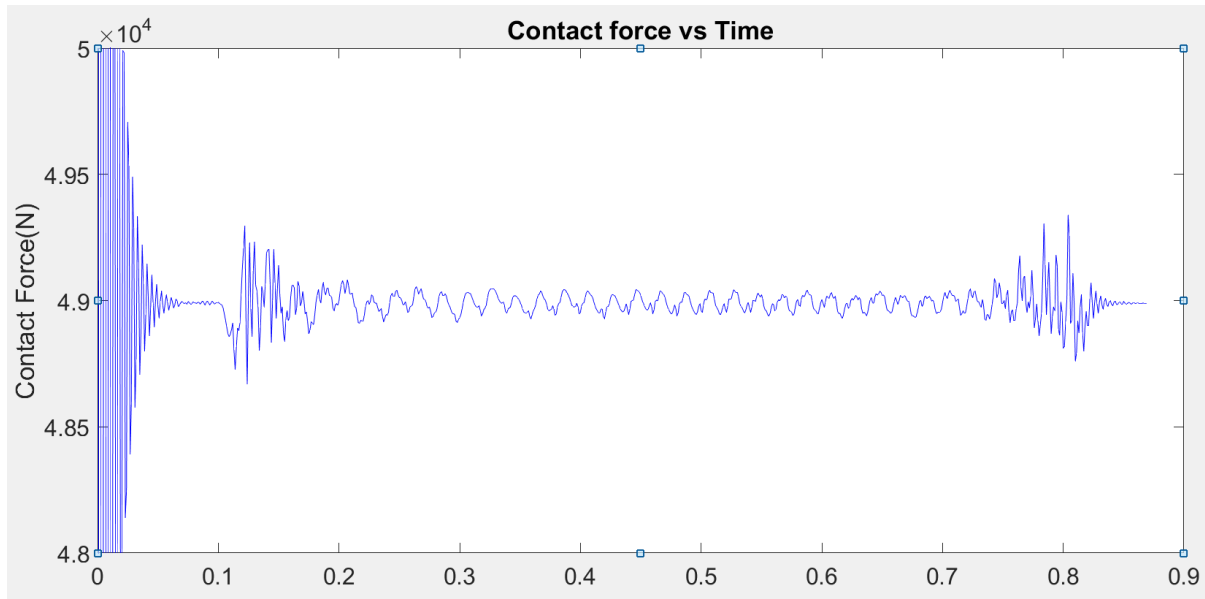
Figure 20:Contact forces on the rail nodes due to the moving wheelset

The contact forces that are applied on the rail by the suspended wheelset are shown in the

figure (20). These forces agree well with the ones examined in El-Ghandour et.al (21).

6.3 Displacement, Stress and strain in the substructure and building:
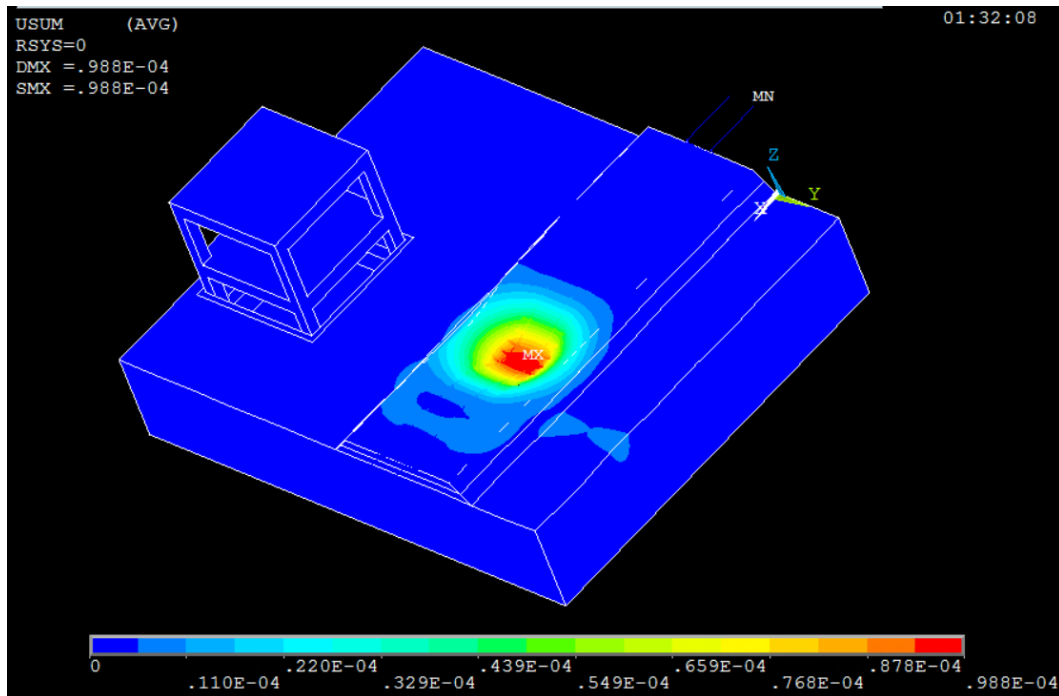
Figure 21:Displacement magnitude at the ballast and the subballast at time t = 0.54 s from the start of the wheel-rail contact.
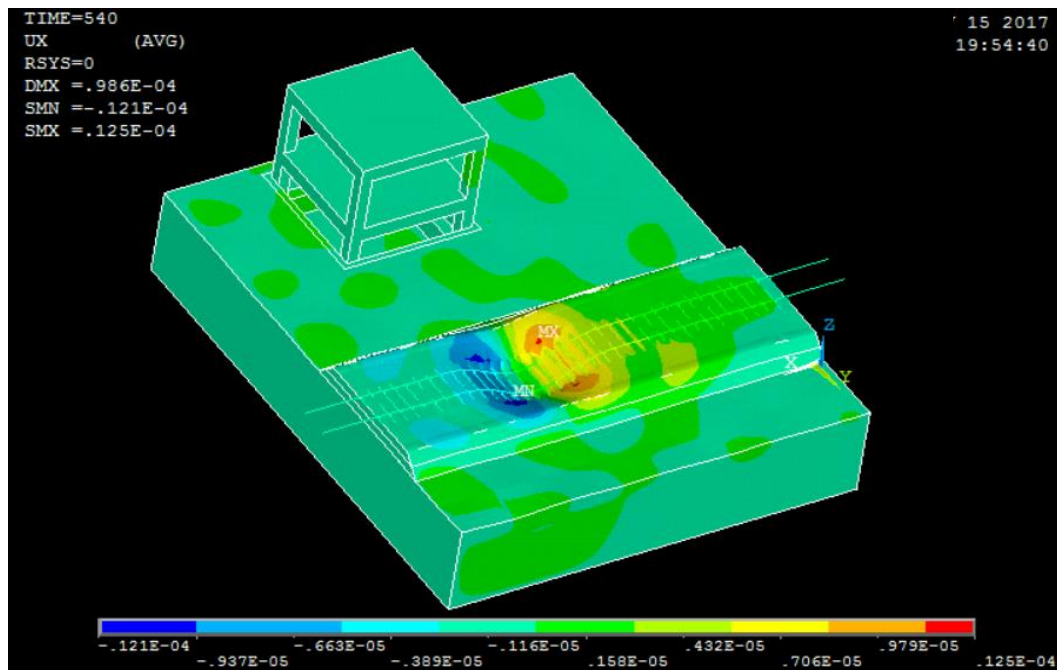
Figure 22:X-Displacement at the ballast and the subballast at time t = 0.54 s from the start of the wheel-rail contact.

Figure 23:Y-Displacement at the ballast and the subballast at time t = 0.54 s from the start of the wheel-rail contact.

Figure 24:Z-Displacement at the ballast and the subballast at time t = 0.54 s from the start of the wheel-rail contact.
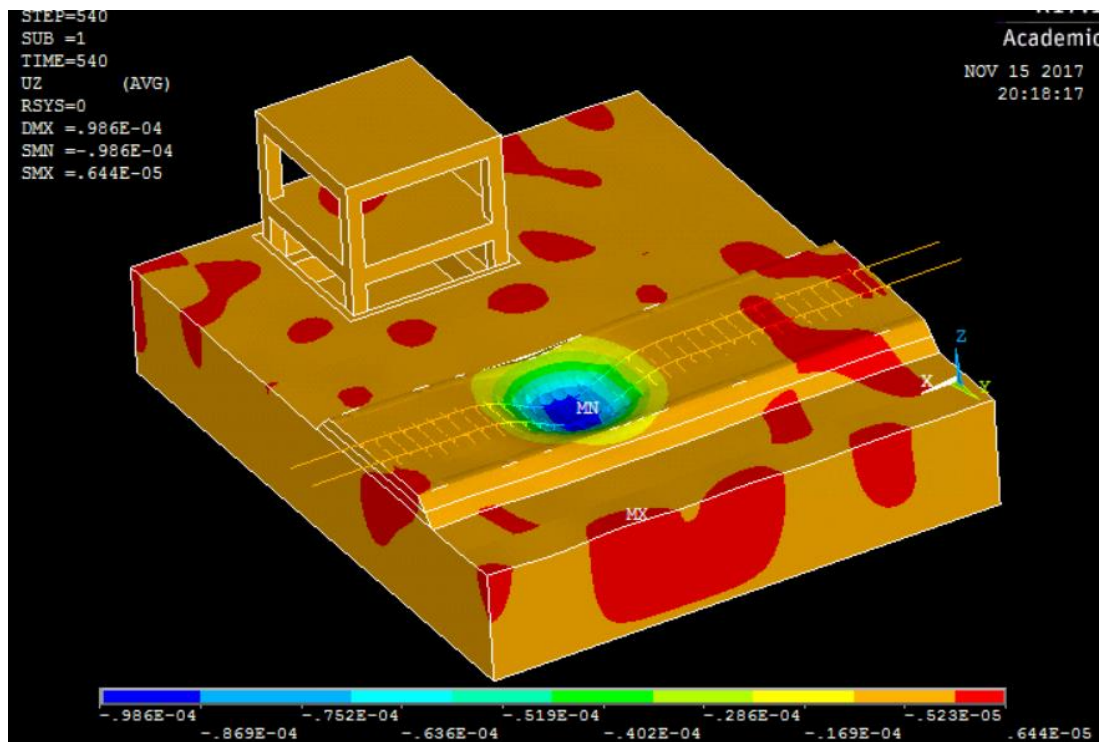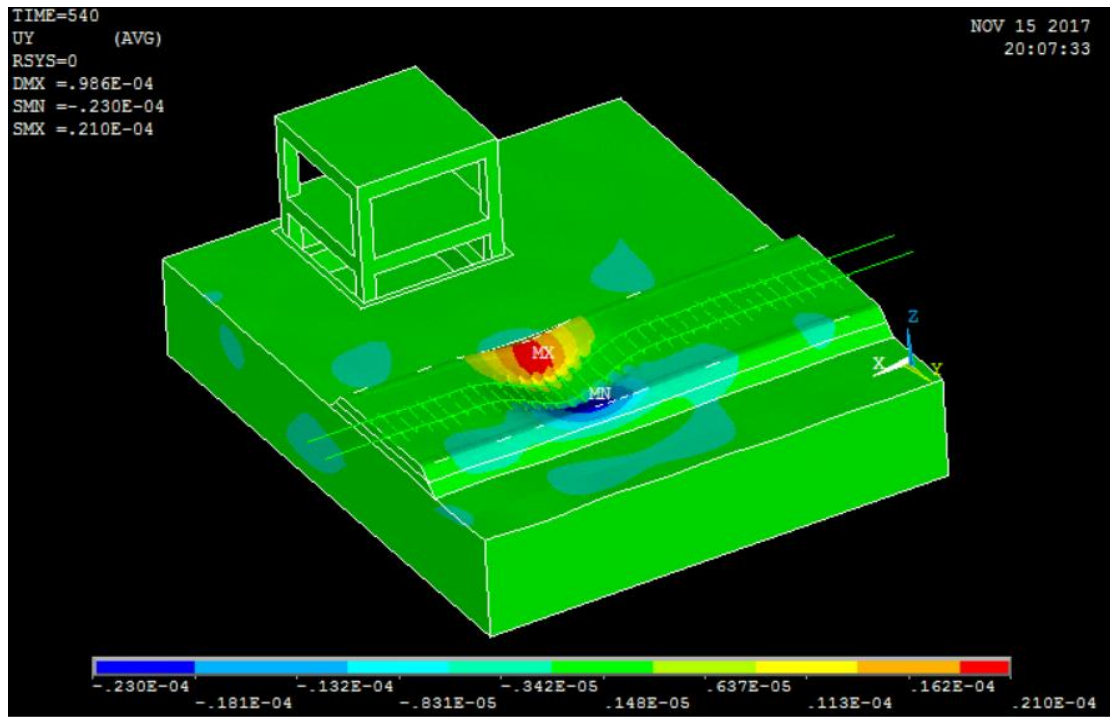
The reconstructed values of total nodal deformation are shown in Figure (21), while the X, Y and Z displacements are shown in Figures (22),(23) and (24) respectively. At this particular time step for which the nodal displacement contour is being plotted on ANSYS, the train is in line with the building structure. It is observed that the maximum displacement is experienced at the ballast due to the effect of moving contact forces on the rail and the sleepers. The weight of the moving suspended wheelset causes maximum vertical deflection as it moves over the rail in the region near the ballast and subballast. The rail and ballast are observed to experience comparatively larger displacement as compared to the building structure as the forces are more concentrated here. The maximum longitudinal displacement at the building is 0.528×10^{-5} m while the transverse displacement is 0.283×10^{-5} m. It is also observed, however small the displacement values are, that they are greater in the longitudinal direction at the building structure than in the transverse directions and the vibrations are transmitted through the substructure to the building.
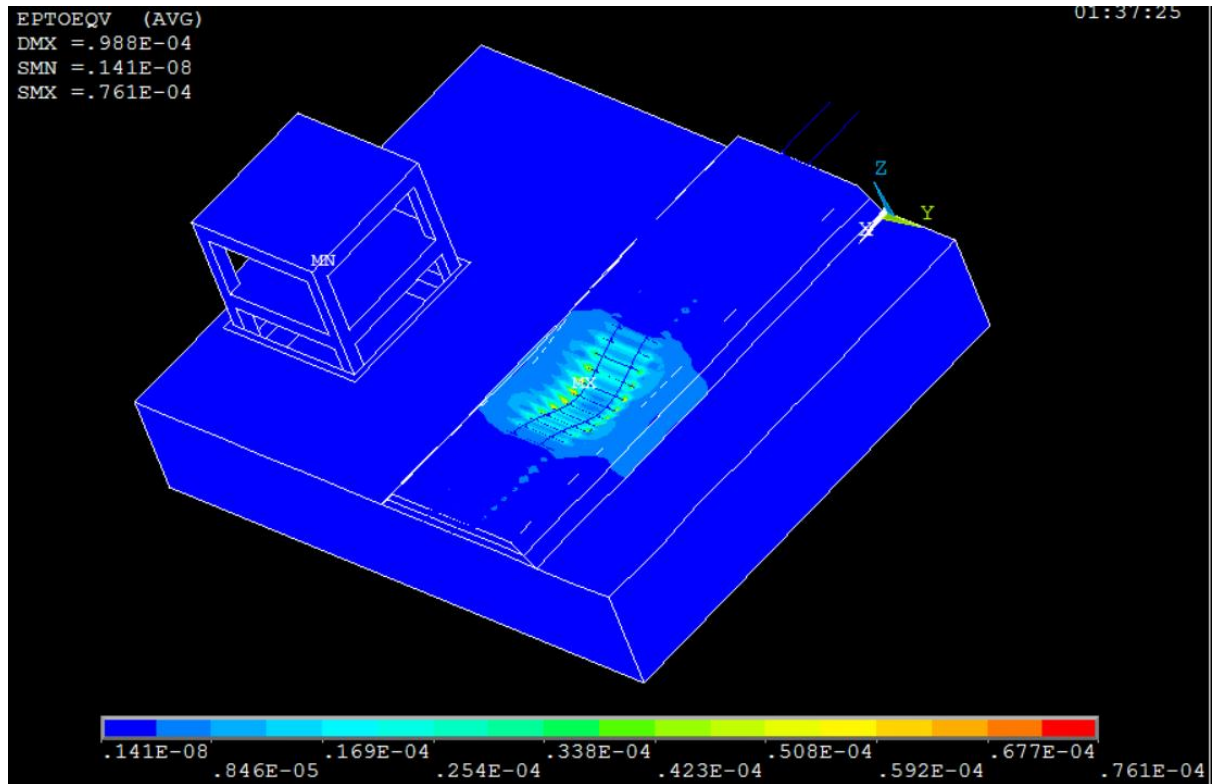
Figure 25:Equivalent strain at the ballast and the subballast at time t =0.54 s from the start of the wheel-rail contact.

The equivalent strain of the substructure is shown in Figure (25). It is noticed that the equivalent strain values are found to be larger near the ballast and the subballast layers and then it eases off further down the substructure. This was expected since there is not much displacement found in the substructure nor the building. The strain concentration near the ballast can be interpreted as a result of more concentrated forces.
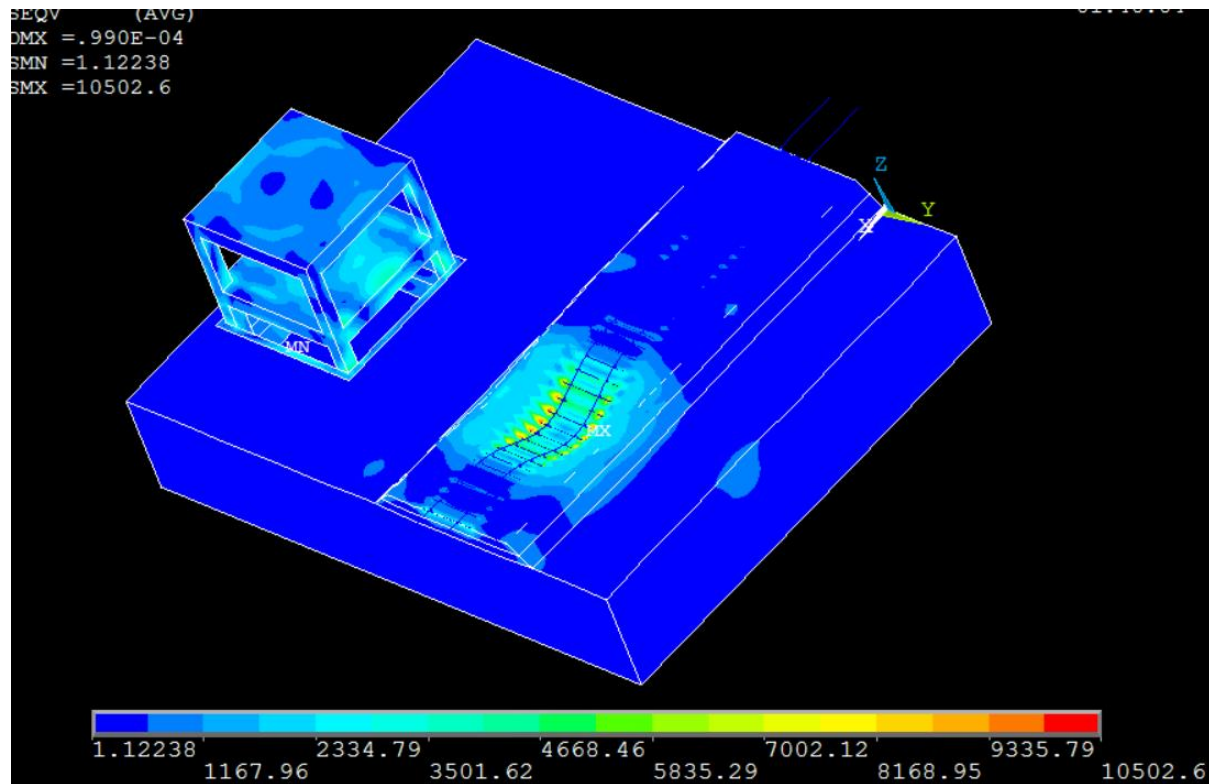
Figure 26: vonMises stress observed at the ballast, subballast and the building structure at time   t=0.61 seconds from the start of the wheel-rail contact.

The sleeper and the ballast experience greater von Mises stress since the deformations are larger due to the direct impact of the moving load. When it comes to the building, it is observed that the basement wall, flexible footing and the level 1 column are subjected to larger von Mises stress in the range of 3580 to 4170 N/m^2 as compared to stresses experienced at top level of the building which are in the range of 30 to 920 N/m^2. This means that the basement wall along with flexible footing and bottom column are susceptible to greater structural damage as compared to the higher level columns and slabs due to fatigue caused by constant vibrations.

6.4 <u>Displacement at the building over the time domain:</u>
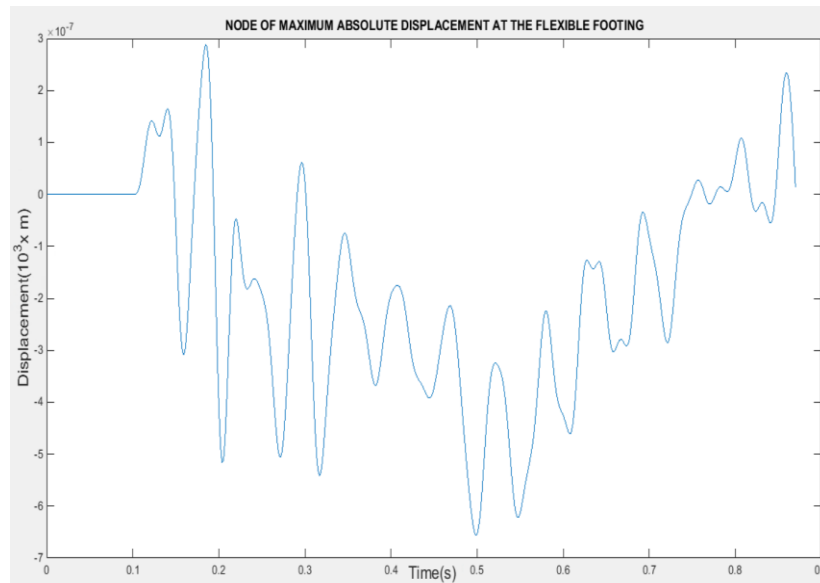
Figure 27:Displacement vs time plot at a node of flexible footing in the building
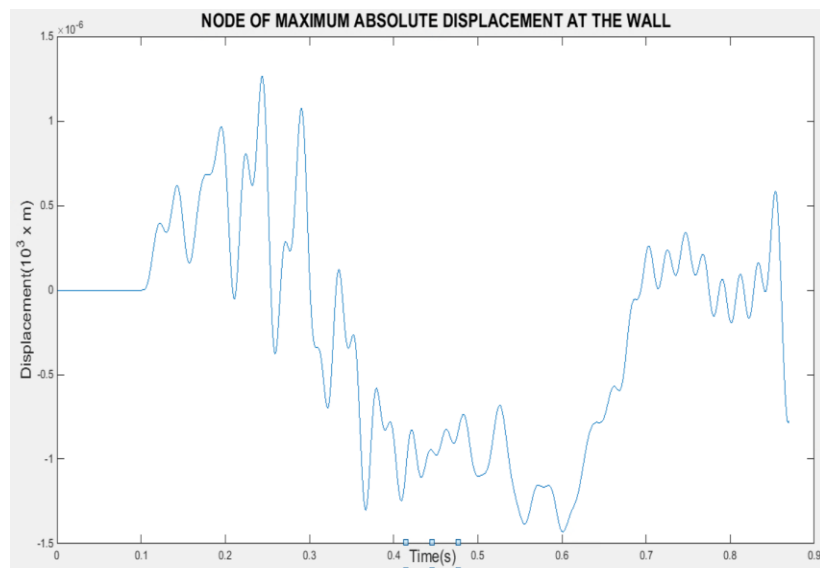
Figure 28:Displacement vs time plot at a node of the basement wall in the building

The displacement vs time plots shown in Figure (27) and (28) represent the total horizontal displacement at the flexible footing of the building structure. It is observed that as the train is in

line with the building structure the displacement increases. In the displacement vs time plot, the train approaches the building at time t=0.54 seconds and is it clearly seen in the plot that the amplitude reaches its peak value between time 0.5 and 0.55 seconds. These graphs were plotted in MATLAB and the displacement contours are reconstructed in ANSYS after calculation nodal displacements in MATLAB. Poisson effects create an elastic displacement as the train passes with the superimposed vibrational motion.

6.5 Vibration Quantification at the building structure:

Nodal displacements are derived from modal displacements in MATLAB by using the formulation given earlier. In a similar way, nodal accelerations can also be calculated from the available modal acceleration data from SAMS. These nodal acceleration values are then sorted in MATLAB and analyzed to determine maximum accelerations for the different parts of the building at different locations for the entire time domain of simulation.

Since acceleration is the most important parameter when it comes to studying the occupant discomfort and structural damage caused to the building, we need to analyze the acceleration plots when the train is approaching the building or when it is in line with the building on the rail track.
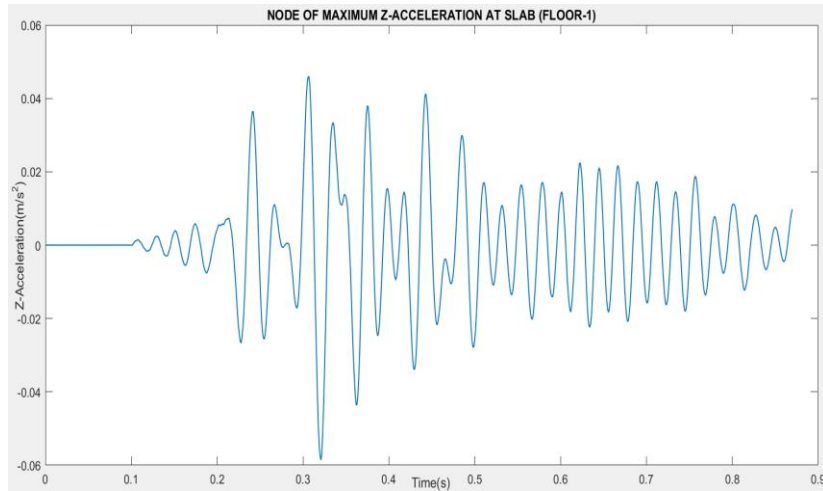
Figure 29:Z-Acceleration vs time graph at a node on slab level-1
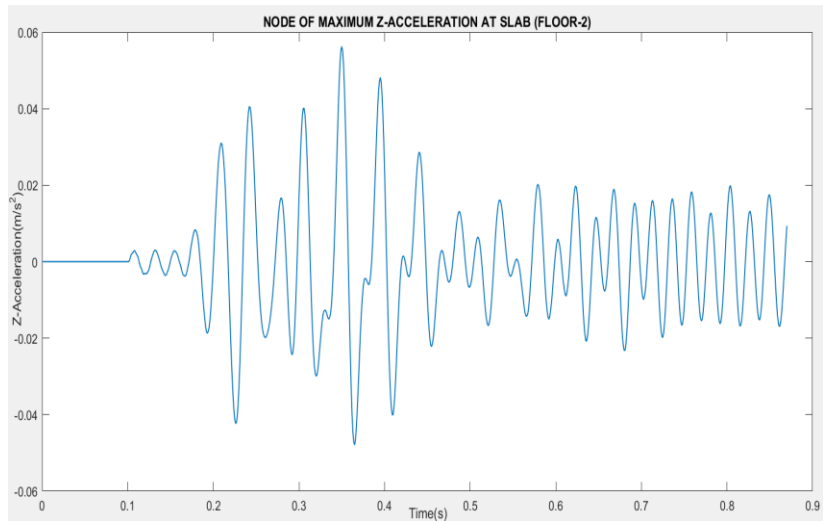
Figure 30:Z-Acceleration vs time graph at a node on slab level- 2

Maximum Z-acceleration (vertical acceleration) at a node on level 1 slab is 0.06 m/s^2 at a time step between 0.3 and 0.4 seconds when the train is closer to the building, and at the same time step the maximum vertical acceleration at a node on level 2 slab is 0.045 m/s^2 which shows that the vertical acceleration decreases with height.
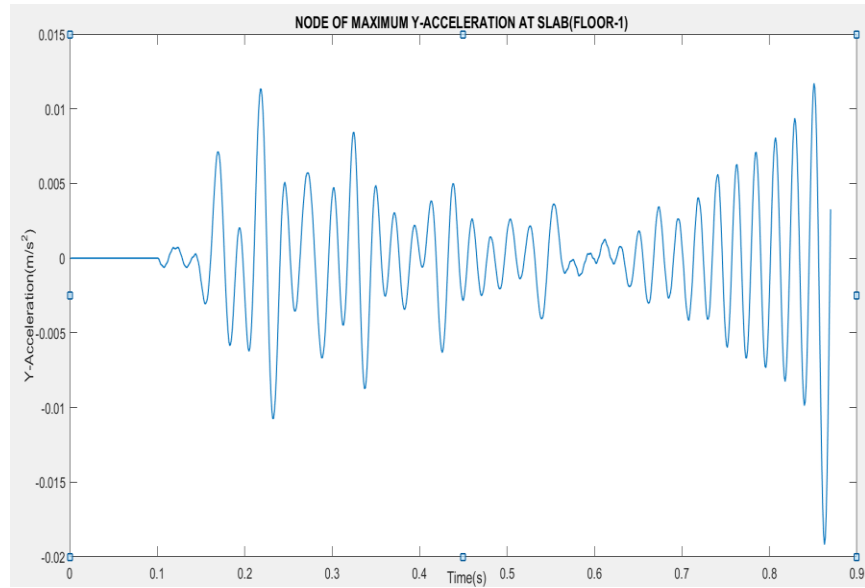
Figure 31:Y-Acceleration vs time graph at a node on slab level- 1
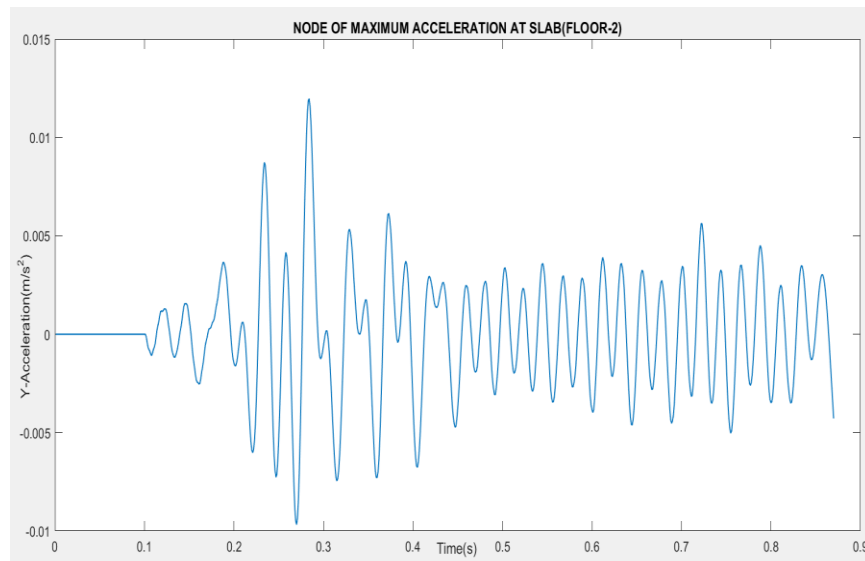
Figure 32:Y-Acceleration vs time graph at a node on slab level- 2

It is observed that the amplitude of Y-acceleration (horizontal acceleration) at a node on level 1 slab is approximately 25% less in magnitude than the Y-acceleration at a node on level 2 slab when the train passes through the rail track in line with the building. This shows that there is an effect of bending at the upper stories.

6.6 <u>Wave propagation speed:</u>

6.6.1 <u>*Longitudinal wave*</u>

In longitudinal waves, the direction of wave propagation is parallel to direction of displacement of the medium particles. Hence, according to the coordinate system used in this model, the longitudinal or the bulk wave will cause deflection in X and Y direction and therefore we observe the same in the plots that are generated. In this problem, displacement caused by bulk waves roughly corresponds to the Y-displacement.

The wave propagation speeds for longitudinal and shear waves through the sub-structure were calculated analytically and compared with the acceleration plots to check if the first rise in the amplitude is obtained at that time instant when the wave is expected to reach the building. The acceleration of the node at basement wall was observed since it will be the first thing that will be subjected to wave incidence.

Longitudinal wave velocity is given as:

$$V_L = \sqrt{\frac{E(1-v)}{\rho(1+v)(1-2v)}}$$

where V_L is the longitudinal wave velocity also called the bulk wave speed, E is the Young's modulus of the subgrade, v is the Poisson's ratio of the subgrade and ρ is its density. The theoretical longitudinal wave velocity was calculated to be 346.4 m/s. The distance between the building wall and the point when the train enters the flexible part of the rail is 20.2 meters and the therefore by the dividing it by the time instant, here 0.16 seconds when the first peak is observed at the basement wall, it is observed that the actual longitudinal wave velocity comes out to be 337

m/s. The error in the actual and theoretical value is only 2.8%, which shows that the longitudinal wave reaches when it is expected.

6.6.2 *Shear wave*

In shear waves, the direction of wave propagation is perpendicular to the direction of displacement of the medium particles. Therefore, in this model, the deflections of the substructure and the building will be affected in the Z-direction according to the co-ordinate system followed.

The shear wave velocity is calculated as

$$V_S = \sqrt{\frac{E}{2\rho(1+v)}}$$

where, V_s is the shear wave velocity, E is the Young's modulus of the subgrade, v is the Poisson's ratio of the subgrade and ρ is its density. The shear wave velocity calculated comes out to be 212.2 m/s for the sub-grade properties used in this model. The first peak in the acceleration vs time graph for the node on the basement wall is observed to be at 0.2 seconds after the first instance of rail-wheel contact. Therefore, the actual shear wave velocity is calculated as 202 m/s. The error in the theoretical and actual shear wave velocity is 4.9% which is within an acceptable range.

Therefore, this comparison between the analytical and actual wave velocities that are observed in this model ensures that the behavior of wave transmission is verified to a good extent.

6.7 <u>Wave reflection:</u>

A wave reflection check was conducted to ensure that the outputs obtained are not affected by bouncing back of waves from the external boundaries of the model, which might lead to deceptive conclusions. The effect of constructive and destructive interference in the incidence and reflected waves can cause the resultant waves to be far from the desired results. In the finite element model, there is a chance of artificial waves being reflected from the boundaries at either ends of the model. El-Ghandour et al.(21) in his research observed the rail deflections and suggested that when a modal damping of 3% is used, it is seen that undesired excitation of waves from the boundary are eliminated. However, this reflection is a function of geometry, and must be checked for different problems.

In this research, to eliminate the wave reflections, we followed a different approach along with application of modal damping. Here, we designed three different models with lesser depth (Model 1), greater depth (Model 2) and greater width (Model 3) of the substructure and compared their behavior.
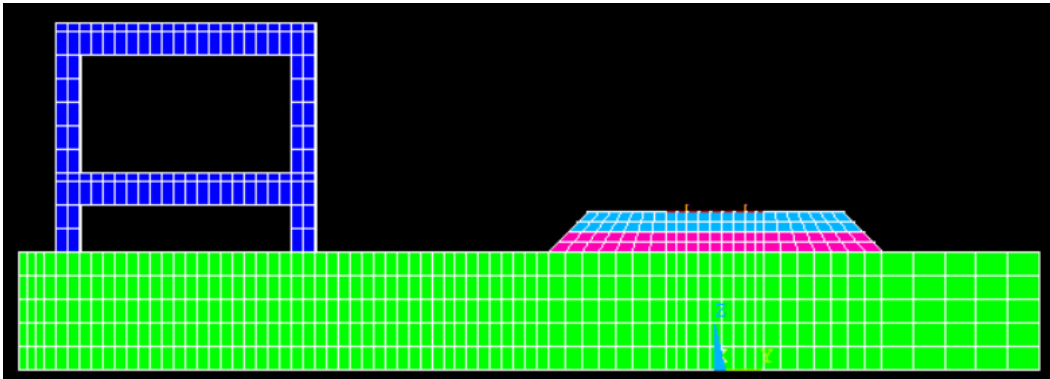
Figure 33:FE model of the system with lesser depth of the sub grade(Model 1)
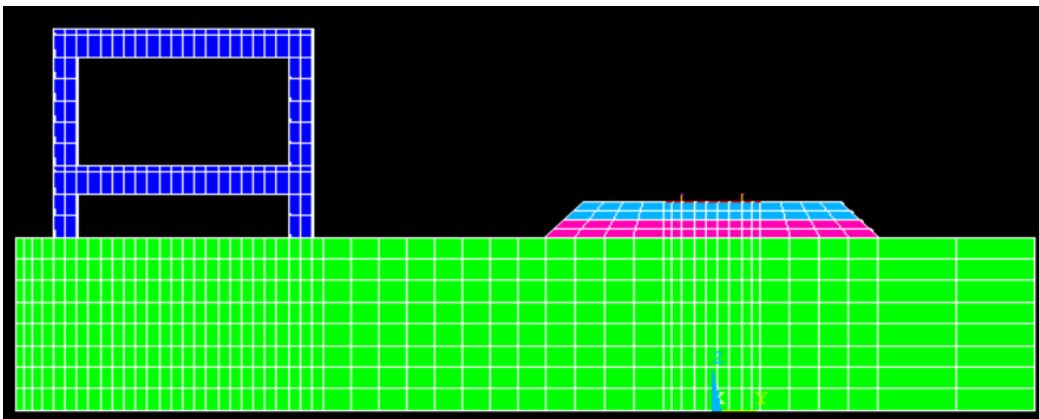
Figure 34:FE model of the system with greater depth of the sub grade(Model 2)
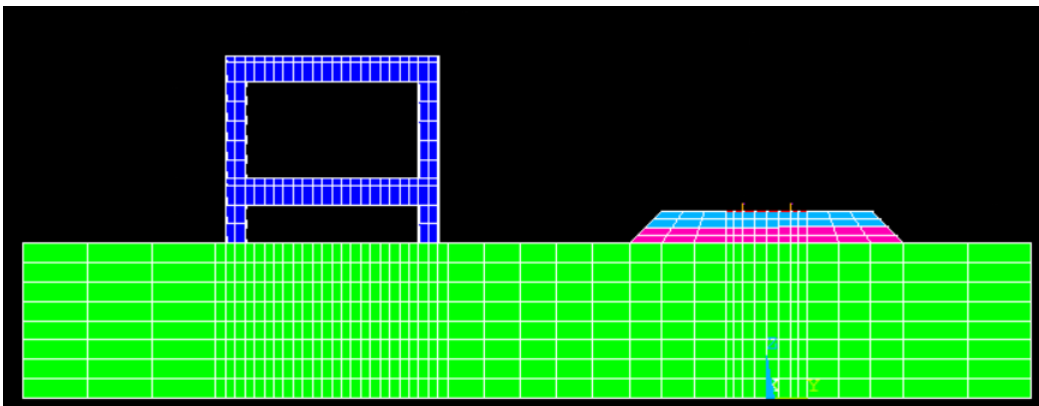
Figure 35:FE model of the system with lesser width of the sub grade to the left of the building (Model 2)
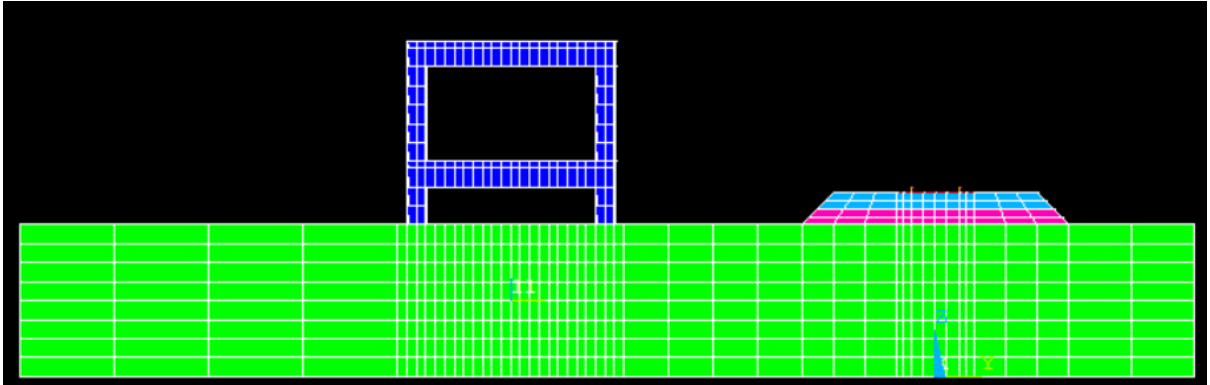
Figure 36:FE model of the system with greater width of the subgrade to the left of the building(Model 3)

The first model had a depth of 3 meters which was increased to 5 meters in the second model and then was checked for convergence of the acceleration. After ensuring that the results are converged for the increased depth, another model was created by increasing the length by 2 meters and width in the direction perpendicular to the rail and between the building and external boundary by 6 meters respectively. Again this model was checked for convergence in the accelerations to ensure that there is no presence of wave reflection.
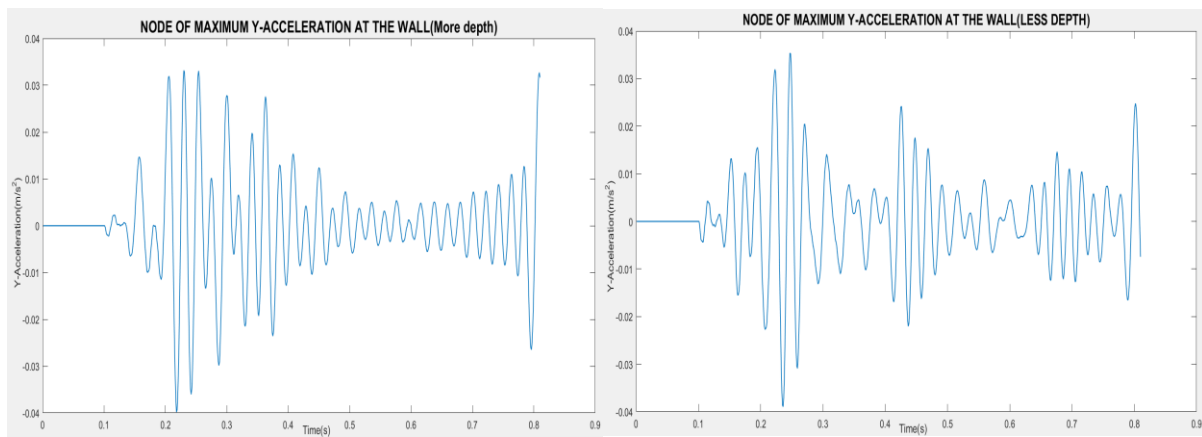
Figure 37:Y-Acceleration vs Time at the basement wall (deeper model on the left and less deeper model on the right)
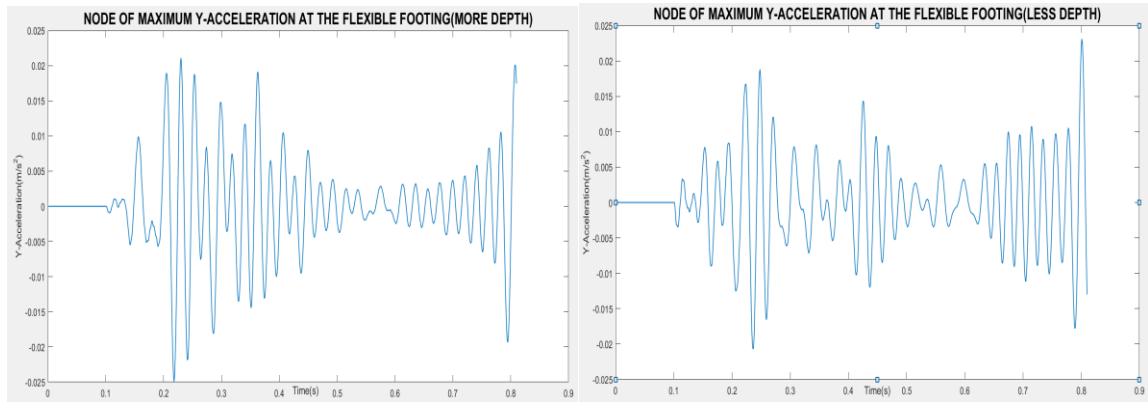
Figure 38:Y-Acceleration vs Time at the flexible footing (deeper model on the left and less deeper model on the right)
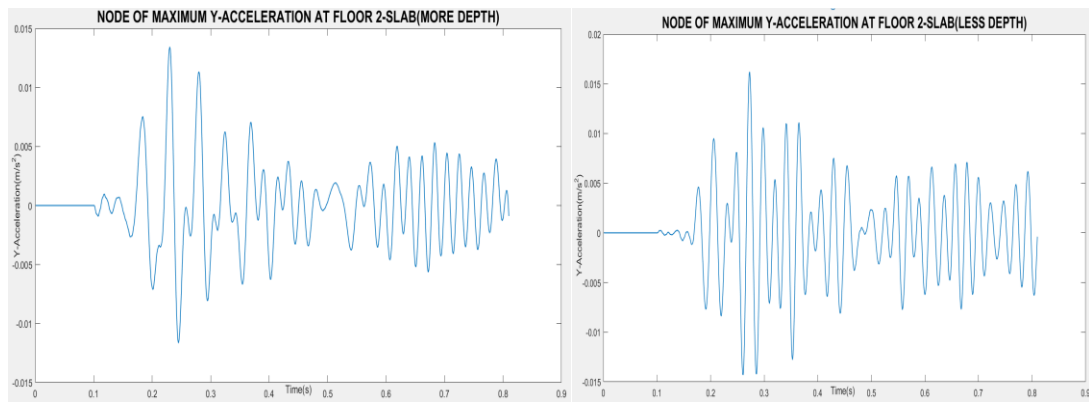
Figure 39:Y-Acceleration vs Time at the slab-2 (deeper model on the left and less deeper model on the right)
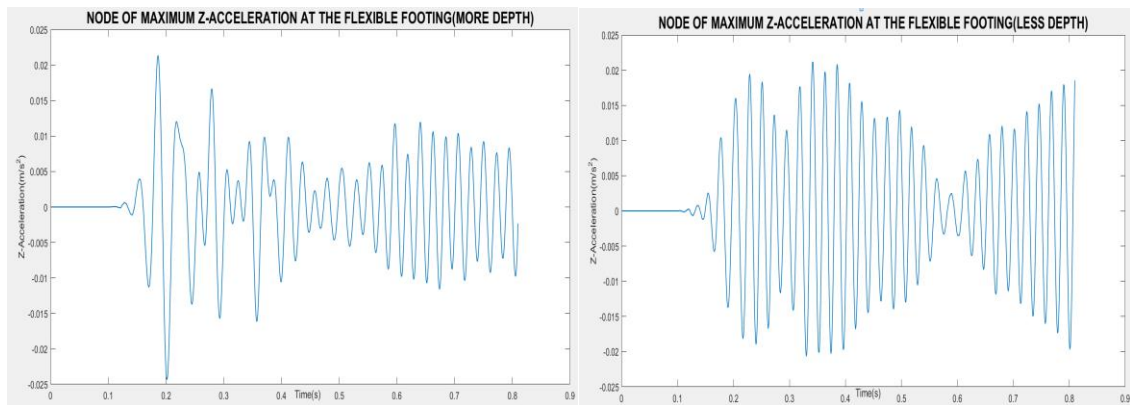
Figure 40:Z-Acceleration vs Time at the flexible footing (deeper model on the left and less deeper model on the right)
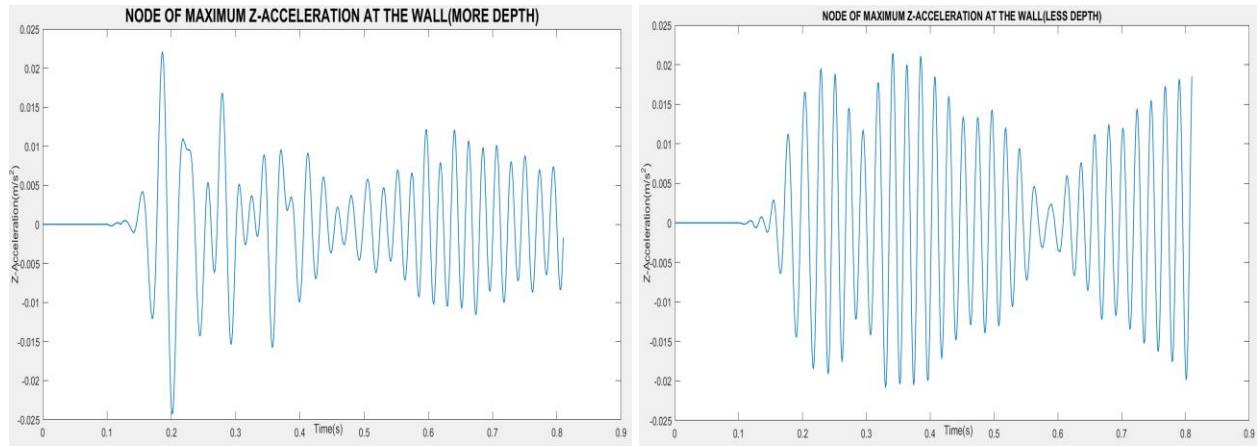
Figure 41:Z-Acceleration vs Time at the basement wall (deeper model on the left and less deeper model on the right)
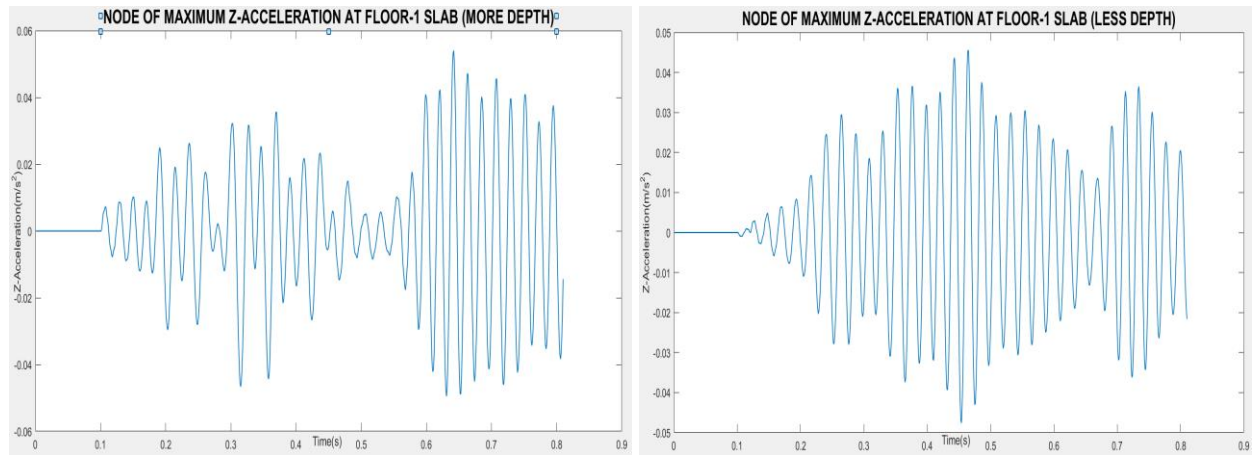
Figure 42:Z-Acceleration vs Time at slab-1 (deeper model on the left and less deeper model on the right)
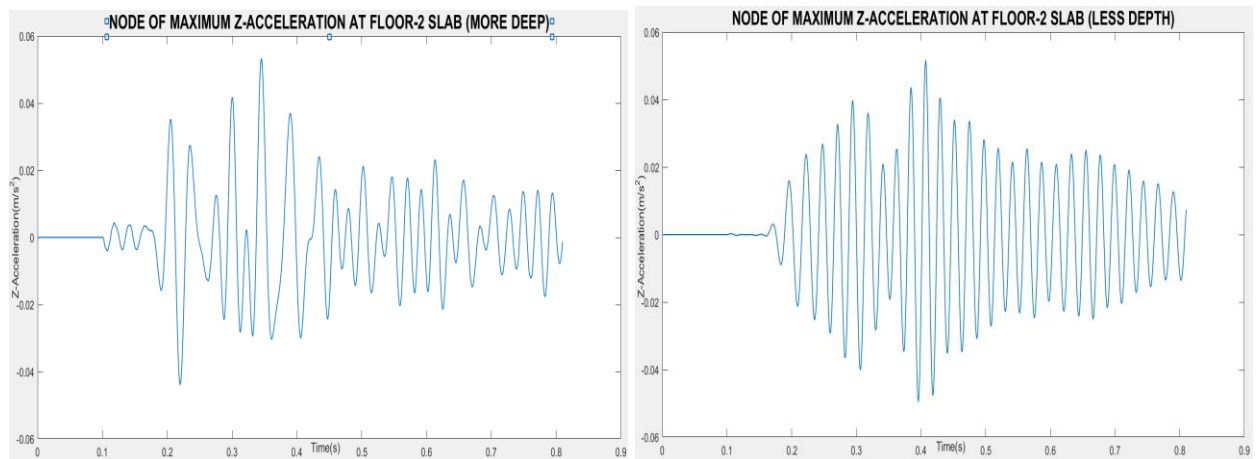
Figure 43:Z-Acceleration vs Time at slab-2 (deeper model on the left and less deeper model on the right)

Here, it is observed that when the depth of the model is increased, the amplitude of the acceleration at the different locations in the building remains similar though there is a little difference in the frequency of the plots for Z-acceleration.This is because the lesser deep model has only a short distance between the bottom surface of the model and the base of the building,which causes more frequent perturbations. Since, the amplitudes of the accelerations are similar,wave reflection from the bottom of the model does not appear to be a major issue.
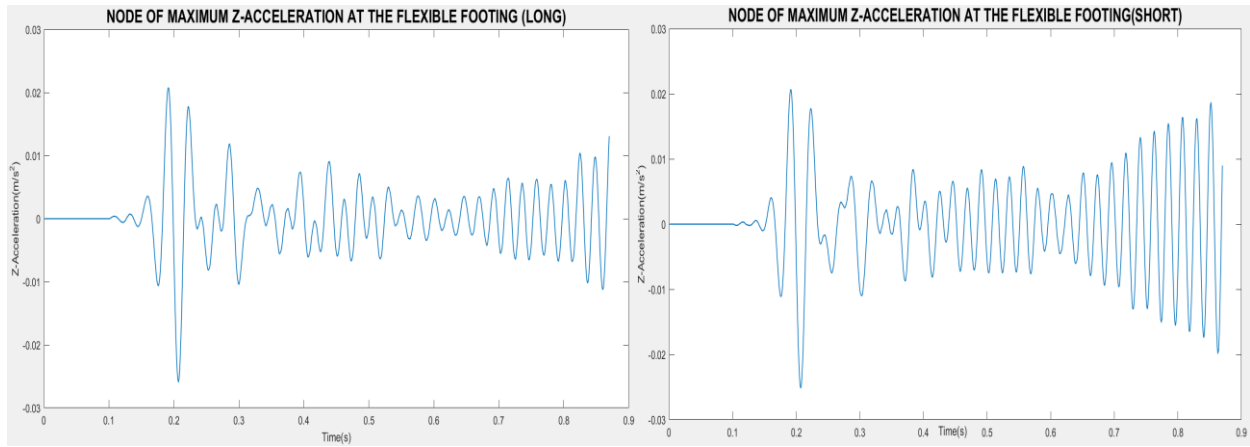
Figure 44:Z-Acceleration vs Time at the flexible footing for the 2nd model on the right and 3rd model on the left
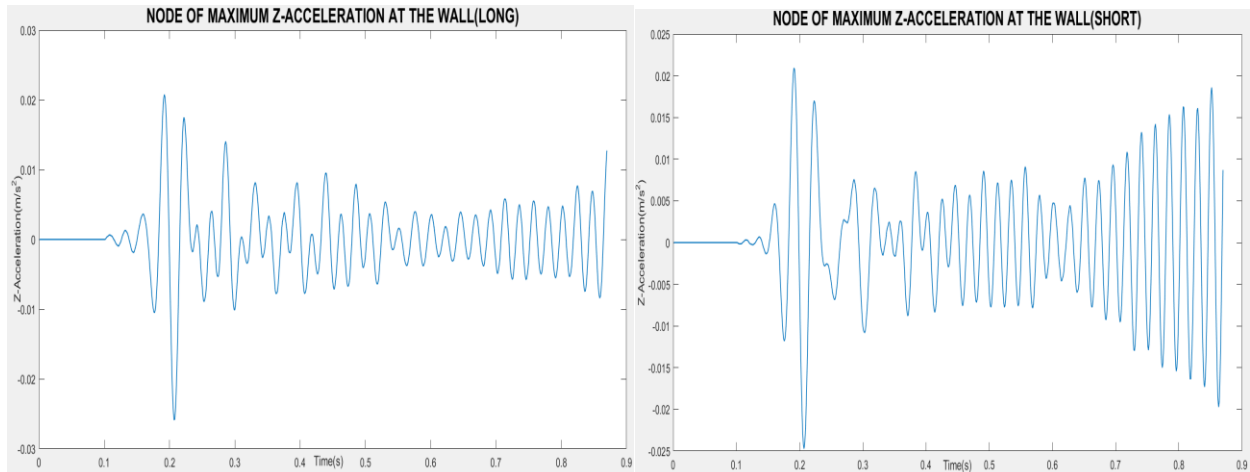
Figure 45:Z-Acceleration vs Time at the basement wall for the 2nd model on the right and 3rd model on the left
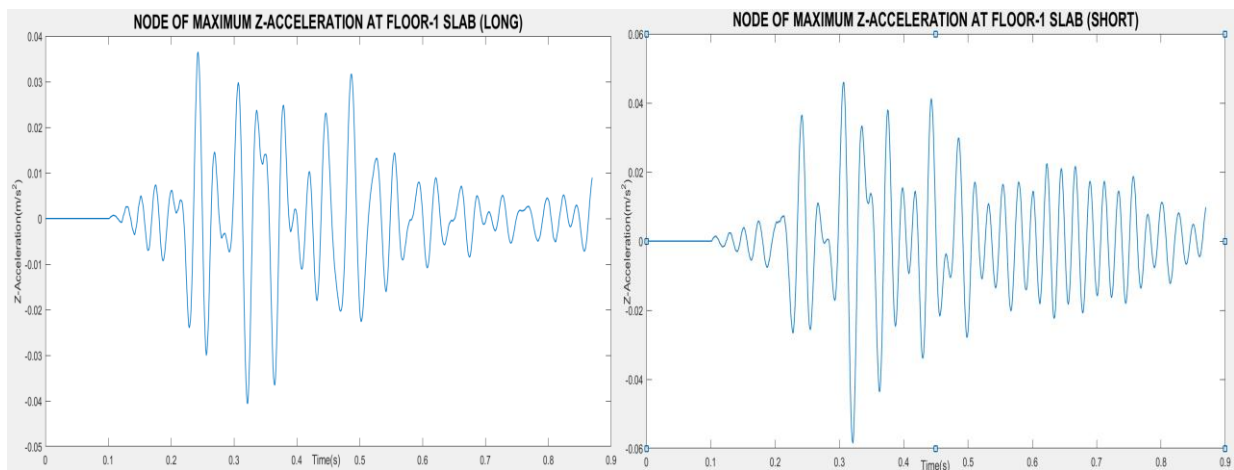
Figure 46:Z-Acceleration vs Time at the first floor slab for the 2nd model on the right and 3rd model on the left
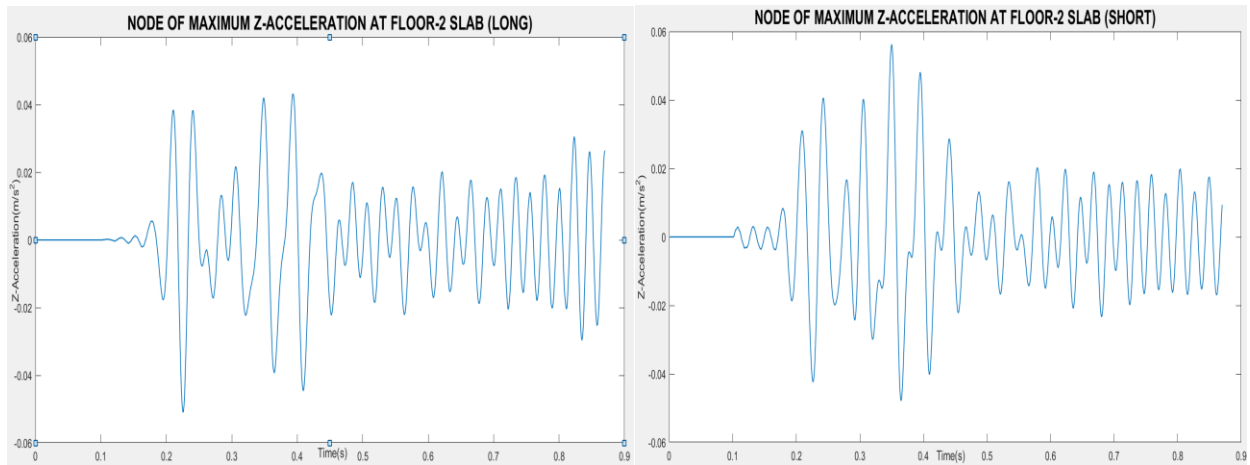
Figure 47:): Z-Acceleration vs Time at the second floor slab for the 2nd model on the right and 3rd model on the left
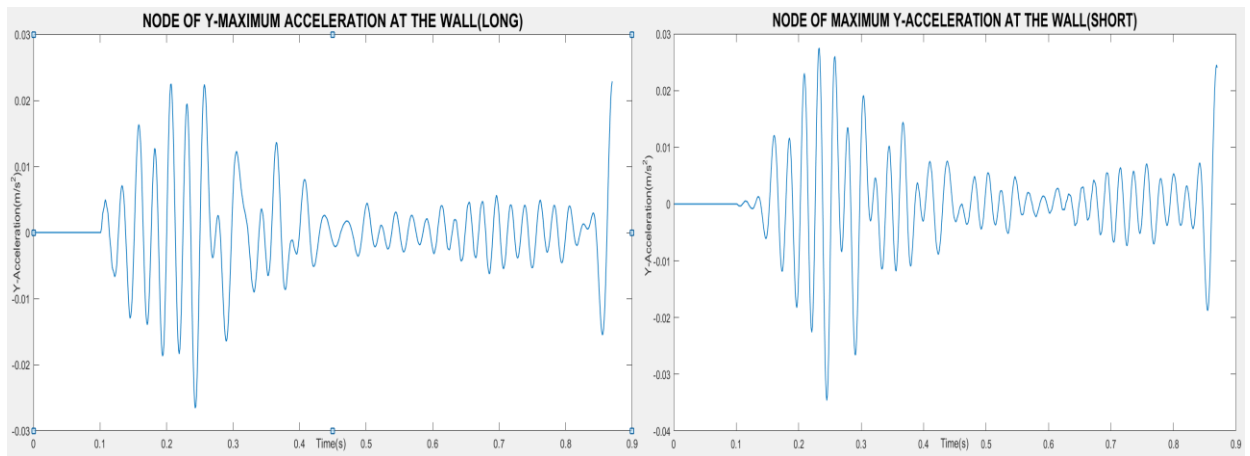
Figure 48:Y-Acceleration vs Time at the basement wall for the 2nd model on the right and 3rd model on the left
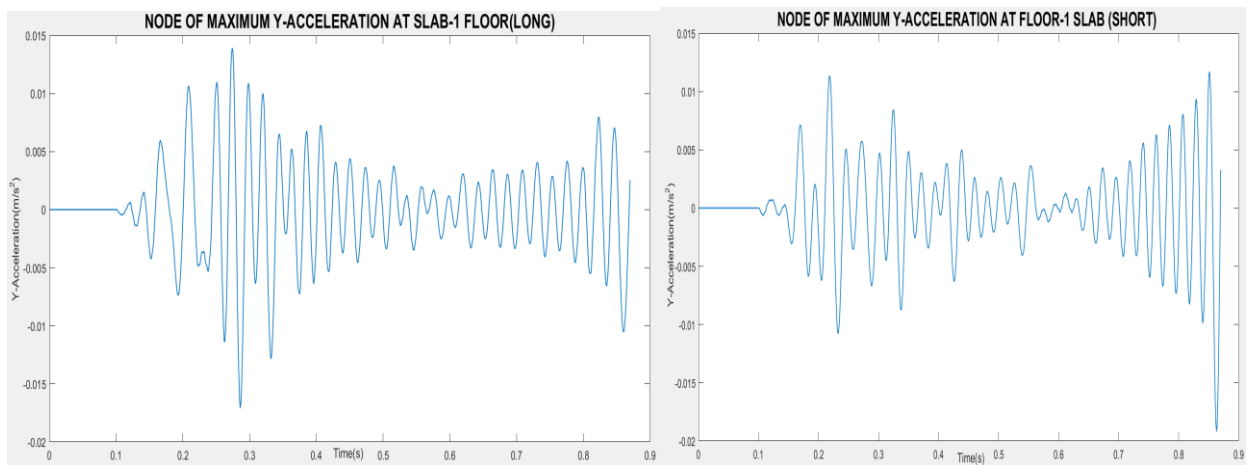
Figure 49:Y-Acceleration vs Time at the first floor slab for the 2nd model on the right and 3rd model on the left
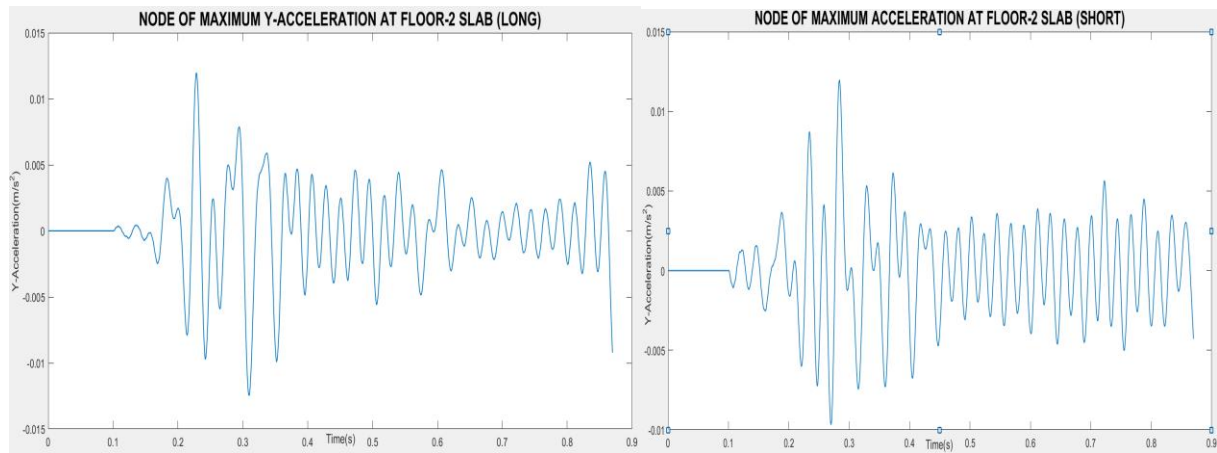
Figure 50:Y-Acceleration vs Time at the second floor slab for the 2nd model on the right and 3rd model on the left

It is observed in Figures (44)-(50) at different locations in the building that the maximum acceleration in the transverse and longitudinal directions do not vary and the pattern of vibrations are similar which ensures that there are no wave reflections bouncing off the external vertical boundaries of the model. In this way, the model was checked for convergence in acceleration when the length and width is increased. The wave reflections are thereby knocked out giving us a converged model and accurate results.

6.8 Mesh density study

- A mesh convergence test was conducted to validate the accuracy of the results obtained for the finite element model after simulation. Here, we meshed the model till we reached a set of elements for which the results obtained were within 5% range.

- Initially the model was coarsely meshed to a total number of nodes as 46582.

- For the model which was finely meshed, the total number of nodes were 56403 and the amplitude of vertical and horizontal accelerations were found out to be similar which ensured that there is mesh convergence.

- Because of cost limitations, refinement was performed in key areas.
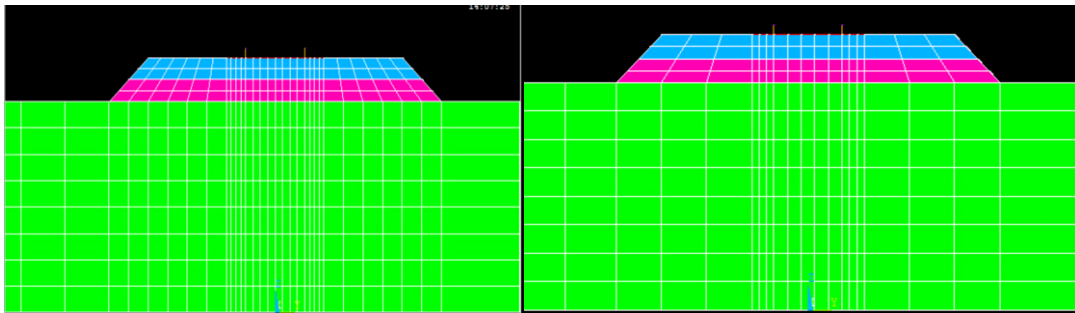
Figure 51: Finer mesh (Left side) and Coarser mesh (Right side)
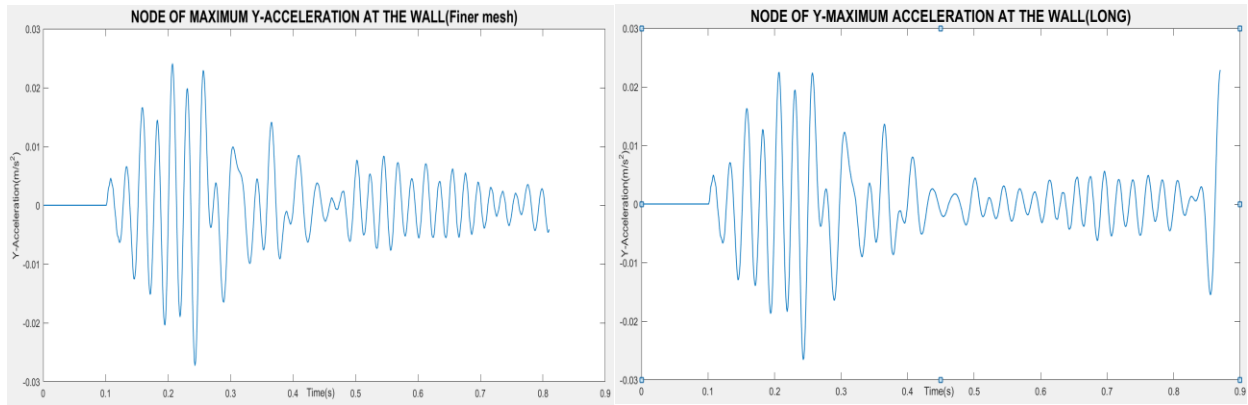
Figure 52:Y-acceleration values at the basement wall : Finer mesh (Left side) and Coarser mesh (Right side)
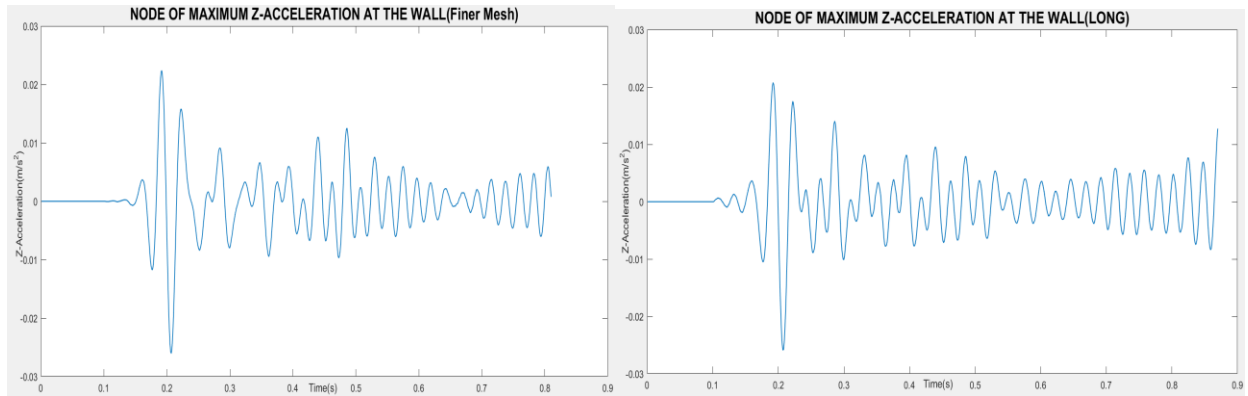
Figure 53:Z-acceleration values at the basement wall : Finer mesh (Left side) and Coarser mesh (Right side)

6.9 <u>Check for occupant discomfort</u>

After getting a converged model after increasing the length, width and the depth to make sure that the waves which are reflected from the fixed boundaries of the model vanish, we plot the total acceleration graphs at the different locations of the building to check for discomfort level of the occupants inside. Since the occupants are present on the slab at level 1 and level 2 and there is a higher possibility of feeling vibrations in this region, we examine the total acceleration values at these two places of the building.
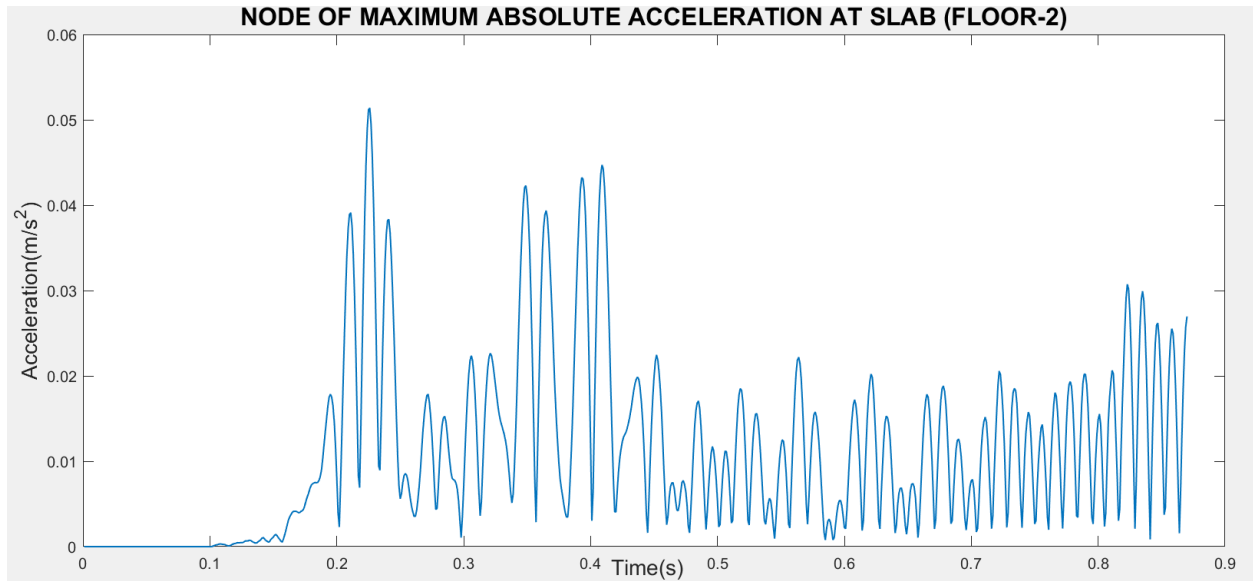
Figure 54:Magnitude of acceleration at the node on the 2nd floor slab of the building
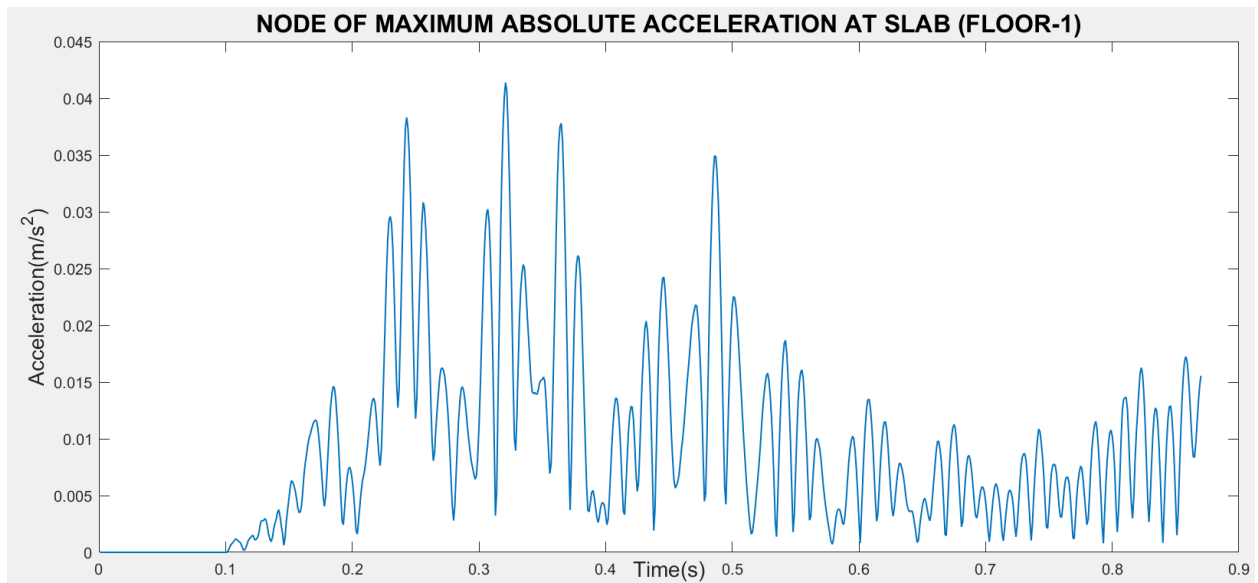
Figure 55:Total acceleration at the node on the 1st floor slab of the building

Bednarz and Targosz (29) suggested that the occupants tend to feel uncomfortable when the amplitude of the acceleration is above 0.005 times the gravitational constant. Another comfort criteria that was suggested by Murray (30) proposed that the range of values where the occupants have an unpleasant feeling due to accelerated vibrations is between 0.5% and 5% of the gravitational constant value. Here, we observe in the acceleration graphs at different regions of the building structure that at the 1st floor, the maximum total acceleration value is 0.041 m/s^2 which is above the discomfort level while it is 0.052 m/s^2 at the 2nd floor slab which is below the discomfort level. The minimum limit above which discomfort is experienced is 0.049 m/s^2.Therefore, occupants are bound to feel a bit uncomfortable since values obtained at some parts are above the comfort limit. In taller buildings, the acceleration in upper floors is higher due to bending of the structure.

CHAPTER 7

CONCLUSIONS AND FUTURE WORK

7.1 Conclusions

Many researchers who are currently working on problems faced by the railroad industry have developed different models and tools to solve for appropriate solutions with cost-effective methods. In this research, in order to study the railroad system, an approach was used where the tools in finite element and multibody dynamics systems were applied in combination. A comprehensive model of a rail track was proposed and implemented in this method. This model was created for fulfilling the objective of inspecting the vibrations caused at different locations in the building structure transmitted through the soil due to the passing train.

A three-dimensional finite element model of a railway track consisting of the rail, sleepers, ballast, subballast, subgrade and a building structure with a foundation and wall was constructed in a finite element package ANSYS. The ballast, subballast, subgrade and the concrete structure were modeled using 3D solid brick elements while the rail and sleepers were modeled using 3D beam elements. The rail pads and fasteners connecting the rail and the sleepers were modeled spring-damper elements. A modal analysis was run for the entire model to extract the mode shapes and natural frequencies of the model along with its mass and stiffness matrices. This data was then used to extract the modal information for the rail nodes only using a nodal elimination technique. This method improves efficiency while allowing more complex details in the model. This rail specific information was given to a multibody code to run the simulation of wheel rail interaction in the time domain. The multibody code computed the contact forces, modal displacements and

acceleration for the rail system. Later, corresponding nodal displacements and nodal accelerations were mathematically reconstructed in MATLAB. This reconstructed data was again fed back to ANSYS in the post-processing stage so that the results obtained can be visualized and studied easily. Also, the nodal data was sorted and analyzed in MATLAB to plot graphs required to study the behavior of the moving train on the building structure and quantify the vibrations. Occupant discomfort was considered to study the vibrations at different levels of the building and checked for the given human comfort range. It was concluded that there is sufficient amount of vibration that would cause discomfort in some parts of the building structure, though not at all. It can be concluded that taller buildings can have higher vibrations in the higher levels than lower levels,. This is due to the fact that the effect of bending and torsion due to structural flexibility can result in greater vibrations at higher levels of the building than as compared to levels which are close to the base of the building.

Also, it was concluded that the wave reflection check done by comparing the results of two different models by changing the length, depth of soil and width after the building ensures that there are no reflected waves from the boundary. The reflected waves die down before they impact the building again and therefore do not cause any kind of constructive or destructive interference of waves near the building.

7.2 <u>Future work</u>

The model built in this research can provide results and help us study the behavior of moving trains over the substructure and its effects on adjacent building. But there is further need to validate these results obtained from simulation and compared with the ones taken experimentally at different points on the building to measure the acceleration. Once validated, the model can be used to investigate various techniques for mitigating vibrations. Examining different rail pads, ballast materials, insulation for the building or other approaches to mitigating vibrations could help determine the most cost-effective techniques for mitigating vibrations in a given scenario.

The nodal deformations in the substructure can be used further to study settlement of soil. The model built in this research work with some additional changes like using different material properties for the fasteners or considering the plastic behavior of soil along with a non-linear approach could lead to a very realistic and powerful model to analyze rail problems with minimum assumptions and accurate results.

APPENDICES

APPENDIX A

ANSYS APDL CODE

This is the Finite element ANSYS-APDL code used to build the railroad model and the building structure nearby. This code also does the modal analysis and then reconstructs the full displacement field.

```
fini
/clear
/prep7
!-----------!
ET,1,BEAM188                              !--- The Rail, the sleepers
ET,2,SOLID185                             !--- The Soil layers
ET,3,SOLID185                             !--- Concrete parts
ET,4,SHELL181
ET,5,COMBIN14                  !--- The spring elements connecting rails and sleepers
ET,6,COMBIN14                             !--- The spring elements connecting rails and sleepers
ET,7,COMBIN14                             !--- The spring elements connecting rails and sleepers

!-----------!
KEYOPT,5,1,0
KEYOPT,5,2,1              !--- Ux
KEYOPT,5,3,0
!-----------!
KEYOPT,6,1,0
KEYOPT,6,2,2           !--- Uy
KEYOPT,6,3,0
!-----------!
KEYOPT,7,1,0
KEYOPT,7,2,3           !--- Uz
KEYOPT,7,3,0
!-----------!
!-----------!
SECTYPE,1, BEAM, I, , 0     ! rail
SECOFFSET, CENT
SECDATA,0.1524,0.07,0.19,0.0165,0.045,0.0175,0,0,0,0,0,0
!*
SECTYPE,2, BEAM, QUAD, , 0  ! sleeper
SECOFFSET, CENT
SECDATA,-0.135,-0.11,.135,-.11,.090,.11,-.090,.11,8,10,0,0

R,7,70e8,5e5,                             !--- the data of spring in x-dirction
R,8,70e8,5e5,                          !--- the data of spring in y-dirction
R,9,70e8,5e5,                          !--- the data of spring in z-dirction
!-------------------------------------------------------------------------!
!-----------   the material info for the corresponding element   ---------!
!-------------------------------------------------------------------------!
MP,EX,1,210e9                    !--- the data of the rails
MP,PRXY,1,0.30
MP,ALPD,1,0
MP,BETD,1,1e-6
MP,DENS,1,7700
!*
```

APPENDIX A (CONTINUED)

```
MP,EX,2,210e10
MP,PRXY,2,0.30                        !--- RIGID RAIL
MP,ALPD,2,0  !6
MP,BETD,2,1e-6 !5e-4
MP,DENS,2,7700
!*
MP,EX,3,64e9                          !--- the data of the sleepers
MP,PRXY,3,0.25
MP,ALPD,3,0   !5
MP,BETD,3,10e-4
MP,DENS,3,2570
!*


MP,EX,4,260e6                         !--- the data of the ballast
MP,PRXY,4,0.25
MP,ALPD,4,0    !5.5
MP,BETD,4,12e-4
MP,DENS,4,1800
!*
MP,EX,5,200e06                         !--- the data of the sub_ballast
MP,PRXY,5,0.2
MP,ALPD,5,0    !5.5
MP,BETD,5,15e-4
MP,DENS,5,1850
!*
MP,EX,6,200e6                          !--- the data of the sub_grade
MP,PRXY,6,0.2
MP,ALPD,6,0    !5.5
MP,BETD,6,15e-4
MP,DENS,6,1850


MP,EX,7,50E9 !12                       !---the data of spring elements(X)
MP,PRXY,7,0.1
MP,ALPD,7,0     !5.4
MP,BETD,7,1e-6 !5e-4
!*
MP,EX,8,50E9 !12                       !---the data of spring elements(Y)
MP,PRXY,8,0.1
MP,ALPD,8,0
MP,BETD,8,1e-6 !5e-4
!*
MP,EX,9,50E9 !12                       !---the data of spring elements(Z)
MP,PRXY,9,0.1
MP,ALPD,9,0
MP,BETD,9,1e-6 !5e-4




MP,EX,10,31e9                       !--- Concrete building
MP,PRXY,10,0.25
MP,ALPD,10,0
MP,BETD,10,10e-4
MP,DENS,10,2500
!*
!----------------------Variables--------------------!
X0=0                    !--->> RIGID RAIL STARTS
X1=3                    !--->> RIGID RAIL ENDS
X2=12.6                       !--->> BUILDING STRUCTURE STARTS
X3=19.8                       !--->> BUILDING STRUCTURE ENDS
X4=24.6          !--->> SOIL ENDS HERE
```

APPENDIX A (CONTINUED)

```
YS0=8.25
YS1=-4.25                   !--->> Y- coordinate where ballast and sub-ballast ends
YS2=-9.9                    !--->> Y- coordinate where building starts
YS3=-17.1                   !--->> Y- coordinate where building ends

YS4=-29.1                   !--->> Y- coordinate where sub-grade ends
Z0=0
Z1=4.8                      !------>> Z co-ordinate of top surface of subgrade
Z2=5.3                      !------>> Z co-ordinate of top surface of sub-ballast (common surface shared by
ballast and sub-ballast)
Z3=5.8                      !------>> Z co-ordinate of top surface of ballast
Z4=6.00424

XBB=16.2                    !--->> X co-ordinate of base of the building
YBB=-13.5                   !--->> Y co-ordinate of base of the building
ZBB=2.4                     !--->> Z co-ordinate of base of the building

HSF=0.6                            !--->> Height of flexible spread footing
R_Gage=2*0.75565
Rigid=3
Rail_length=21.6
No_sleeper_div_total=36
No_sleeper_div_X1_X2=16                      !--->>Till the building
No_sleeper_div_BLDG=12                       !--->>Start to end of building
No_sleeper_div_X3_X4=8                        !--->>After the building
No_rail_ele_betwn_sleeper=5
No_soil_ele_betwn_sleeper_B=4                     !---->> In-line with the building
No_soil_ele_betwn_sleeper_NB=2                    !---->> where there is no building
Distance_betw_sleepers=0.6
SLP_OUT_ELE=2
SLP_MID_ELE=4
BEAM_LENGTH=5.4
BEAM_WIDTH=0.6
Z_SLAB1_BASE=4.2
Z_SLAB2_BASE=8
WALL_WIDTH=0.3
DIST_BETWEN_SF=4.8                  ! Distance between flexible spread footing
!-----------------------Creating the Rigid part------------------!
TYPE,1
MAT,2
secnum,1
*GET,Elem_RR_RG1,ELEM,,COUNT, , , ,                      !--->> Getting the !elem# before right rigid rail 1


K,1,0,R_Gage/2,Z4
K,2,Rigid,R_Gage/2,Z4
L,1,2
LESIZE,1,,,1,,1,,,1
LMESH,1
!-----------Creating the right rail---------------------------------------!
TYPE,1
MAT,1
secnum,1
K,3,Rigid+((Rail_length/No_sleeper_div_total)/No_rail_ele_betwn_sleeper),R_Gage/2,Z4
L,2,3
LESIZE,2,,,1,,1,,,1
LMESH,2
LGEN,5*No_sleeper_div_total,2, ,,((Rail_length/No_sleeper_div_total)/No_rail_ele_betwn_sleeper) ,
```

APPENDIX A (CONTINUED)

```
,,1,0,0
!LGEN, ITIME, NL1, NL2, NINC,DX,DY,DZ,KINC,NOELEM,IMOVE
!----Getting scalar parameter: KP number just before the Rigid  rail
*GET,KP_RR_RGEND,KP,,COUNT, , , ,                                    !*GET, Par, Entity, ENTNUM,
Item1, IT1NUM, Item2, IT2NUM
*GET,Line_RR_RGEND,LINE,,COUNT, , , ,              !--->> Line_RR_RGEND stands for Right rail
Rigid end part
MAT,2
K,KP_RR_RGEND+1,2*Rigid+Rail_length,R_Gage/2,Z4
KP_RR_END=KP_RR_RGEND+1


L,KP_RR_RGEND,KP_RR_RGEND+1
Line_RR_END= Line_RR_RGEND+1

*GET,Elem_RR_RG2,ELEM,,COUNT, , , ,

LESIZE,Line_RR_END,,,1,,1,,,1
LMESH,Line_RR_END

!-----------Creating the left rail---------------------------------------!

*GET,Elem_LR_RG1,ELEM,,COUNT, , , ,

LGEN,2,1,Line_RR_END,1 , , -R_Gage, ,0,0,0    !LGEN, ITIME, NL1, NL2, NINC, DX, DY, DZ,
KINC, NOELEM, IMOVE

*GET,Elem_LR_RG2,ELEM,,COUNT, , , ,               !--->>*** Here it fetches elem# after left rigit
rail 2 is created
*GET,Node_end_of_rails,NODE,,COUNT,,,,
!----------------Creating sleepers-----------------------------!
TYPE,1
MAT,3
SECNUM,2

*GET,KP_LR_END,KP,,COUNT, , , ,                !-->> RR stands for Right Rail
KP_LR_RGEND=KP_LR_END-1

*GET,Line_LR_END,LINE,,COUNT, , , ,
Line_LR_RGEND=Line_LR_END-1

K,KP_LR_END+1,Rigid,-1.25,Z3
K,KP_LR_END+2,Rigid,-R_Gage/2,Z3
K,KP_LR_END+3,Rigid,R_Gage/2,Z3
K,KP_LR_END+4,Rigid,1.25,Z3



L,KP_LR_END+1,KP_LR_END+2
L,KP_LR_END+2,KP_LR_END+3
L,KP_LR_END+3,KP_LR_END+4

SL1=Line_LR_END+1
SL2=Line_LR_END+2
SL3=Line_LR_END+3

LSEL,S,LINE,,SL1,SL3,2
LESIZE,ALL,,,SLP_OUT_ELE,,1,,,1
```

APPENDIX A (CONTINUED)

```
LSEL,S,LINE,,SL2,,0
LESIZE,ALL,,,,SLP_MID_ELE,,1,,,1


LSEL,S,LINE,,SL1,SL3,1
LMESH,ALL

ALLSEL
LGEN,No_sleeper_div_total+1,SL1,SL3,1,Distance_betw_sleepers,,,,0,0
!---------------- Creating keypoints for ballast, sub-ballast,subgrade-------------
*GET,KP_SLP_END,KP,,COUNT, , , ,
*GET,Line_SLP_END,LINE,,COUNT, , , ,

K,KP_SLP_END+1,X1,R_Gage/2,Z3
K,KP_SLP_END+2,X1,R_Gage/2,Z2
K,KP_SLP_END+3,X1,R_Gage/2,Z1
K,KP_SLP_END+4,X1,R_Gage/2,Z0


K,KP_SLP_END+5,X1,1.25,Z3
K,KP_SLP_END+6,X1,1.25,Z2
K,KP_SLP_END+7,X1,1.25,Z1
K,KP_SLP_END+8,X1,1.25,Z0
K,KP_SLP_END+9,X1,3.25,Z3
K,KP_SLP_END+10,X1,3.75,Z2
K,KP_SLP_END+11,X1,-YS1,Z1
K,KP_SLP_END+12,X1,-YS1,Z0


K,KP_SLP_END+25,X1,YS0,Z1
K,KP_SLP_END+26,X1,YS0,Z0
K,KP_SLP_END+27,X1,YS4,Z1
K,KP_SLP_END+28,X1,YS4,Z0

!-----------------Creating Areas for ballast, sub-ballast,subgrade-----------------
A,KP_SLP_END+1,KP_SLP_END+5,KP_SLP_END+6,KP_SLP_END+2
A,KP_SLP_END+6,KP_SLP_END+7,KP_SLP_END+3,KP_SLP_END+2
A,KP_SLP_END+7,KP_SLP_END+8,KP_SLP_END+4,KP_SLP_END+3
A,KP_SLP_END+9,KP_SLP_END+10,KP_SLP_END+6,KP_SLP_END+5
A,KP_SLP_END+10,KP_SLP_END+11,KP_SLP_END+7,KP_SLP_END+6
A,KP_SLP_END+11,KP_SLP_END+12,KP_SLP_END+8,KP_SLP_END+7
ARSYM,Y,1,6 ,1 , ,0,0
A,KP_SLP_END+1,KP_SLP_END+2,KP_SLP_END+16,KP_SLP_END+13
A,KP_SLP_END+2,KP_SLP_END+3,KP_SLP_END+18,KP_SLP_END+16
A,KP_SLP_END+3,KP_SLP_END+4,KP_SLP_END+20,KP_SLP_END+18
A,KP_SLP_END+25,KP_SLP_END+26,KP_SLP_END+12,KP_SLP_END+11
!A,KP_SLP_END+23,KP_SLP_END+24,KP_SLP_END+28,KP_SLP_END+27

!++++++++++++++++++++++++++++++++++++++++++++++++++++++++++++++++++++++++++++++++

LSEL,S,LOC,X,X1
LSEL,R,LENG,,R_Gage
LESIZE,ALL,,,,SLP_MID_ELE,,1,,,1


LSEL,S,LOC,X,X1
LSEL,R,LENG,,1.25-(R_Gage/2)
LESIZE,ALL,,,,SLP_OUT_ELE,,1,,,1
```

APPENDIX A (CONTINUED)

```
LSEL,S,LOC,X,X1
LSEL,R,LOC,Z,Z0,Z3,1
LSEL,R,LOC,Y,1.26,3.24,1
LSEL,A,LOC,Y,-1.26,-3.24,1
LESIZE,ALL,,,3,,1,,,1


LSEL,S,LOC,X,X1
LSEL,R,LENG,,Z1-Z0
LSEL,U,LINE,,Line_SLP_END+15,Line_SLP_END+17,2
LSEL,U,LINE,,Line_SLP_END+32,Line_SLP_END+34,2
LESIZE,ALL,,,8,,1,,,1


LSEL,S,LINE,,Line_SLP_END+2,Line_SLP_END+4,2
LSEL,A,LINE,,Line_SLP_END+5,Line_SLP_END+7,2
LSEL,A,LINE,,Line_SLP_END+11,Line_SLP_END+31,10
LSEL,A,LINE,,Line_SLP_END+14,Line_SLP_END+24,5
LSEL,A,LINE,,Line_SLP_END+22,Line_SLP_END+28,6
LESIZE,ALL,,,2,,1,,,1



LSEL,S,LINE,,Line_SLP_END+40,Line_SLP_END+41,1
LESIZE,ALL,,,2,,1,,,1

ALLSEL
TYPE,4
AMESH,1,16,1
!=============Extruding the ballast ===========!
TYPE,2
MAT,4
EXTOPT,ESIZE,(No_soil_ele_betwn_sleeper_NB)*(No_sleeper_div_X1_X2)
EXTOPT,ACLEAR,1
VEXT,1,13,3,X2-X1,,,
ASEL,S,LOC,X,X2,,0,1
EXTOPT,ESIZE,(No_soil_ele_betwn_sleeper_B)*(No_sleeper_div_BLDG)
VEXT,ALL,,,X3-X2,,,
ASEL,S,LOC,X,X3,,0,1
EXTOPT,ESIZE,(No_soil_ele_betwn_sleeper_NB)*(No_sleeper_div_X3_X4)
VEXT,ALL,,,X4-X3,,,
ALLSEL
!=============Extruding the sub-ballast===========!

TYPE,2
MAT,5
EXTOPT,ESIZE,(No_soil_ele_betwn_sleeper_NB)*(No_sleeper_div_X1_X2)
EXTOPT,ACLEAR,1
VEXT,2,14,3,X2-X1,,,


ASEL,S,LOC,X,X2,,0,1
ASEL,R,LOC,Z,Z1,Z2,1
EXTOPT,ESIZE,(No_soil_ele_betwn_sleeper_B)*(No_sleeper_div_BLDG)
VEXT,ALL,,,X3-X2,,,


ASEL,S,LOC,X,X3,,0,1
ASEL,R,LOC,Z,Z1,Z2,1
```

APPENDIX A (CONTINUED)

```
EXTOPT,ESIZE,(No_soil_ele_betwn_sleeper_NB)*(No_sleeper_div_X3_X4)
VEXT,ALL,,,X4-X3,,,
ALLSEL


!==============Extruding the sub-grade(except the portion where there is a
building)============!

TYPE,2
MAT,6
EXTOPT,ESIZE,(No_soil_ele_betwn_sleeper_NB)*(No_sleeper_div_X1_X2)
EXTOPT,ACLEAR,1
ASEL,S,AREA,,3,15,3
ASEL,A,AREA,,16,,0
VEXT,ALL,,,X2-X1,,,
ALLSEL


ASEL,S,LOC,X,X2,,0,1
ASEL,R,LOC,Z,Z0,Z1,1
EXTOPT,ESIZE,(No_soil_ele_betwn_sleeper_B)*(No_sleeper_div_BLDG)
VEXT,ALL,,,X3-X2,,,


ASEL,S,LOC,X,X3,,0,1
ASEL,R,LOC,Z,Z0,Z1,1
EXTOPT,ESIZE,(No_soil_ele_betwn_sleeper_NB)*(No_sleeper_div_X3_X4)
VEXT,ALL,,,X4-X3,,,
ALLSEL
!============Creating the fastner springs===============  !

!--------X-------------!
TYPE,5
MAT,7
REAL,7
*GET,KP_FS1,KP,,COUNT, , , ,                          !-->>>> KP_FS1 stands for KP# just before
creating Fast spring KPs(X)
*GET,Line_FS1,LINE,,COUNT, , , ,
K,KP_FS1+1,Rigid,-(R_Gage/2),Z4
K,KP_FS1+2,Rigid,-(R_Gage/2),Z3
K,KP_FS1+3,Rigid, 0.75565,Z4
K,KP_FS1+4,Rigid, 0.75565,Z3

L,KP_FS1+1,KP_FS1+2
L,KP_FS1+3,KP_FS1+4
LSEL,S,LINE,,Line_FS1+1,Line_FS1+2,1
LESIZE,ALL,,,1,,1,,,1
LMESH,ine_FS1+1,Line_FS1+2,1
LGEN,No_sleeper_div_total+1,Line_FS1+1,Line_FS1+2,1,Distance_betw_sleepers,,,0,0,0
        !LGEN, ITIME, NL1, NL2, NINC, DX, DY, DZ, KINC, NOELEM,IMOVE
ALLSEL
!-----------Y-------------!
TYPE,6
MAT,8
REAL,8
*GET,KP_FS2,KP,,COUNT, , , ,                          !-->>>> KP_FS2 stands for KP# just before
creating Fast spring KPs(Y)
*GET,Line_FS2,LINE,,COUNT, , , ,


K,KP_FS2+1,Rigid,-(R_Gage/2),Z4
```

APPENDIX A (CONTINUED)

```
K,KP_FS2+2,Rigid,-(R_Gage/2),Z3
K,KP_FS2+3,Rigid, 0.75565,Z4
K,KP_FS2+4,Rigid, 0.75565,Z3

L,KP_FS2+1,KP_FS2+2
L,KP_FS2+3,KP_FS2+4

LSEL,S,LINE,,Line_FS2+1,Line_FS2+2,1
LESIZE,ALL,,,1,,1,,,1

LMESH,Line_FS2+1,Line_FS2+2,1
LGEN,No_sleeper_div_total+1,Line_FS2+1,Line_FS2+2,1,Distance_betw_sleepers,,,0,0,0

ALLSEL

!------------------Z----------------------------!

TYPE,7
MAT,9
REAL,9


*GET,KP_FS3,KP,,COUNT, , , ,                              !-->>>> KP_FS3 stands for KP# just before
creating Fast spring KPs(Z)
*GET,Line_FS3,LINE,,COUNT, , , ,


K,KP_FS3+1,Rigid,-(R_Gage/2),Z4
K,KP_FS3+2,Rigid,-(R_Gage/2),Z3
K,KP_FS3+3,Rigid, 0.75565,Z4
K,KP_FS3+4,Rigid, 0.75565,Z3

L,KP_FS3+1,KP_FS3+2
L,KP_FS3+3,KP_FS3+4


LSEL,S,LINE,,Line_FS3+1,Line_FS3+2,1
LESIZE,ALL,,,1,,1,,,1

LMESH,Line_FS3+1,Line_FS3+2,1
LGEN,No_sleeper_div_total+1,Line_FS3+1,Line_FS3+2,1,Distance_betw_sleepers,,,0,0,0
ALLSEL

!+++++++++++++++++++++++++++++++++++++++++++++++++++++++++++++++++++++++++++++++++++
++++++++++++++++++++++++++++
!+++++++++++++++++++++++++++++++++++++++++++++++++++++++++++++++++++++++++++++++++++
++++++++++++++++++++++++++++


!-----------------------------Creating a local co-ordinate system for the building:

LOCAL, 11, CART, XBB, YBB, ZBB, 0, 0, 0, ,
CSYS,11
*GET,KP_BLDG_STR,KP,,COUNT, , , ,
*GET,Line_BLDG_STR,LINE,,COUNT, , , ,
!---------------------------------------Base of the building-----------------------------------!

FX1=2.4
FX2=2.7
```

APPENDIX A (CONTINUED)

FX3=3.3
FX4=3.6

FY1=2.4
FY2=2.7
FY3=3.3
FY4=3.6

! ----------------------Flexible spread footing(Keypoints)----------!
K,KP_BLDG_STR+1,FY4,-FY4,0
K,KP_BLDG_STR+2,FX1,-FY4,0
K,KP_BLDG_STR+3,FX1,-FY1,0
K,KP_BLDG_STR+4,FY4,-FY1,0
K,KP_BLDG_STR+5,-FX1,-FY4,0
K,KP_BLDG_STR+6,-FX4,-FY4,0
K,KP_BLDG_STR+7,-FX4,-FY1,0
K,KP_BLDG_STR+8,-FX1,-FY1,0

K,KP_BLDG_STR+9,-FX1,FY1,0
K,KP_BLDG_STR+10,-FX4,FY1,0
K,KP_BLDG_STR+11,-FX4,FY4,0
K,KP_BLDG_STR+12,-FX1,FY4,0

K,KP_BLDG_STR+13,FY4,FY1,0
K,KP_BLDG_STR+14,FX1,FY1,0
K,KP_BLDG_STR+15,FX1,FY4,0
K,KP_BLDG_STR+16,FY4,FY4,0

!------Beams at the base[1st layer] - (Keypoints)-------!

K,KP_BLDG_STR+17,FX1,-FY3,0
K,KP_BLDG_STR+18,-FX1,-FY3,0
K,KP_BLDG_STR+19,-FX1,-FY2,0
K,KP_BLDG_STR+20,FX1,-FY2,0

K,KP_BLDG_STR+21,-FX2,-FY1,0
K,KP_BLDG_STR+22,-FX3,-FY1,0
K,KP_BLDG_STR+23,-FX3,FY1,0
K,KP_BLDG_STR+24,-FX2,FY1,0

K,KP_BLDG_STR+25,FX1,FY2,0
K,KP_BLDG_STR+26,-FX1,FY2,0
K,KP_BLDG_STR+27,-FX1,FY3,0
K,KP_BLDG_STR+28,FX1,FY3,0

K,KP_BLDG_STR+29,FX3,-FY1,0
K,KP_BLDG_STR+30,FX2,-FY1,0
K,KP_BLDG_STR+31,FX2,FY1,0
K,KP_BLDG_STR+32,FX3,FY1,0

!--!

APPENDIX A (CONTINUED)

!--------------------Area defined by the flexible spread footings and base beam(1st layer)--------------!

```
*GET,A_BEFORE_BLDG,AREA,0,COUNT
A,KP_BLDG_STR+1,KP_BLDG_STR+2,KP_BLDG_STR+3,KP_BLDG_STR+4
A,KP_BLDG_STR+5,KP_BLDG_STR+6,KP_BLDG_STR+7,KP_BLDG_STR+8
A,KP_BLDG_STR+9,KP_BLDG_STR+10,KP_BLDG_STR+11,KP_BLDG_STR+12
A,KP_BLDG_STR+13,KP_BLDG_STR+14,KP_BLDG_STR+15,KP_BLDG_STR+16

A,KP_BLDG_STR+17,KP_BLDG_STR+18,KP_BLDG_STR+19,KP_BLDG_STR+20
A,KP_BLDG_STR+21,KP_BLDG_STR+22,KP_BLDG_STR+23,KP_BLDG_STR+24
A,KP_BLDG_STR+25,KP_BLDG_STR+26,KP_BLDG_STR+27,KP_BLDG_STR+28
A,KP_BLDG_STR+29,KP_BLDG_STR+30,KP_BLDG_STR+31,KP_BLDG_STR+32
```

```
!---------Dividing the base beam (length(parallel to rail)) into 0.15m elements---------!
LSEL,S,LINE,,Line_BLDG_STR+17,Line_BLDG_STR+31,2
LESIZE,ALL,0.15
```

```
!---------Dividing the base beam (width(length perpendicular to rail)) into 0.3m elements---------!
LSEL,S,LINE,,Line_BLDG_STR+18,Line_BLDG_STR+32,2
LESIZE,ALL,0.3
```

```
!--------Dividing sides of flexible footing parallel to the rails by 8 ----!
LSEL,S,LINE,,Line_BLDG_STR+1,Line_BLDG_STR+15,2
LESIZE,ALL,,,8,,1,,,1
```

```
!--------Dividing sides of flexible footing perpendicular to the rails by 4 ----!
LSEL,S,LINE,,Line_BLDG_STR+2,Line_BLDG_STR+16,2
LESIZE,ALL,,,4,,1,,,1
TYPE,4
MAT,10
AMESH,A_BEFORE_BLDG+1,A_BEFORE_BLDG+8,1
```

```
!----Extruding the spread footing and the beam by 0.6 m (1 element)---!
TYPE,3
MAT,10
REAL,1

EXTOPT,ESIZE,1
EXTOPT,ACLEAR,1
VEXT,A_BEFORE_BLDG+1,A_BEFORE_BLDG+8,1,,,HSF
```

```
*GET,VOL_BEFORE_BLDG,VOLU,0,COUNT
```

!--Keypoints for Columns(0.8x0.8m)-------------!

```
ALLSEL
*GET,KP_COLUMN1,KP,,COUNT, , , ,
*GET,Line_COLUMN1,LINE,,COUNT, , , ,
*GET,A_BEFORE_COLUMN1,AREA,0,COUNT
CX1=2.7
CX2=3.3
```

APPENDIX A (CONTINUED)

```
CY1=2.7
CY2=3.3

K,KP_COLUMN1+1,CX2,-CY2,HSF
K,KP_COLUMN1+2,CX1,-CY2,HSF
K,KP_COLUMN1+3,CX1,-CY1,HSF
K,KP_COLUMN1+4,CX2,-CY1,HSF
K,KP_COLUMN1+5,-CX1,-CY2,HSF
K,KP_COLUMN1+6,-CX2,-CY2,HSF
K,KP_COLUMN1+7,-CX2,-CY1,HSF
K,KP_COLUMN1+8,-CX1,-CY1,HSF
K,KP_COLUMN1+9,-CX1,CY1,HSF
K,KP_COLUMN1+10,-CX2,CY1,HSF
K,KP_COLUMN1+11,-CX2,CY2,HSF
K,KP_COLUMN1+12,-CX1,CY2,HSF
K,KP_COLUMN1+13,CX2,CY1,HSF
K,KP_COLUMN1+14,CX1,CY1,HSF
K,KP_COLUMN1+15,CX1,CY2,HSF
K,KP_COLUMN1+16,CX2,CY2,HSF

!-------------------------------------------Creating areas for columns--------------!

A,KP_COLUMN1+1,KP_COLUMN1+2,KP_COLUMN1+3,KP_COLUMN1+4
A,KP_COLUMN1+5,KP_COLUMN1+6,KP_COLUMN1+7,KP_COLUMN1+8
A,KP_COLUMN1+9,KP_COLUMN1+10,KP_COLUMN1+11,KP_COLUMN1+12
A,KP_COLUMN1+13,KP_COLUMN1+14,KP_COLUMN1+15,KP_COLUMN1+16

!--------------Dividing sides of the column parallel to rail into 0.15 m -----------!

LSEL,S,LINE,,Line_COLUMN1+1,Line_COLUMN1+15,2
LESIZE,ALL,0.15

!--------------Dividing sides of the column perpendicular to rail into 0.3 m -----------!
LSEL,S,LINE,,Line_COLUMN1+2,Line_COLUMN1+16,2
LESIZE,ALL,0.3


TYPE,4
AMESH,A_BEFORE_COLUMN1+1,A_BEFORE_COLUMN1+4,1



!------------------Extrusion for columns(to 6 element{length=3.6 m}) --------------------------!

TYPE,3
MAT,10
EXTOPT,ESIZE,6
EXTOPT,ACLEAR,1
VEXT,A_BEFORE_COLUMN1+1,A_BEFORE_COLUMN1+4,1,,,3.6

!-------------------Keypoints for beams -----------------------------!
ALLSEL
*GET,KP_BEAM1,KP,,COUNT, , , ,

*GET,Line_BEAM1,LINE,,COUNT, , , ,

K,KP_BEAM1+1,CX1,-FY3,HSF
K,KP_BEAM1+2,-CX1,-FY3,HSF
K,KP_BEAM1+3,-CX1,-FY2,HSF
```

APPENDIX A (CONTINUED)

```
K,KP_BEAM1+4,CX1,-FY2,HSF
K,KP_BEAM1+5,-FX2,-CY1,HSF
K,KP_BEAM1+6,-FX3,-CY1,HSF
K,KP_BEAM1+7,-FX3,CY1,HSF
K,KP_BEAM1+8,-FX2,CY1,HSF
K,KP_BEAM1+9,CX1,FY2,HSF
K,KP_BEAM1+10,-CX1,FY2,HSF
K,KP_BEAM1+11,-CX1,FY3,HSF
K,KP_BEAM1+12,CX1,FY3,HSF
K,KP_BEAM1+13,FX3,-CY1,HSF
K,KP_BEAM1+14,FX2,-CY1,HSF
K,KP_BEAM1+15,FX2,CY1,HSF
K,KP_BEAM1+16,FX3,CY1,HSF



!-------------------Areas for beams----------------!
*GET,A_BEAM1,AREA,,COUNT, , , ,


A,KP_BEAM1+1,KP_BEAM1+2,KP_BEAM1+3,KP_BEAM1+4
A,KP_BEAM1+5,KP_BEAM1+6,KP_BEAM1+7,KP_BEAM1+8
A,KP_BEAM1+9,KP_BEAM1+10,KP_BEAM1+11,KP_BEAM1+12
A,KP_BEAM1+13,KP_BEAM1+14,KP_BEAM1+15,KP_BEAM1+16

!----Dividing the side of beam1 perpendicular to rail into 0.3 m elements----!
LSEL,S,LINE,,Line_BEAM1+2,Line_BEAM1+16,2
LESIZE,ALL,0.3

!----Dividing the side of beam1 parallel to rail into 0.15 m elements----!
LSEL,S,LINE,,Line_BEAM1+1,Line_BEAM1+15,2
LESIZE,ALL,0.15


TYPE,4
AMESH,A_BEAM1+1,A_BEAM1+4,1


!---------------Extruding beam1 by 1 element(length= 0.6m)----------!
ALLSEL
TYPE,3
MAT,10
EXTOPT,ESIZE,1
EXTOPT,ACLEAR,1
VEXT,A_BEAM1+1,A_BEAM1+4,1,,,0.6



!------Creating keypoints for beam 2

*GET,KP_BEAM2,KP,,COUNT, , , ,
*GET,Line_BEAM2,LINE,,COUNT, , , ,
*GET,A_BEAM2,AREA,,COUNT, , , ,

K,KP_BEAM2+1,CX1,-FY3,3.6
K,KP_BEAM2+2,-CX1,-FY3,3.6
K,KP_BEAM2+3,-CX1,-FY2,3.6
K,KP_BEAM2+4,CX1,-FY2,3.6
K,KP_BEAM2+5,-FX2,-CY1,3.6
```

APPENDIX A (CONTINUED)

```
K,KP_BEAM2+6,-FX3,-CY1,3.6
K,KP_BEAM2+7,-FX3,CY1,3.6
K,KP_BEAM2+8,-FX2,CY1,3.6
K,KP_BEAM2+9,CX1,FY2,3.6
K,KP_BEAM2+10,-CX1,FY2,3.6
K,KP_BEAM2+11,-CX1,FY3,3.6
K,KP_BEAM2+12,CX1,FY3,3.6
K,KP_BEAM2+13,FX3,-CY1,3.6
K,KP_BEAM2+14,FX2,-CY1,3.6
K,KP_BEAM2+15,FX2,CY1,3.6
K,KP_BEAM2+16,FX3,CY1,3.6


!---Creating areas for Beam2----!


A,KP_BEAM2+1,KP_BEAM2+2,KP_BEAM2+3,KP_BEAM2+4
A,KP_BEAM2+5,KP_BEAM2+6,KP_BEAM2+7,KP_BEAM2+8
A,KP_BEAM2+9,KP_BEAM2+10,KP_BEAM2+11,KP_BEAM2+12
A,KP_BEAM2+13,KP_BEAM2+14,KP_BEAM2+15,KP_BEAM2+16



!----Dividing the side of beam2 perpendicular to rail into 0.3 m elements----!
LSEL,S,LINE,,Line_BEAM2+2,Line_BEAM2+16,2
LESIZE,ALL,0.3

!----Dividing the side of beam2 parallel to rail into 0.15 m elements----!
LSEL,S,LINE,,Line_BEAM2+1,Line_BEAM2+15,2
LESIZE,ALL,0.15


TYPE,4
AMESH,A_BEAM2+1,A_BEAM2+4,1


!--------------------Extruding beam2 by 1 elements(length= 0.6 m)-----------!

TYPE,3
MAT,10
EXTOPT,ESIZE,1
EXTOPT,ACLEAR,1
VEXT,A_BEAM2+1,A_BEAM2+4,1,,,0.6


!------------------Creating 1st slab------------------!
ALLSEL
*GET,KP_SLAB1,KP,,COUNT
*GET,LINE_SLAB1,LINE,,COUNT
*GET,A_SLAB1,AREA,,COUNT


K,KP_SLAB1+1,CX2,-CY2,Z_SLAB1_BASE
K,KP_SLAB1+2,-CX2,-CY2,Z_SLAB1_BASE
K,KP_SLAB1+3,-CX2,CY2,Z_SLAB1_BASE
K,KP_SLAB1+4,CX2,CY2,Z_SLAB1_BASE

A,KP_SLAB1+1,KP_SLAB1+2,KP_SLAB1+3,KP_SLAB1+4
```

APPENDIX A (CONTINUED)

```
!------------Dividing side of slab1 perpendicular to rail into 0.3 m elements----!
LSEL,S,LINE,,LINE_SLAB1+2,LINE_SLAB1+4,2
LESIZE,ALL,0.3

!----Dividing the side of slab1 parallel to rail into 0.15 m elements----!
LSEL,S,LINE,,LINE_SLAB1+1,LINE_SLAB1+3,2
LESIZE,ALL,0.15


TYPE,4
AMESH,A_SLAB1+1

!-----------------Extruding Slab1 by 1 element(length=0.2m)-------!

TYPE,3
MAT,10
EXTOPT,ESIZE,1
EXTOPT,ACLEAR,1
VEXT,A_SLAB1+1,,0,,,0.2

!--------------------------------Copying areas of columns on the slab1 surface (Offset distance DZ= 3.8m)--
--------------------!

ALLSEL
*GET,KP_COLUMN2,KP,,COUNT
*GET,LINE_COLUMN2,LINE,,COUNT
*GET,A_BEFORE_COLUMN2,AREA,,COUNT

AGEN,2,A_BEFORE_COLUMN1+1,A_BEFORE_COLUMN1+4,1,,,3.8,,0,0


!------------Dividing side of column2 perpendicular to rail into 0.3 m elements----!
LSEL,S,LINE,,LINE_COLUMN2+2,LINE_COLUMN2+16,2
LESIZE,ALL,0.3


!-------Dividing the side of column2 parallel to rail into 0.15 m elements----!
LSEL,S,LINE,,LINE_COLUMN2+1,LINE_COLUMN2+15,2
LESIZE,ALL,0.15


TYPE,4
AMESH,A_BEFORE_COLUMN2+1,A_BEFORE_COLUMN2+4,1



!-----------------Extrusion of columns2 to 6 elements(length 3.6 m)--------------------------!

TYPE,3
MAT,10
EXTOPT,ESIZE,6
EXTOPT,ACLEAR,1
VEXT,A_BEFORE_COLUMN2+1,A_BEFORE_COLUMN2+4,1,,,3.6


!-------------------Copying and offsetting areas of beam below the topmost slab(Offset distance=3.8 m)-----
-------------------------!
```

APPENDIX A (CONTINUED)

```
ALLSEL
*GET,KP_BEAM3,KP,,COUNT, , , ,
*GET,Line_BEAM3,LINE,,COUNT, , , ,
*GET,A_BEAM3,AREA,,COUNT, , , ,

AGEN,2,A_BEAM2+1,A_BEAM2+4,1,,,3.8,,0,0
!----Dividing the side of beam3 perpendicular to rail into 0.3 m elements----!
LSEL,S,LINE,,Line_BEAM3+2,Line_BEAM3+16,2
LESIZE,ALL,0.3

!----Dividing the side of beam3 parallel to rail into 0.15 m elements----!
LSEL,S,LINE,,Line_BEAM3+1,Line_BEAM3+15,2
LESIZE,ALL,0.15


TYPE,4
AMESH,A_BEAM3+1,A_BEAM3+4,1


!--------------------Extruding beam3 by 1 elements(length= 0.6 m)-----------!

TYPE,3
MAT,10
EXTOPT,ESIZE,1
EXTOPT,ACLEAR,1
VEXT,A_BEAM3+1,A_BEAM3+4,1,,,0.6




!---------------Creating the topmost slab----------------!
ALLSEL
*GET,KP_SLAB2,KP,,COUNT
*GET,LINE_SLAB2,LINE,,COUNT
*GET,A_SLAB2,AREA,,COUNT


K,KP_SLAB2+1,CX2,-CY2,Z_SLAB2_BASE
K,KP_SLAB2+2,-CX2,-CY2,Z_SLAB2_BASE
K,KP_SLAB2+3,-CX2,CY2,Z_SLAB2_BASE
K,KP_SLAB2+4,CX2,CY2,Z_SLAB2_BASE

A,KP_SLAB2+1,KP_SLAB2+2,KP_SLAB2+3,KP_SLAB2+4


!------------Dividing side of slab2 perpendicular to rail into 0.3 m elements----!
LSEL,S,LINE,,LINE_SLAB2+2,LINE_SLAB2+4,2
LESIZE,ALL,0.3


!----Dividing the side of slab2 parallel to rail into 0.15 m elements----!
LSEL,S,LINE,,LINE_SLAB2+1,LINE_SLAB2+3,2
LESIZE,ALL,0.15


TYPE,4
AMESH,A_SLAB2+1
```

APPENDIX A (CONTINUED)

```
!----------------Extruding Slab2 by 1 element(length=0.2m)-------!

TYPE,3
MAT,10
EXTOPT,ESIZE,1
EXTOPT,ACLEAR,1
VEXT,A_SLAB2+1,,0,,,0.2




!++++++++++++++++++++++++ Wall 1 ++++++++++++++++++++++++!

ALLSEL
*GET,KP_WALL1,KP,,COUNT
*GET,LINE_WALL1,LINE,,COUNT
*GET,A_WALL1,AREA,,COUNT


K,KP_WALL1+1,FX1,-FY4,0
K,KP_WALL1+2,-FX1,-FY4,0
K,KP_WALL1+3,-FX1,-FY3,0
K,KP_WALL1+4,FX1,-FY3,0

K,KP_WALL1+5,-FX3,-FY1,0
K,KP_WALL1+6,-FX4,-FY1,0
K,KP_WALL1+7,-FX4,FY1,0
K,KP_WALL1+8,-FX3,FY1,0

K,KP_WALL1+9,FX1,FY3,0
K,KP_WALL1+10,-FX1,FY3,0
K,KP_WALL1+11,-FX1,FY4,0
K,KP_WALL1+12,FX1,FY4,0

K,KP_WALL1+13,FX4,-FY1,0
K,KP_WALL1+14,FX3,-FY1,0
K,KP_WALL1+15,FX3,FY1,0
K,KP_WALL1+16,FX4,FY1,0


A,KP_WALL1+1,KP_WALL1+2,KP_WALL1+3,KP_WALL1+4
A,KP_WALL1+5,KP_WALL1+6,KP_WALL1+7,KP_WALL1+8
A,KP_WALL1+9,KP_WALL1+10,KP_WALL1+11,KP_WALL1+12
A,KP_WALL1+13,KP_WALL1+14,KP_WALL1+15,KP_WALL1+16

LSEL,S,LINE,,LINE_WALL1+1,LINE_WALL1+15,2
LESIZE,ALL,0.15


LSEL,S,LINE,,LINE_WALL1+2,LINE_WALL1+16,2
LESIZE,ALL,0.3


TYPE,4
ASEL,S,AREA,,A_WALL1+1,A_WALL1+4,1
AMESH,A_WALL1+1,A_WALL1+4,1


TYPE,3
MAT,10
```

APPENDIX A (CONTINUED)

```
EXTOPT,ESIZE,4
EXTOPT,ACLEAR,1
VEXT,A_WALL1+1,A_WALL1+4,1,,,Z1-ZBB


!===================================================
!==============Wall-2============================

ALLSEL
*GET,KP_WALL2,KP,,COUNT
*GET,LINE_WALL2,LINE,,COUNT
*GET,A_WALL2,AREA,,COUNT


K,KP_WALL2+1,FX4,-FY4,HSF
K,KP_WALL2+2,FX1,-FY4,HSF
K,KP_WALL2+3,FX1,-CY2,HSF
K,KP_WALL2+4,FX4,-CY2,HSF


K,KP_WALL2+5,-FX1,-FY4,HSF
K,KP_WALL2+6,-FX4,-FY4,HSF
K,KP_WALL2+7,-FX4,-CY2,HSF
K,KP_WALL2+8,-FX1,-CY2,HSF
K,KP_WALL2+9,-FX1,CY2,HSF
K,KP_WALL2+10,-FX4,CY2,HSF
K,KP_WALL2+11,-FX4,FY4,HSF
K,KP_WALL2+12,-FX1,FY4,HSF
K,KP_WALL2+13,FX4,CY2,HSF
K,KP_WALL2+14,FX1,CY2,HSF
K,KP_WALL2+15,FX1,FY4,HSF
K,KP_WALL2+16,FX4,FY4,HSF
A,KP_WALL2+1,KP_WALL2+2,KP_WALL2+3,KP_WALL2+4
A,KP_WALL2+5,KP_WALL2+6,KP_WALL2+7,KP_WALL2+8
A,KP_WALL2+9,KP_WALL2+10,KP_WALL2+11,KP_WALL2+12
A,KP_WALL2+13,KP_WALL2+14,KP_WALL2+15,KP_WALL2+16

LSEL,S,LINE,,LINE_WALL2+1,LINE_WALL2+15,2
LESIZE,ALL,0.15


LSEL,S,LINE,,LINE_WALL2+2,LINE_WALL2+16,2
LESIZE,ALL,0.3
TYPE,4
AMESH,A_WALL2+1,A_WALL2+4,1
TYPE,3
MAT,10
EXTOPT,ESIZE,3
EXTOPT,ACLEAR,1
VEXT,A_WALL2+1,A_WALL2+4,1,,,(Z1-ZBB)-HSF


!================ WALL 3 ================!
ALLSEL
*GET,KP_WALL3,KP,,COUNT
*GET,LINE_WALL3,LINE,,COUNT
*GET,A_WALL3,AREA,,COUNT
K,KP_WALL3+1,FX4,-CY2,HSF
```

APPENDIX A (CONTINUED)

```
K,KP_WALL3+2,CX2,-CY2,HSF
K,KP_WALL3+3,CX2,-FY1,HSF
K,KP_WALL3+4,FX4,-FY1,HSF
K,KP_WALL3+5,-CX2,-CY2,HSF
K,KP_WALL3+6,-FX4,-CY2,HSF
K,KP_WALL3+7,-FX4,-FY1,HSF
K,KP_WALL3+8,-CX2,-FY1,HSF
K,KP_WALL3+9,-CX2,FY1,HSF
K,KP_WALL3+10,-FX4,FY1,HSF
K,KP_WALL3+11,-FX4,CY2,HSF
K,KP_WALL3+12,-CX2,CY2,HSF
K,KP_WALL3+13,FX4,FY1,HSF
K,KP_WALL3+14,CX2,FY1,HSF
K,KP_WALL3+15,CX2,CY2,HSF
K,KP_WALL3+16,FX4,CY2,HSF
A,KP_WALL3+1,KP_WALL3+2,KP_WALL3+3,KP_WALL3+4
A,KP_WALL3+5,KP_WALL3+6,KP_WALL3+7,KP_WALL3+8
A,KP_WALL3+9,KP_WALL3+10,KP_WALL3+11,KP_WALL3+12
A,KP_WALL3+13,KP_WALL3+14,KP_WALL3+15,KP_WALL3+16
LSEL,S,LINE,,LINE_WALL3+1,LINE_WALL3+15,2
LESIZE,ALL,0.15
LSEL,S,LINE,,LINE_WALL3+2,LINE_WALL3+16,2
LESIZE,ALL,0.3
TYPE,4
AMESH,A_WALL3+1,A_WALL3+4,1
TYPE,3
MAT,10
EXTOPT,ESIZE,3
EXTOPT,ACLEAR,1
VEXT,A_WALL3+1,A_WALL3+4,1,,,(Z1-ZBB)-HSF
!-----------------------Soil Keypoints on the building-side-----------!
CSYS,0                          !---->>> Changing co-ordinate axis back to global cartesian

ALLSEL
*GET,KP_SOIL,KP,,COUNT
*GET,LINE_SOIL,LINE,,COUNT
*GET,A_SOIL,AREA,,COUNT
K,KP_SOIL+1,X1,YS3,Z1
K,KP_SOIL+2,X1,YS3,Z0
K,KP_SOIL+3,X1,YS2,Z1
K,KP_SOIL+4,X1,YS2,Z0
K,KP_SOIL+5,X1,YS3,ZBB
K,KP_SOIL+6,X1,YS2,ZBB
A,KP_SLP_END+28,KP_SLP_END+27,KP_SOIL+1,KP_SOIL+2
A,KP_SOIL+2,KP_SOIL+5,KP_SOIL+6,KP_SOIL+4
A,KP_SOIL+4,KP_SOIL+3,KP_SLP_END+23,KP_SLP_END+24
A,KP_SOIL+5,KP_SOIL+1,KP_SOIL+3,KP_SOIL+6
LSEL,S,LINE,,LINE_SOIL+1,LINE_SOIL+9,2
LSEL,A,LINE,,LINE_SOIL+12,LINE_SOIL+14,2
LESIZE,ALL,0.6
LSEL,S,LINE,,LINE_SOIL+6,LINE_SOIL+10,2
LSEL,A,LINE,,LINE_SOIL+11,LINE_SOIL+13,2
LSEL,U,LINE,,LINE_SOIL+10,LINE_SOIL+11,1
LESIZE,ALL,0.3

LSEL,S,LINE,,LINE_SOIL+10,LINE_SOIL+11,1
LESIZE,ALL,,,5,1,,,1
LSEL,S,LINE,,LINE_SOIL+2,LINE_SOIL+4,2
LESIZE,ALL,,,3,1,,,1
```

APPENDIX A (CONTINUED)

```
TYPE,4
AMESH,A_SOIL+1,A_SOIL+4,1
TYPE,2
MAT,6
EXTOPT,ESIZE,(No_sleeper_div_X1_X2)*(No_soil_ele_betwn_sleeper_NB)
EXTOPT,ACLEAR,1
VEXT,A_SOIL+1,A_SOIL+3,1,X2-X1,,
ASEL,S,LOC,X,X2,,0
ASEL,U,LOC,Y,YS0,YS1,1
ASEL,R,LOC,Z,Z0,ZBB,1
ASEL,A,LOC,Y,YS1,YS2,1
ASEL,R,LOC,X,X2,,0
ASEL,A,LOC,Y,YS3,YS4,1
ASEL,R,LOC,X,X2,,0
TYPE,2
EXTOPT,ESIZE,(No_sleeper_div_BLDG)*(No_soil_ele_betwn_sleeper_B)
VEXT,ALL,,,X3-X2,,
ASEL,S,LOC,X,X3,,0
ASEL,U,LOC,Y,YS0,YS1,1
ASEL,R,LOC,Z,Z0,ZBB,1
ASEL,A,LOC,Y,YS1,YS2,1
ASEL,R,LOC,X,X3,,0
ASEL,A,LOC,Y,YS3,YS4,1
ASEL,R,LOC,X,X3,,0
TYPE,2
EXTOPT,ESIZE,(No_sleeper_div_X3_X4)*(No_soil_ele_betwn_sleeper_NB)
EXTOPT,ACLEAR,1
VEXT,ALL,,,X4-X3,,
ALLSEL
ASEL,S,AREA,,A_SOIL+4,,0
TYPE,2

EXTOPT,ESIZE,(No_soil_ele_betwn_sleeper_NB)*((X2-X1)/Distance_betw_sleepers)
EXTOPT,ACLEAR,1
VEXT,ALL,,0,(X2-X1),,
ALLSEL
AGEN,2,A_SOIL+4,,0,X3-X1,,,,0,0
ALLSEL
*GET,KP_SOIL_END,KP,,COUNT
*GET,LINE_SOIL_END,LINE,,COUNT
*GET,A_SOIL_END,AREA,,COUNT
TYPE,4
ASEL,S,AREA,,A_SOIL_END,,0
AMESH,A_SOIL_END,,0
TYPE,2
MAT,6
EXTOPT,ESIZE,(No_soil_ele_betwn_sleeper_NB)*((X4-X3)/Distance_betw_sleepers)
EXTOPT,ACLEAR,1
VEXT,A_SOIL_END,,0,(X4-X3),,
ALLSEL
EPLOT
!================================Initial
Conditions=========================================!

ALLSEL
NUMMRG,NODE
NUMCMP,NODE
NUMCMP,ELEM
```

APPENDIX A (CONTINUED)

```
NSEL,ALL
IC,ALL,ALL,0,0
!=========================BOUNDARY
CONDITIONS=============================================!
!-----------------Fixing the base---------------!
ALLSEL
NSEL,S,LOC,Z,0
D,ALL,UX,0
D,ALL,UY,0
D,ALL,UZ,0

!--------------Fixing X displacement for the nodes on the outer face of soil perpendicular to the rails----------------!
ALLSEL
NSEL,S,LOC,X,X1
NSEL,A,LOC,X,X4
D,ALL,UX,0
!--------------Fixing Y displacement for the nodes on the outer face of soil perpendicular to the above
face---------------!
ALLSEL
NSEL,S,LOC,Y,YS4
NSEL,A,LOC,Y,YS0
D,ALL,UY,0
!------------------Selecting elements of rigid rails and applying fixed support to all its nodes---------------!
ALLSEL
ESEL,S,MAT,,2
NSLE
D,ALL,UX,0
D,ALL,UY,0
D,ALL,UZ,0

D,ALL,ROTX,0
D,ALL,ROTY,0
D,ALL,ROTZ,0
!----------------Constraining the rotations at the nodes of sleepers------------!
ALLSEL
ESEL,S,MAT,,3

NSLE
D,ALL,ROTX,0
D,ALL,ROTY,0
D,ALL,ROTZ,0
!----------------Constraining the rotation of the common nodes between rail and spring elements-----------!
ALLSEL
NSEL,S,NODE,,7,177,5
NSEL,A,NODE,,190,360,5

D,ALL,ROTX,0
D,ALL,ROTY,0
D,ALL,ROTZ,0

ALLSEL
EPLOT
!-------------------------MODAL ANALYSIS----------------------------------------------------------------!
/SOLU
ALLSEL
OUTRES,ALL,ALL
ANTYPE,MODAL          ! Choose modal analysis type
MODOPT,LANB,300      ! Choose the subspace mode-extraction method,
MXPAND,300       !Specifies the number of modes to expand and write for a modal or buckling analysis.
SOLVE
```

APPENDIX A (CONTINUED)

```
FINISH
/solu
n_Col=6          !number of columns in the data sheet
to_skip=0        !number of lines to skip
num_tim_step=810 !1201  !number of time steps
Num_Nodes=63884     !number of nodes in the model

/INQUIRE,numlines,LINES,Nodal_coord,csv
to_read=numlines-to_skip
!
*DEL,bc_table,,NOPR
! Number of rows reduced by one:
*DIM,bc_table,TABLE,to_read-1,n_Col-1            ! table array to hold data
*TREAD,bc_table,Nodal_coord,csv,,to_skip
 ! Move data to numerical Array
*DEL,bc_array,,NOPR
*DIM,bc_array,ARRAY,to_read,n_Col
 *do,j,1,n_Col
*vfun,bc_array(1,j),copy,bc_table(0,j-1)    ! Shift down and right
*enddo
 *do,j,1,num_tim_step
   *do,i,1,Num_Nodes,
    D,i,UX,bc_array(i+Num_nodes*(J-1),1)
    D,i,UY,bc_array(i+Num_nodes*(J-1),2)
    D,i,UZ,bc_array(i+Num_nodes*(J-1),3)
    D,i,ROTX,bc_array(i+Num_nodes*(J-1),4)
    D,i,ROTY,bc_array(i+Num_nodes*(J-1),5)
    D,i,ROTZ,bc_array(i+Num_nodes*(J-1),6)
   *enddo
/solu
Time,j
allsel
solve
 OUTRES,all,all
 save

*enddo
FINISH
!*
```

APPENDIX B

This ANSYS APDL code is used to extract the required data to be given to SAMS as input from the Modal analysis

```
NumExportModes = 300
StartMode = 1
!***** End of User-specified Data *****
EndMode = StartMode + NumExportModes - 1
/POST1
*cfopen, FEM_Output, txt, ,

!!!!!!!!!!!!!!!!
! Output NumNodes
!!!!!!!!!!!!!!!!

*get, NumNodes, NODE, 0, COUNT
*vwrite, 'NumNodes'
(a8)
*vwrite, NumNodes
(f8.0)
*vwrite, 'NumModes'
(a8)
*vwrite, NumExportModes
(f6.0)
!-------- IMPORTANT --------------!
!--------------------------------!

! the following is the density of each part,
! these values varies depnds on the used model.
! part1=Rails, part2= Sleepers,
! part3=Ballast, part4=sub-ballast
! part5=Sub-grade, part6=spring-x
! part7= spring-y, Part8=spring-z
! part9=Concrete

!---------------------------------------!
!_____ MODIFY _____!
!_____!

!----  the beam elemnts parts: Rails, sleepers
MassDensity_P1= 7700
MassDensity_P2= 2570


!----  the soil layers: Ballast, Sub-ballast, Sub_grade
MassDensity_P3= 1800
MassDensity_P4= 1850
MassDensity_P5= 1850

!----  the spring elemnts :
MassDensity_P6= 0
MassDensity_P7= 0
MassDensity_P8= 0
!---- Concrete structure:
MassDensity_P9=2500
!!!!!!!!!!!!!!!!
! Output nodal positions
!!!!!!!!!!!!!!!!

*vwrite, 'Node Pos'
```

APPENDIX B (CONTINUED)

```
 (a8)
*get, StartNode, NODE, 0, NUM, MIND
NodeI = StartNode

EnumI = 1
*dowhile, NodeI
  NodeX = nx(NodeI)
  NodeY = ny(NodeI)
  NodeZ = nz(NodeI)

  *vwrite, EnumI, NodeI, NodeX, NodeY, NodeZ
  (2f8.0, 3e25.16)

  NodeI = ndnext(NodeI)
  EnumI = EnumI + 1
*enddo


!!!!!!!!!!!!!!!
! Output frequencies
!!!!!!!!!!!!!!!

*vwrite, 'Freqs'
(a5)

*do, ModeI, StartMode, EndMode
  *get, ModeFreq, MODE, ModeI, FREQ
  *vwrite, ModeI, ModeFreq
  (f6.0, e24.16)
*enddo


!!!!!!!!!!!!!!!
! Output all mode shapes
!!!!!!!!!!!!!!!

*vwrite, 'Mode Sha', 'pe'
(a8, a2)

!Skip to the first displacements that represent
!the first mode that is desired to be output.
SET, FIRST
*if, StartMode, NE, 1, then
  *do, ModeI, 1, StartMode-1
    SET, NEXT
  *enddo
*endif

*do, ModeI, StartMode, EndMode
  *vwrite, 'Mode ', ModeI
  (a5, f5.0)

  !!!!!!!!!!!!!!!
  ! Output one mode shape
  !!!!!!!!!!!!!!!

  NodeI = StartNode

  !For each node, output its mode shape
  EnumI = 1
  *dowhile, NodeI
```

APPENDIX B (CONTINUED)

```
    DispX = ux(NodeI)
    DispY = uy(NodeI)
    DispZ = uz(NodeI)
    RotX  = rotx(NodeI)
    RotY  = roty(NodeI)
    RotZ  = rotz(NodeI)

    *vwrite, EnumI, NodeI, DispX, DispY, DispZ, RotX, RotY, RotZ
    (2f8.0, 6e25.16)


    NodeI = ndnext(NodeI)
    EnumI = EnumI + 1
  *enddo

  SET, NEXT
*enddo


!!!!!!!!!!!!!!!!
! Compute nodal masses
!!!!!!!!!!!!!!!!

!Allocate mem for nodes
*get, NodeMaxI, NODE, 0, NUM, MAXD
*dim, NodalMass, , NodeMaxI

! initializing the nodal mass.
*do, NodeI, 1, NodeMaxI
  NodalMass(NodeI) = 0
*enddo

!Compute mass of each elem and add mass to each node in the elem
!----------------------------------------!
!_____ MODIFY _____!
!_____!
*get, ElemI, ELEM, 0, NUM, MIND
*dowhile, ElemI

  *get, ElemVol, elem, ElemI, VOLU

  *if,ElemI,GE,1,AND,ElemI,LE,660,then
    *if,ElemI,GE,1,AND,ElemI,LE,364,then
     MassDensity=MassDensity_P1
    *elseif,ElemI,GE,365,AND,ElemI,LE,660,then
     MassDensity=MassDensity_P2
    *endif

       Node1 = nelem(ElemI, 1)
       Node2 = nelem(ElemI, 2)

       PartialMass = ElemVol*MassDensity/2

       NodalMass(Node1) = NodalMass(Node1) + PartialMass
       NodalMass(Node2) = NodalMass(Node2) + PartialMass

  *elseif,ElemI,GE,661,AND,ElemI,LE,18324,then

    *if,ElemI,GE,661,AND,ElemI,LE,3348,then
     MassDensity=MassDensity_P3
    *elseif,ElemI,GE,3349,AND,ElemI,LE,6036,then
```

APPENDIX B (CONTINUED)

```
    MassDensity=MassDensity_P4
 *elseif,ElemI,GE,6037,AND,ElemI,LE,18324,then
   MassDensity=MassDensity_P5

  *endif

     Node1 = nelem(ElemI, 1)
     Node2 = nelem(ElemI, 2)
     Node3 = nelem(ElemI, 3)
     Node4 = nelem(ElemI, 4)
     Node5 = nelem(ElemI, 5)
     Node6 = nelem(ElemI, 6)
     Node7 = nelem(ElemI, 7)
     Node8 = nelem(ElemI, 8)


     PartialMass = ElemVol*MassDensity/8

     NodalMass(Node1) = NodalMass(Node1) + PartialMass
     NodalMass(Node2) = NodalMass(Node2) + PartialMass
     NodalMass(Node3) = NodalMass(Node3) + PartialMass
     NodalMass(Node4) = NodalMass(Node4) + PartialMass
     NodalMass(Node5) = NodalMass(Node5) + PartialMass
     NodalMass(Node6) = NodalMass(Node6) + PartialMass
     NodalMass(Node7) = NodalMass(Node7) + PartialMass
     NodalMass(Node8) = NodalMass(Node8) + PartialMass



 *elseif,ElemI,GE,18325,AND,ElemI,LE,18546,then

   *if,ElemI,GE,18325,AND,ElemI,LE,18398,then
    MassDensity=MassDensity_P6
   *elseif,ElemI,GE,18399,AND,ElemI,LE,18472,then
    MassDensity=MassDensity_P7
   *elseif,ElemI,GE,18473,AND,ElemI,LE,18546,then
    MassDensity=MassDensity_P8
      *endif

     Node1 = nelem(ElemI, 1)
     Node2 = nelem(ElemI, 2)

     PartialMass = ElemVol*MassDensity/2

     NodalMass(Node1) = NodalMass(Node1) + PartialMass
     NodalMass(Node2) = NodalMass(Node2) + PartialMass


 *elseif,ElemI,GE,18547,AND,ElemI,LE,42762,then

   *if,ElemI,GE,18547,AND,ElemI,LE,22794,then
    MassDensity=MassDensity_P9
   *elseif,ElemI,GE,22795,AND,ElemI,LE,42762,then
    MassDensity=MassDensity_P5


   *endif

     Node1 = nelem(ElemI, 1)
```

APPENDIX B (CONTINUED)

```
        Node2 = nelem(ElemI, 2)
        Node3 = nelem(ElemI, 3)
        Node4 = nelem(ElemI, 4)
        Node5 = nelem(ElemI, 5)
        Node6 = nelem(ElemI, 6)
        Node7 = nelem(ElemI, 7)
        Node8 = nelem(ElemI, 8)

        PartialMass = ElemVol*MassDensity/8

        NodalMass(Node1) = NodalMass(Node1) + PartialMass
        NodalMass(Node2) = NodalMass(Node2) + PartialMass
        NodalMass(Node3) = NodalMass(Node3) + PartialMass
        NodalMass(Node4) = NodalMass(Node4) + PartialMass
        NodalMass(Node5) = NodalMass(Node5) + PartialMass
        NodalMass(Node6) = NodalMass(Node6) + PartialMass
        NodalMass(Node7) = NodalMass(Node7) + PartialMass
        NodalMass(Node8) = NodalMass(Node8) + PartialMass
   *endif
 ElemI = elnext(ElemI)
*enddo
! Output nodal masses

*vwrite, 'Node Mas', 's'
(a8, a1)
NodeI = StartNode
EnumI = 1
*dowhile, NodeI
  SingleMass = NodalMass(NodeI)
  *vwrite, EnumI, NodeI, SingleMass
  (2f8.0, e25.16)
  NodeI = ndnext(NodeI)
  EnumI = EnumI + 1
*enddo
*cfclos
FINISH
```

APPENDIX C

This is the Matlab code to reconstruct nodal accelerations of the entire model from the modal accelerations of the rail

```matlab
%--- constants
NN=63884;  % Total number of nodes in the system
NNR=336;   % Number of nodes on the rails
NM=300;      % Number of mode shapes
DOF=6;     % number of nodal DOF
%----  CHECK you entered the needed data above ---%
%-------------------------------------------------%
%--- Reading the Modal coordinates data (q) ---%
%
fid_1 = fopen('Sams_modal_acc.dat','r');
[cn,count1]=fscanf(fid_1,'%f %f %f %f %f %f %f %f %f',[NM+1,inf]);
Q=cn';
q=Q(:,2:end);  % FOR ALL TIME STEPS (timestemps X number of modes)


%--- Reading the Frequencies (f) ---%
fid_2 = fopen('Freqs.txt','r');
[cn1,count2]=fscanf(fid_2,'%f %f',[2,NM]);
f=cn1(2,:)';  %  frequencies
Omeg=f*2*pi;


for i=1:NM
    q(:,i)=q(:,i)/Omeg(i);
end

%--- Reading the mode shapes of the whole system ---%
fid_3 = fopen('MODE_SHAPES.txt','r');     %  This file was extuded as
FEM_Output but only for mode shapes
[cn,count1]=fscanf(fid_3,'%f %f %f %f %f %f %f %f %f',[DOF+2,inf]);
MODES=cn';

PHI=MODES(:,3:end);  %---  The all modes for the whole system  (NN*NM)X DOF

phi=PHI';
phi=phi(:);

modes_modif=zeros(NN*DOF,NM);
for i=1:NM
modes_modif(:,i)=phi(1+NN*DOF*(i-1):NN*DOF*i); % NDOFXNM
end

TS=length(Q);  % the number of time steps

A=zeros(NN*TS,DOF);   % Initializing U

for i=1:TS;
```

APPENDIX C (CONTINUED)

```
  a=modes_modif*q(i,:)';
  a1=reshape(a,DOF,NN)';
  A(1+NN*(i-1):NN*i,:)=a1;
end;

%--- Writing A for a file ---%
%-------------------------------%

csvwrite('Nodal_accln.csv',A);

fclose('all');
```

CITED LITERATURE

1. Moncef Toumi, Hugues Chollet, and Honoré Yin: Finite element analysis of the frictional wheel-rail rolling contact using explicit and implicit methods, An International Journal on the Science and Technology of Friction, Lubrication and Wear, pages 157-166, June 08 2016.

2. Xin Zhao, Zili Li: The solution of frictional wheel–rail rolling contact with a 3D transient finite element model: Validation and error analysis, An International Journal on the Science and Technology of Friction, Lubrication and Wear, Pages 444-451, October 10 2010.

3. A. Rovira, A. Roda, M.B. Marshall, H. Brunskill, R. Lewis: Experimental and numerical modelling of wheel–rail contact and wear,911-924,March 29 2011

4. H.E.M Hunt: Modelling Of Rail Vehicles and Track for Calculation of Ground-Vibration Transmission into Buildings, Journal of Sound and Vibration (1996) 1983(1), 185-194, November 20 1995.

5. T.G. Gutowski, C.L. Dym, Propagation of ground vibration: A review, Journal of Sound and Vibration, Volume 49, Issue 2, Pages 179-193, ISSN 0022-460X, 22 November 1976.

6. P. Galvin, J. Dominguez, High-speed train-induced ground motion and interaction with structures, Journal of Sound and Vibration 307 (2007) 755–777, August 23 2007.

7. G. Kouroussis, L. van Parys, C. Conti, and O. Verlinden, "Using three-dimensional finite element analysis in time domain to model railway-induced ground vibrations," Advances in Engineering Software, vol. 70, pp. 63–76, 2014.

8. V. Krylov. On the theory of railway-induced ground vibrations. Journal de Physique IVColloque, 04 (C5), pp.C5-769-C5-772, 1994.

9. Verbraken, H, Eysermans, H., Dechief, E., François, S., Degrande, G. and Lombaert, G.: Development of a hybrid prediction method for railway induced vibration.

10. Yeong-bin yang and hsiao-hui hung:A parametric study of wave barriers for reduction of train-induced vibrations, international journal for numerical methods in engineering, vol. 40, 3729-3747 (1997)

11. L.Andersen , S.R.K. Nielsen , Reduction of ground vibration by means of barriers or soli improvement along a railway track, Soil Dynamics and Earthquake engineering,Vol.25,pages 701-716, October 2005

12. M. Sanayei, P.Maurya, and J. A.Moore, "Measurement of building foundation and ground-borne vibrations due to surface trains and subways," Engineering Structures, Vol. 53, pp. 102–111,2013

13. Ebrahimi, S. and Eberhard, P.: Aspects of contact problems in computational multibody dynamics. In Multibody Dynamics, Pages 23–47. Springer, 2007.

14. Kumaran, G., Menon, D., and Nair, K.: Dynamic studies of rail track sleepers in a track structure system. Journal of Sound and Vibration, 268(3):485–501, Nov 27 2003.

15. Shabana A. A., Zaazaa K. E., S. H.: Railroad vehicle dynamics: A computational approach. Boca Raton, FL, Taylor and Francis/CRC, 2007.

16. Recuero A.M., Escalona J.L., and S.A.A.: Finite- element analysis of unsupported sleepers using three dimensional wheelrail contact formulation. Proceedings of the Institute of Mechanical Engineers, Part K: Journal of Multi-body Dynamics, 225 (2): 153-165, 2011.

17. Rosario Chamorro , Jose L.Escalona, Manuel Gonzalez , An approach for modeling long flexible bodies with application to railroad dynamics, Multibody Syst Dyn (2011) 26:135–152, May 2011.

18. Tanabe, M., Wakui, H., Sogabe, M., Matsumoto, N., and Tanabe, Y.: A combined multi- body and finite element approach for dynamic interaction analysis of high-speed train and railway structure including post-derailment behavior during an earthquake. IOP Conference Series: Materials Science and Engineering, 10(1):012144, 2010.

19. Galvín, P., Romero, A., and Domínguez, J.: Fully three-dimensional analysis of high-speed train–track–soil-structure dynamic interaction, Journal of Sound and Vibration, 329(24):5147–5163, 2010.

20. Liang Ling, Xin-Biao Xiao, Xue-Song Jin: Development of a simulation model for dynamic derailment analysis of high-speed trains, Acta Mechanica Sinica (2014) 30(6):860–875, September 3 2014.

21. El-Ghandour, A. I., Hamper, M. B., and Foster, C. D.: Coupled finite element

and multibody system dynamics modeling of a three-dimensional railroad system, Proceedings of the Institution of Mechanical Engineers, Part F: Journal of Rail and Rapid Transit, Vol.230(I) 283-294,2016

22. Vlasenko, D. and Kasper, R.: Generation of equations of motion in reference frame formulation for fem models. Engineering Letters, 16(4):537–544, 2008.

23. Rathod, C., Chamorro, R., Escalona, J., El-Sibaie, M., and Shabana, A.: Validation of three-dimensional multi-body system approach for modelling track flexibility. Proceedings of the Institution of Mechanical Engineers, Part K: Journal of Multi-body Dynamics, 223(4):269–282, 2009.

24. Shabana, A. : Dynamics of Multibody systems, Cambridge University press,2005

25. Meli, E. and Pugi, L.: Preliminary development, simulation and validation of a weigh in motion system for railway vehicles, Meccanica, 48(10):2541–2565, 2013.

26. Kalker, J.: Three-Dimensional Elastic Bodies in Rolling Contact. Kluwer Academic Publ, Dordrecht, 1 edition, 1990.

27. Shabana, A. A. and Yakoub, R. Y.: Three dimensional absolute nodal coordinate formulation for beam elements: theory. Journal of Mechanical Design, 123(4):606–613, 2001.

28. Shampine, L. F. and Gordon, M. K.: Computer solution of ordinary differential equations: the initial value problem. WH Freeman San Francisco, 1975.

29. Bednarz, J. and Targosz, J.: Finite elements method in analysis of vibrations wave propagation in the soil. Journal of KONES Powertrain and transport, 18(3), 2011.

30. Murray, T.M., Allen, D.E., and Ungar, E.E: Floor vibrations due to human activity, American Institute of Steel Construction, 2003.

31. American Railway Engineering and Maintenance-of-Way Association, 2009. Monfared, V.: Contact stress analysis in rolling bodies by finite element method statically, 2012.

VITA

SARVESH SURESH MASUREKAR

1012 S Oakley blvd , Apt 1, Chicago, IL-60612
smasur2@uic.edu   Contact no: +1-312-874-8247
www.linkedin.com/in/sarveshm21

OBJECTIVE: Seeking Fulltime/Intern position as a Mechanical Engineer.

EDUCATION:

Masters of Science, Mechanical Engineering	*GPA 3.67/4.00*
University of Illinois at Chicago	*DECEMBER-2017*
Bachelor of Engineering, Mechanical	*GPA 3.7/4.00*
Don Bosco Institute of Technology, Mumbai University	*JUNE-2015*

ACHIEVEMENTS

- **University topper** in '*Engineering Mechanics*' with a score of **100/100**.
- **University topper** in '*Engineering Drawing*' with a score of **73/75**.

WORK EXPERIENCE

- **Summer Internship at RB PNEUMATIC TOOLS PVT.LTD**   *JUL to AUG-2013*
  Worked as *Production engineer intern* where the major role was to ergonomically design machinery and pneumatic tools on SolidWorks which included advanced modelling and assembly techniques in component shafts, gears, couplings, flanges, housings, clutches, bearings. Learnt about manufacturing processes such as Milling, Forming, Sheet metal work, injection molding, blow molding and acquired knowledge about power tools.

- **Intern at MEDIMEK INDUSTRIES**
  JUN to JUL-2014
  Worked as *Assistant design engineer* where the major role was to inspect and design manufacturing drawings of hospital furniture,its assembly modelling, detailing, error diagnostics and template creation on SolidWorks. Also interface with suppliers for component selection, manufacturing and quality control, component validation and processing.Read and interpret technical drawings,specifications,tolerances,schematics and documentation of reports.

RESEARCH EXPERIENCE

- **THESIS: 3D FINITE ELEMENT METHOD AND MULTIBODY SYSTEM COUPLING OF RAILROAD DYNAMICS WITH VIBRATION OF SURROUNDING BUILDING :(Presented at *MIDWEST rail conference* 2017)**   *JUNE 2016- Current*
  Quantified vibrations in the building structure due to a passing train to minimize the discomfort of occupants by applying concepts of modal analysis and then reconstructing displacement fields in ANSYS from SAMS (multibody simulation software) by using coupling of Finite element analysis and MBS to model a 3D railway track system.

- **INDEPENDENT STUDY-RESEARCH IN FINITE ELEMENT MODELING OF OPTIC NERVE HEAD BIOMECHANICS:**

The goal of this study was to characterize the biomechanics of the optic nerve head and studying the stresses using computer modelling and analytical techniques on ANSYS WORKBENCH, SolidWorks and Microsoft Excel. *MAY 2016.*

SOFTWARES: SOLIDWORKS,AUTODESK INVENTOR,ANSYS,PRO-E,CATIA V5,CREO,AutoCAD,ABAQUS,NX-CAD,NX-NASTRAN,MATLAB,HYPERWORKS,MSC-ADAMS,MSC-NASTRAN,MS OFFICE|Programming Lang. :C,C++, and JAVA

ACADEMIC PROJECTS

- **DYNAMIC ANALYSIS OF A FLUID FLOWING THROUGH A POROUS MEDIUM:** In a consolidation problem, concepts of Poromechanics and Advanced FEA were applied to calculate pore pressure and to track displacement under a loaded flexible footing on soil using *MATLAB*.
  NOV 2016
- **METAL 3D PRINTER OPERATED BY INDUSTRIAL ROBOTIC ARM (UR-5):** Over the course of this application project, a multi-axis industrial robotic arm mounted with an automatic weld gun along with the workstation was designed and simulated to make it work as a free form 3D metal printer using a simulation software *ROBO-DK*. *MARCH 2016*
- **DESIGN OF A COTTER JOINT:** Calculated the stresses induced in the cotter joint for an effective transmission of a non-varying load in ANSYS and thereby designed suitable dimensions for the joint to avoid failure. *OCTOBER 2015*
- **SOLAR POWERED REFRIGERATION SYSTEM:**
  Built a solar powered refrigeration system which works on '*Electrolux Absorption System*' principle.
  MARCH 2015
- **AUTOMOBILE- ALL TERRAIN VEHICLE:** Designed & manufactured an innovative '*Steering System*' for an 'All-Terrain Vehicle 'which participated in *SAE INDIA BAJA competition.*
  JUNE 2014
- **INDUSTRIAL SAFETY MECHANISM** Designed an industrial safety electro-mechanical device for a punching setup based on Electro pneumatic principles and components using *FESTO SIM* software.
  JAN 2013

RELATED COURSEWORK: Advanced FEA, CAD/CAM/CAE,Applied Stress Analysis, Solid Mechanics,Strength of Materials, Multibody dynamics,Machine Design,Engineering Drawing, Mechanical vibration ,Fluid mechanics, Thermodynamics, Mechatronics, Theory of machines, HVAC, Material Technology, Manufacturing processes, 3D Printing,

CERTIFICATIONS

- Certified as 'Professional *in Product design and Analysis*' in **SolidWorks, ANSYS, PRO-E, CATIA** at *CADD centre*.
- Certified and trained on 'CNC *828D Milling Programming and operation'* at **SIEMENS LIMITED**.